Three Essays on Temporal Network Analysis in Financial and Social Systems

SHAUNETTE TAMEIKA FERGUSON nee MARCH

(Degree)
博士（経済学）

(Date of Degree)
2022-09-25

(Date of Publication)
2024-09-25

(Resource Type)
doctoral thesis

(Report Number)
甲第8419号

(URL)
https://hdl.handle.net/20.500.14094/0100477845

博　士　論　文

令和4年6月

神戸大学大学院経済学研究科
経済学専攻
指導教員　小林　照義
SHAUNETTE TAMEIKA FERGUSON née MARCH

博　士　論　文

Three Essays on Temporal Network Analysis in Financial and Social Systems
（金融・社会システムにおけるテンポラル・ネットワーク解析に関する三編の論文）

令和4年6月

神戸大学大学院経済学研究科
経済学専攻
指導教員　小林　照義
SHAUNETTE TAMEIKA FERGUSON née MARCH

ACKNOWLEDGEMENT

Without the encouragement and support of many individuals, this doctoral dissertation would not have been possible. To them, I am sincerely grateful for their unrelenting support, words of encouragement, and acts of kindness. I would first like to thank God for his grace in sustaining my health of mind, body and spirit throughout this process. I am most grateful for this spirit of resilience that he has endowed me with; despite being broken at times, it continues to find a way to keep pursuing the best of my abilities ('Age Quod Agis'). The unwavering support of my family has also been critical in keeping me grounded, humble and strong. Here, I highlight the contribution of two indefatigable champions: my father, Noel March and my grandfather, Alexander Gayle. Their passing undoubtedly brought great anguish during my first year and the penultimate year of my tenure. However, their remarkable display of courage serves as a daily reminder that I should not fear but instead be bold in entering any arena. I can recall numerous times during this process when I encountered challenges that appeared impossible; I would often think back on my grandfather, who would mischievously ask: "Did it [the challenge] beat you? Did you really allow it to beat you?" This dissertation is partly the result of asking myself that question each challenging encounter. For these reasons, I dedicate this work to the loving memory of Alexander Gayle and Noel March.

I am forever grateful to my loving husband and life partner, Keson Ferguson, for his continued patience, kindness, and belief in my ability. This journey was made easier with your presence and words of encouragement in particularly turbulent times. My mother, Una Gayle and sister, Shanique March have also been instrumental in providing the familiarity of home and an environment for restoration. I must make special mention of my dearest uncle Paul Hastings-Gayle who has been on every academic and professional journey from beginning to end, he is never too busy to provide meaningful guidance and a fresh perspective.

The steadfast support of my friends in Jamaica and the diaspora in the United Kingdom and the United States of America has been unfailing; I am grateful. Thank you to my dearest friend Love Odih Kumuyi for her constant encouragement and for maintaining our imperishable friendship. I

am forever indebted to Dr. Dania Dwyer, Mrs. Althea Heron and my mentors, Dr. Robert Mullings and Dr. Naila Smith, for their wise counsel, ideas and advice during particularly challenging times when I doubted my ability. When I embarked on this journey as a new research student in Japan, I met Akira Matsui who has maintained a keen interest in my progress, eager to help me navigate the unknown and unfamiliar aspects of my new academic life in Japan. I am sincerely appreciative of the continued support and friendship.

I also must acknowledge the support of the Japanese Government in providing funding assistance via the Ministry of Education, Culture, Sports, Science and Technology (Monbukagakusho: MEXT) scholarship for the first three years of my research. My gratitude also extends to the staff of the Embassy of Japan in Jamaica, Ms. Reika Inoue and Ms. Megan Barrett, for their support and patience in navigating the scholarship application procedures and the entry requirements for Japan. The scholarship has allowed me to pursue this entire endeavor at Kobe University whose academic and student support staff have been tremendously encouraging and supportive. Special thank you to Ms. Aemee Inoue and Ms. Megumi Tamura for their continued patience, encouragement, and availability to provide help throughout the various academic and student affairs processes. I am sincerely grateful.

Finally, I acknowledge the able supervision of Professor Kobayashi whose advice has never failed to improve my research. His support has helped tremendously in developing my technical and analytical skills in this field of network theory which was practically new to me five years ago. Most importantly, his patience throughout this process and his continued encouragement to break boundaries has made a significant contribution in bringing this dissertation to fruition. I also thank Dr. Sadamori Kojaku for his contribution to my research and for graciously making time to provide advice and motivation.

TABLE OF CONTENTS

CHAPTER 1

Introduction

Many systems in the real world can be modeled as temporal networks[1–4] due to their complex architecture that change as they interact with and adapt to the wider environment. Networks are generally used as a convenient way of representing complex patterns of connection between the constituents (i.e., nodes) that are linked by relational ties (i.e., edges).[5] Traditionally, networks depict these relationships as static representations by considering either a single snapshot in time or an aggregation of the relationships over a time window. Despite their usefulness in simplifying some aspects of the network architecture for real systems, static representations can ignore other realistic features that characterize complex systems.[6–15] Modeling complex systems as temporal networks, preserves the time dimension of the underlying data; therefore providing much richer information on the time-varying behavior of nodes and the dynamics of the edges between them.[16,17] Two well-known networks that constitute a considerable part of our daily lives fall into this category of systems with a time-varying structure: social networks and financial systems. The network science literature has seen an explosion of studies on financial and social networks; however, the application of temporal network models is considerably advanced in the latter while still relatively nascent for financial systems.

Over the last decade and a half, the world has experienced substantial disruptions to the global financial system and to the way we interact with each other in common social settings (e.g. schools, workplaces) due to pandemics. The danger lies in the tendency for breakdowns in these systems to permeate other aspects of our lives and other systems that rely on them to function; thus signaling their importance. System malfunctions of this kind are, therefore, constant reminders of why we study financial and social complexity exhibited, respectively, in the behavior of humans and financial institutions. The overall objective of studying any system is to understand it well enough to prevent or mitigate collapse due to threats, and to enable greater control over them. By using temporal networks, we can fully consider the realistic structure of the time-varying dependencies at a microscale which is key to uncovering how social and financial systems operate at the core.[15]

This, therefore, enables us in answering questions such as: How do node level interactions lead to global effects. Moreover, the richness of temporal data also presents the opportunity to go beyond the microlevel to uncover informative details about the source of changes in the network as a whole. It is against this background that we establish the purpose of this work as being twofold. First, we investigate how the dynamical local interactions and properties of banks generate systemic risk in an empirical financial network. Second, we explore the source of dynamical changes in the global properties of social systems using empirical data on human interaction in face-to-face networks.

Our study of financial systemic risk is conducted within the context of an interbank market that facilitates banks in managing liquidity through bilateral exchange of loans. The novel feature of this work is that we use timestamped data on unsecured overnight interbank loans which we rely on to measure systemic risk by aggregating the trades over a quarter-hourly timescale. The use of such a small timescale enables us to observe the evolution of systemic risk via the interbank linkages as the day progresses. At best, previous empirical studies aggregate trades over an entire day;[18–20] however most consider much coarser timescales[21–24] (e.g. monthly, quarterly or yearly), which discounts the possibility that systemic risk has its own diurnal dynamical pattern. Furthermore, we study the systemic risk patterns in close to 4,000 days that span relatively calm and turbulent periods alike; thus contextualizing and differentiating the findings based on economic conditions. The existence of intraday fluctuations in systemic risk may imply that the timing of certain activities in interbank markets needs closer monitoring. Moreover, it may signal that the study of financial systemic risk in other layers of the system should respect the inherent timescale of the given layer.

We adopt the broad definition of systemic risk as seen in the financial network literature which defines it as the possibility that an initially localized shock triggers global instability via a cascading effect.[25–30] Due to the existence of various transmission channels that can propagate risk, different financial network models are often used to represent and study each channel separately. For example, models of interbank networks define banks as nodes that are linked by bilateral claims and obligations; however, when the portfolios of institutions overlap, one could also define nodes as financial institutions in general with edges between those that have common assets in their portfo-

lios. Interbank markets feature extensively in the study of financial systemic risk for a few reasons that include the interest generated by the 2007-2008 global financial crisis which witnessed a partial collapse of interbank markets globally.[20] Moreover, interbank markets reflect many general features of financial systems such as their ability to: capture complexity of exposures among banks,[31–33] incorporate banks' balance sheets,[33] consider uncertainties surrounding financial contracts (as banks depend on promises regarding future payments).[31,32]

Early studies of interbank obligations assumed stylized random network structures that are static;[27,34–36] however, other works employ the use of empirical data to examine the role played by real interbank network structures.[18–24,37–40] The empirical findings highlight that systemic risk is overestimated in financial networks with random structures that characterize banks as having homogeneous sizes and/or degrees.[20,38,41] To motivate our departure from static representations of financial networks and random network structures, we highlight findings from studies on social networks indicating that the time-varying activity of nodes can influence spreading phenomena such as infectious diseases, opinions and rumors.[2,3,42,43] More specifically, the work on epidemic spreading in temporal networks show that contagion can be altered fundamentally by the burstiness of human contacts,[44,45] either mitigating spread[46–48] or causing it to accelerate.[42,49] It is also shown that coarser resolutions i.e., aggregating contacts over long time scales, can average out material temporal information by treating old contacts and new contacts in the same way, and also by considering neither the possibility that temporal correlations may exist between consecutive contacts nor the impact that one contact can have on multiple edges.[50–54] A temporal network analysis of the Italian interbank market, i.e., the data set that is used in our investigation, indicates that the daily interbank transactions exhibit interaction patterns that are essentially the same as those that characterize human social communication;[55] this means, banks trade with counterparties in much the same way as friends interact via phone calls and face-to-face communications.[8,56] Our review of the works on financial systemic risk highlights only a few studies that investigate contagion in interbank markets at the daily scale.[18–20] We, therefore, recognize a gap that exists in the financial network literature that has not accounted sufficiently for the possibility of a build-up of contagious risk in interbank networks. Early identification of such build-ups could be useful in formulating timely responses to

mitigate systemic risk.

In our study of social systems, we contribute to the network science literature that explores global properties of complex systems. By using four face-to-face empirical human contact data sets from the Sociopatterns project, we investigate the source of dynamical changes often observed in the size of networks — defined in terms of the number of active individuals (i.e., nodes) and the number of connections between them (i.e., edges) at a given point in time. These are two of the most basic metrics common to any system, since all networks consist fundamentally of nodes and edges. To explore the mechanisms behind network expansion and shrinkage, we introduce a new estimation method (i.e., numerical maximum likelihood) to estimate the parameters of a model that takes the aggregate number of nodes and edges at a given time as inputs. The novelty of our estimation method is its ability to estimate simultaneously, the parameters that represent each mechanism. Estimating both parameters in parallel, therefore allows us to identify the origins of the systems' size fluctuations by deconstructing the contribution that each makes and by also observing the interplay between them. Furthermore, since we are relying solely on the aggregate metrics of total nodes and edges, we can apply the method to understand the dynamical changes in practically any system. We highlight previous studies that develop methods to classify the source of such time-varying dynamics in temporal networks[57,58] also employed these basic aggregate metrics; hence, our proposed method serves as an extension of their work.

Existing studies on temporal social networks are interested in the time-varying tendency of interactions between nodes; however, these local interactions represent just one aspect of dynamics in system — the other consists of changes in the properties at the aggregate level. One such global property is the size of networks which has been shown to fluctuate quite often in temporal networks. More specifically, aggregate nodes and edges have a scaling relationship that is referred to as the densification power-law.[57–60] However, this relationship that describes the way aggregate network connections at a given time changes with the number of nodes, has been found to exhibit two distinct patterns. First, the conventional densification scaling shows a constant growth[59,60] in network edges; but in the second case, total edges expands at a rate that is not constant.[57,58]

In both instances, any fluctuations in the aggregate metrics can be traced back to changes in two mechanisms: the system's population, and/or the probability of two nodes connecting (i.e., overall activity level). For a social network with fixed probability of connection, total interacting individuals and total edges (i.e., the total pairs of individuals in contact) will both increase if the population of the network expands. This is because as more persons join, an increasing number of individuals will find partners to maintain the fixed probability of connection in the system. For a network that has a fixed population, however, increasing the connection probability will not only raise the total number of edges between individuals but — if non-interacting persons exist — an increasing probability implies that more of them will become engaged with others which then leads to an increase in the total number of active individuals.

Changes in the system's population and overall activity level precipitate changes not only in the size over time but also the type of densification scaling pattern[57] that emerges. To understand complex systems well enough to control and manipulate them, it is important that we explore the existence of any time-dependent contributions of the mechanisms behind fluctuating network size. In theory, the conventional scaling relationship (i.e., where aggregate edges grow at a constant rate with aggregate nodes) is due to a network population that is changing.[57–60] However, the non-constant growth rate of edges (as number of nodes increases) is due to variations in the overall activity level which modulates the generation of edges.[57,58] Empirical data on social networks and other systems show that, in reality, the relative importance of each mechanism can be changing from time to time. In fact, they showed that neither of the mechanisms was the sole factor affecting the network size in the investigated temporal social networks.[58] Besides this tendency for population size and overall activity level to switch between themselves as the dominant mechanism driving time-varying changes in system size, there also exists the possibility that both mechanism are acting at the same time. To explore such a possibility, the models proposed in these studies would need to be extended to facilitate an estimation of the parameters simultaneously. Our study proposes a method to this end.

The outline of this dissertation is as follows. In chapter two, we survey the literature on two

complex networks that are quite familiar to our daily lives: financial and social networks, which we study closely in chapters three and four, respectively. The purpose of this survey is to establish a concordance between these two areas of study, highlighting the relatively advanced nature of the work on social systems, and precisely how the tools and methods employed in social network analysis can be applied to gain much needed insights about financial systems. To the best of our knowledge, the two areas have been reviewed largely in a disparate manner. Therefore, this survey takes a systematic approach in connecting the two areas with the hope of identifying: how the existing gaps in the financial network literature can be supplemented by highlighting tools and methods in social network analysis that have provided useful insights for social policy design.

In chapter three, we study how local dynamics can precipitate macrolevel changes in financial networks. Although financial interlinkages have been identified as the factor underlying the various types of risks that threaten financial stability via aggregate network effects,[61] heterogeneity among the institutions themselves is also important. We, therefore, employ temporal network analysis to the interbank network to highlight time-variation in bank trades as an important source of heterogeneity with implications for how we detect changes in systemic risk. Our investigation quantifies systemic risk (i.e., fraction of banks to default) due to an initially localized shock that propagates throughout the network. We also explore some possible factors that may be influencing dynamical changes in the level of risk in the system during respective trading days. Finally, we leverage the temporal richness of the data to highlight how differences in structure at a point in time should be considered when quantifying threat levels in the system.

In chapter four, we go beyond the dynamical behavior of nodes (i.e., at the microlevel) to investigate the source of dynamical changes in social network at the aggregate level. In particular, we explore the question of: why do networks expand or shrink at different times? We extend existing works on the topic to develop a numerical maximum likelihood approach that enables us to deconstruct the individual contribution of each mechanism as well as the interplay between them. We conclude our discussion in chapter five.

CHAPTER 2

Social and financial networks as complex adaptive systems

Shaunette T. Ferguson, Graduate School of Economics, Kobe University, Japan

2.1. Introduction

We encounter complex systems almost everywhere:[62–65] from our own immune system which we depend on to survive to those that are man-made such as communication,[66–68] transportation,[69] financial and other[65,70] networks that have enabled greater convenience. Understanding these systems enables us in preventing or mitigating their failure,[71–77] while taking advantage of how we can obtain the maximum benefit from them.[78–80] Social networks have been paramount in understanding and anticipating the spread of social phenomena (e.g. ideas, innovations, fads, diseases and computer viruses) while providing the tools to measure the social standing[81–84] of the individuals participating in them. Much of what we know about the diffusion and persistence of certain epidemics is due to studies about the behavior of social systems as they evolve, and how dynamic processes occur on them. Furthermore, understanding human mobility[85,86] patterns have the potential to help us mitigate the spread of epidemics,[87] enhance crisis responses[88] among other things.[89] Similar to social networks that link individuals according to their social relationships, financial systems are also modeled as networks of financial institutions with links that symbolize the nature of their financial relationship.[35,90] By viewing financial systems in this way we can make sense of financial meltdowns provoked by the failure of institutions that cascade over a highly interconnected and interdependent system.[36,91] Both social and financial systems have a complex architecture due to a non-randomness in their origins and evolution, and this similarity between them has enabled many approaches in social network analysis to be applied in the study of financial systems.

Social network analysis stands as one of the key streams of the network science research most applicable to the study of financial systems, another includes the field of statistical physics.[92,93]

Early developments in social network analysis, particularly in sociology during the mid-20th century, led to findings that provided a pivotal foundation for our understanding of diffusive phenomena (e.g. ideas, habits, behaviors etc.), and the notion that some individuals or group of individuals are more important (central) than others. Formalizing how we investigate these systems and phenomena was due largely to contributions in the field of statistical physics, which began with questions about the design principles of real systems. At first, complex systems were thought to be random, emerging from pairs of individual units connecting with a certain probability p to generate a total of $pN(N-1)/2$ edges between the nodes.[94] However, increasing interest in the workings of real systems, particularly the resilience of their topology, motivated further research and brought into question the realistic nature of empirical systems having a random network structure. Several of these studies that challenge the paradigm of a random network topology in real systems, relied on networks in the natural environment to find that many systems around us are encoded with self-organizing patterns that are anything but random. The advancement of our knowledge about real complex systems have resulted from several factors working in tandem ;[92] namely: 1) greater availability of large-scale computerized data sets in different fields of study, 2) increased computing power and capacity that enable networks with millions of nodes to be studied; thus expanding the research possibilities, 3) increased collaboration between different disciplines which allows access to diverse databases.

Subsequent works pursue the development of tools and metrics to contrive meaning from this wealth of data by quantifying the commonalities and uniqueness of empirical systems. Three fundamental properties became known about complex networks. First, the *small world*[95] property describes the relatively short distance between any two nodes, where distance is the number of edges connecting the pair via the shortest possible path. Second is the tendency for nodes to form clusters (e.g. a clique of friends in social networks) in which everyone in the cluster is acquainted with the other. The presence of such cliques, given by the clustering coefficient[96] metric, tends to be greater for real systems than for random networks. Third, is the non-Poissonian degree distribution that shows few nodes having many edges (or degrees) while a larger number of nodes have relatively fewer edges.[67,92] Studies on the World Wide Web,[66] Internet,[68] metabolic networks[97] and others[67,98,99]

indicate that they belong to a class of scale-free networks[67,100] with degree distributions that are significantly different from that of random networks. Establishing this foundation paved the way for subsequent investigations aimed at identifying *tipping points* (i.e., where small shocks make considerable differences in outcomes[36]), and how statistical properties lead to a more or less resilient network. Some networks are quite robust to drastic attacks with the malfunction of key components leading infrequently to system-wide breakdown.[97,101] However, this robustness is sometimes due to the presence of redundancies built into the underlying network structure (e.g. communication networks[102]). The main question of concern in this aspect of the literature considers the extent of the contribution of network topology, in the absence of redundancies, in maintaining the system's stability.

Although the fields of economics and finance are inherently transdisciplinary[93] and the parallels between financial and complex systems[36,91,103,104] are quite discernible, the extension of network concepts and techniques to the financial system followed much later.[61,93] One explanation for this is the absence of behavioral considerations[36] in some studies which model individual entities (e.g. banks) as passive. Furthermore, the network structure in early studies that applied network techniques, implicitly assumed that nodes (e.g. banks) are either isolated or completely connected[105] (i.e., every node is connected to the other),[61,93] without adequate investigations into the implications of assuming these structures. In fact, financial supervision once considered the balance sheet of individual institutions while ignoring in large part, potentially important information about the relationship between them.[61] In other words, two institutions that lend (or borrow) the same amount may have different effects on the network as a whole; hence, at the very least, nodes should be differentiated on the basis of the number of edges connecting them to others. We also highlight the role played by data unavailability or inaccessibility on relationships between institutions in financial systems. This limitation has been cited in several studies as a debilitating factor to more in-depth investigations using network techniques. Limited availability of data on bilateral exposure of banks and/or balance sheet data, at the appropriate level of granularity, can limit the use of specialized models that exist for simulating systemic risk;[106] thus having negative implications for policy design.[33] For example, the evidence on whether real interbank networks belong to the category of

scale-free networks is mixed: some studies of empirical interbank networks find a power-law degree distribution among banks[107–110] while others[111–113] find degree distributions that have a heavier tail than random networks, but not necessarily scale-free. Since scale-free networks are robust to random failures but more susceptible to the removal of specific nodes that are well connected,[114] it begs the question: what does it mean for financial network stability when the system has an alternative degree distribution[112,113] to the scale-free distribution?

Notwithstanding, the applications of techniques in statistical physics and social network analysis are becoming increasingly present in the work on financial systems. Due to a general urgency to capture complexity and connectivity between institutions and financial markets, more detailed data collection has become the focus of regulators, asset managers and risk managers who are concerned, respectively, with macro prudential supervision, the complex dynamics of financial market interdependencies and early warning signals that can identify emerging systemic risks. By viewing financial systems from a network perspective we have access to the most holistic and straightforward representation of a host of financial relationships[115] where each relationship type can be modeled as separate layers.[116–118] Furthermore, network models can aptly handle heterogeneity of institutions i.e., with all their interconnections, while offering a way to simulate dynamic spread of shocks to identify non-linearities that are typical of systemic instabilities.[36] Existing studies on financial networks highlight similarities in the structure of interbank networks with that of other complex real-world systems; more specifically, financial networks exhibit small-world property, high clustering coefficients, and a non-Poissonian degree distribution.

While structural configuration is a key component of understanding complexity in social and financial networks,[114,119–121] the self-organizing tendency of these systems often leads to new patterns of interaction emerging over time. This means network structure is also evolving, and the dynamism forms part of the system's complexity. Temporal network models capture these changes as nodes and edges switch between the states of being active and inactive;[3,16,122,123] thus encapsulating the inherent time dimension that is evident in the real interaction between the most fundamental network components.The use of temporal network models is well advanced in social network

analysis;[3,16,46,47,122–125] however, their extension to the study of financial systems remains in its infancy.[126] Studies on temporal social networks highlight that non-linear effects can emerge from time-varying behavior at the local level; thus having implications for how the wider system responds to small disturbances.[42,43,46,127,128] Despite the low penetration of temporal models in the study of financial networks, their application is highly relevant especially for financial systemic risk analysis because of the sheer nature of how these systems operate. Several processes are occurring on them, sometimes concurrently, in which the properties of institutions and/or their relationship with others in the system are dynamic. Therefore, the time-varying aspect of the interaction between institutions should not be neglected, and observing these behaviors over extended periods can uncover many hidden properties about them. Furthermore, one of the primary objectives of financial regulation and supervision is to manage financial systemic risk which manifests as non-linear macroscopic effects that emerge when dynamical changes at the institutional level are aggregated. Hence, any meaningful headway on the study of systemic risk hinges on knowledge of the temporal structural dynamics of the financial system under investigation.

In this review, we aim to provide a systematic overview of the existing works on social networks and financial systems. We highlight the parallel between them, and how the tools from social network analysis have been leveraged to better understand financial systems outside of the conventional space of economics and finance. The body of work that has already reviewed the financial network literature increased steadily in the aftermath of the global financial crisis of 2008—2009, signaling an expansion in the use of network concepts and techniques. One of the earliest reviews discussed methodologies and also motivated the use of network representations to study financial systems.[129] Others focused mainly on surveying theoretical studies that investigate the narrow strand that links connectivity and financial stability[130] or the broader range of studies on interbank networks that differentiates on the basis of the type of financial links, shocks, loss propagation, network formation process and structure.[33] The reviews by De Bandt et al.[31] and Benoit et al.[131] surveyed studies that use financial network models and also those that used conventional approaches in economics and finance. Another strand includes studies on simulation methods[115,132] and simulated empirical financial networks.[115,132–134] Recent surveys, however, are more integrated in reviewing works

that employ network models of financial markets to investigate the relationship with systemic risk .[93,135,136] Bardoscia et al[93] specifically highlighted the contribution of the field of statistical physics to that of financial network studies. Here, we take a novel approach to fill the gap in the network science literature by establishing a bridge between social network analysis and financial network studies. We focus particularly on the relevant theoretical frameworks, the empirical applications and their policy implications.

In section 2.2, we provide an overview of temporal networks and the various ways in which empirical data can be simplified to incorporate dynamical properties that are crucial in our understanding of real systems. We follow by highlighting the similarities between social and financial systems in section 2.3. In section 2.4, we discuss the different applications of network analysis to static and time-varying social systems. Finally in section 2.5, we review studies that employ network analysis in the study of financial systems.

2.2. Constructing temporal networks from empirical data

To capture inherent properties that are time-varying in real complex systems, a temporal network representation is frequently employed; hence their widespread use span various fields of social and natural science.[137–140] Similar to their static counterparts, temporal networks consist essentially of nodes with links (formally known as edges) between them. However, active nodes (or even edges) a given time can be different from those at another time. Therefore, temporal networks are more detailed in their representation of when nodes and edges become active and when they go offline;[141] thus encoding the inherent dynamism of the system's structure. In addition to network structure, the dimension of time is particularly relevant in exploring and understanding spreading processes because each edge and the time that they become active, provides an opportunity for propagation.[43,141] Here, we discuss key considerations when constructing temporal networks from empirical data.

2.2.1. General network representation

A network representation can simplify the many complex systems (e.g., world wide web, power grids, transportation systems etc.) that form part of our daily lives. At the foundation of these systems

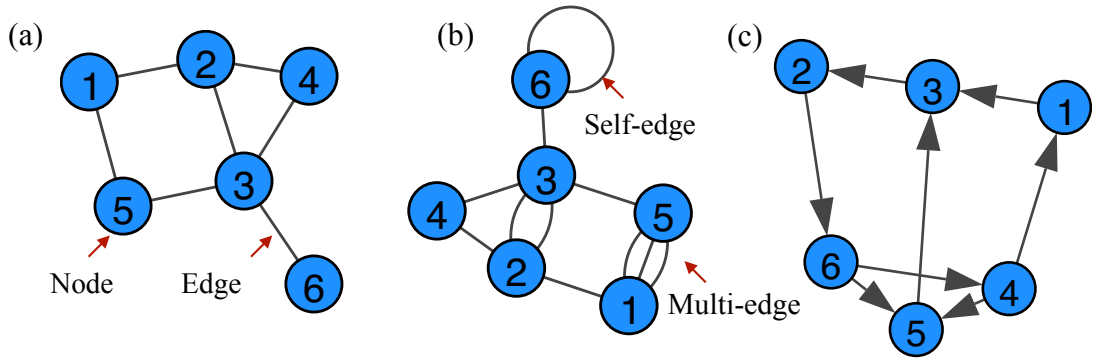

$$U = \begin{bmatrix} 0 & 1 & 0 & 0 & 1 & 0 \\ 1 & 0 & 1 & 1 & 0 & 0 \\ 0 & 1 & 0 & 1 & 1 & 1 \\ 0 & 1 & 1 & 0 & 0 & 0 \\ 1 & 0 & 1 & 0 & 0 & 0 \\ 0 & 0 & 1 & 0 & 0 & 0 \end{bmatrix} \quad M = \begin{bmatrix} 0 & 1 & 0 & 0 & 3 & 0 \\ 1 & 0 & 2 & 1 & 0 & 0 \\ 0 & 2 & 0 & 1 & 1 & 1 \\ 0 & 1 & 1 & 0 & 0 & 0 \\ 3 & 0 & 1 & 0 & 0 & 0 \\ 0 & 0 & 1 & 0 & 0 & 1 \end{bmatrix} \quad D = \begin{bmatrix} 0 & 0 & 1 & 0 & 0 & 0 \\ 0 & 0 & 0 & 0 & 0 & 1 \\ 0 & 1 & 0 & 0 & 0 & 0 \\ 0 & 0 & 0 & 0 & 1 & 0 \\ 1 & 0 & 1 & 0 & 0 & 0 \\ 0 & 0 & 0 & 1 & 1 & 0 \end{bmatrix}$$

Figure 2.1: Visualizing and representing networks. In the upper panel, networks are visualized as graphs with nodes (blue circles) and edges (black line connecting them), and the lower panel shows the respective adjacency matrices. Each row and column identifies the a particular node as the source and target, respectively. (a) The interaction between nodes can be bidirectional which is represented as an undirected network. (b) Network representations can also track the number of bilateral contacts (i.e., pairwise interactions) or whether nodes have made contact with themselves by including multi-edges and self-edges, respectively. (c) In directed networks, edges go from source (initiating) node to target nodes, and this is denoted by unidirectional edges.

are units that are relating among themselves via edges, and we can visualize these fundamental constructs graphically (Fig. 2.1, upper panel) or as elements in a matrix (Fig. 2.1, lower panel). The latter representation is referred to as an adjacency matrix in which the row and column indexes are node identifiers (or node indexes). In the adjacency matrix, a non-zero value means that the nodes identified by the row and column indexes, respectively, have been in contact while nodes with no contact between them have a zero value in place. When the focus is solely on whether two nodes have interacted, a binary adjacency matrix (i.e., entries can be 1 if nodes have interacted and 0 otherwise) may be more appropriate. However, additional information on the nature and diversity of the edges in the networks are sometimes important and therefore, better represented as a weighted graph or adjacency matrix. Finally, if no importance is assigned to the direction of the

contact between nodes, then a symmetrical adjacency matrix, in which all the edges are bidirectional, may suffice (Fig. 2.1a). On the contrary, an asymmetric adjacency matrix takes note of the exact direction of the contact (Fig. 2.1c); hence values contained in the upper triangle and lower triangle of the matrix do not mirror each other (i.e., $A_{ij} \neq A_{ji}$). In networks where individual nodes are not connected themselves (i.e., self-loop), the corresponding adjacency matrix has a diagonal with only zero elements (Fig. 2.1a and Fig. 2.1c, lower panels) while where self-loops exist, the entries on the diagonal can be non-zero (Fig. 2.1b, lower panel).

So far, we have described the basic elements that underlie the topology of complex systems. Such systems are, however, comprised of intricate hierarchical structures with a prominent feature emerging in them: most nodes have only a few edges while a few nodes have a large number of edges linking them to others. This property puts such systems in a class known as scale-free networks where the frequency of highly connected nodes decays as a power-law. Scale-free networks contrast with exponential networks in which nodes have the same number of edges on average, and an exponential decline is exhibited by the number of highly connected nodes.[2] Heterogeneity in the number of edges that emanate from individual nodes (i.e., node degrees) in scale-free networks is an extremely relevant feature because of its strong impact on the robustness and vulnerability of networks.[114,120,142,143] We also note that, in some networks, nodes become active and form connections with others at different times, thus the transient nature of node activity gives rise to a dynamic network structure that requires us to consider the time dimension. Temporal networks enable the reconstruction of a simplified version of systems that can be enriched by incorporating timestamp data that identify when events occur. Different approaches have been employed in the construction of temporal networks from real data, some retain as much information as possible while others focus only on a few temporal features.

2.2.2. Temporal network representations

Series of static networks

A straightforward way to simplify temporal data is by representing the data as a series of static snapshots.[2] The allure of this approach is the many methods available for static-network analysis.[2]

(a)

Time	Node identifier	
	i	j
0	B	D
1	A	E
1	A	C
2	C	D
2	D	F
3	A	B
3	E	F
4	B	D
4	C	D
5	C	F

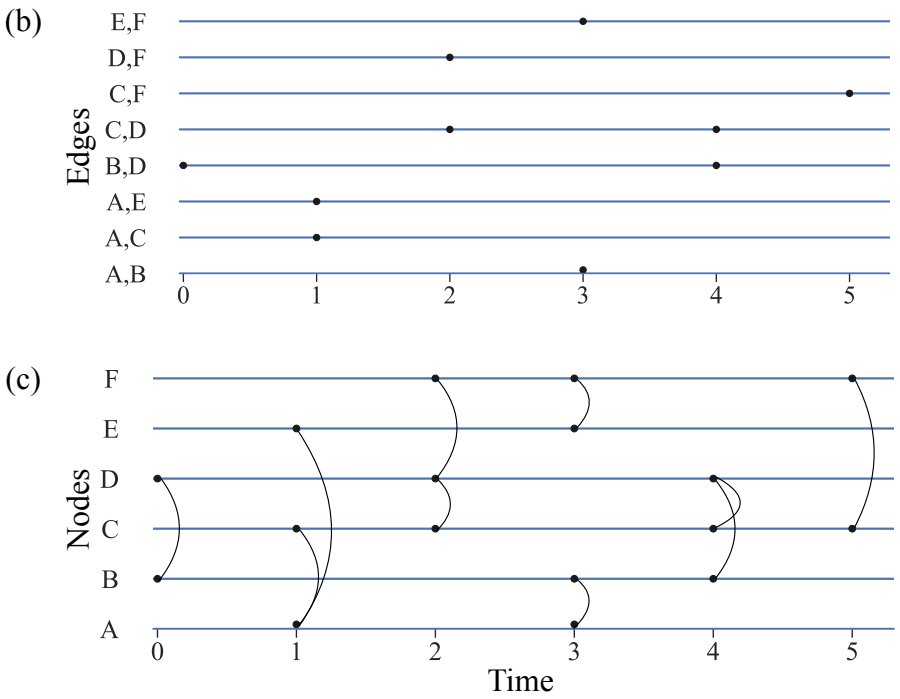

Figure 2.2: Timeline of contacts that involve edges in a network of six nodes. Panel (a) is a sample contact sequence indicating the time of contact between nodes i and j. We show edge activity at consecutive times in panel (b) with each dot representing a contact between a given pair of nodes. The contact duration is the time between the first and the final contact events for an edge. In panel (c), the interaction of each node is shown explicitly. From (b) and (c), the inter-event time is the time between events that involve edges and nodes, respectively.

To construct temporal networks in this way, we define a time-window length ℓ which is used to segment the data into different snapshots. Essentially, a snapshot is an aggregation of the events that occurred within a time-window, beginning at a t_i and ending at t_j where $j > i$ and $\ell = t_j - t_i$.

In Fig. 2.2a, each time point is essentially a snapshot with a time-window length of 1. Of course, larger time-windows that are not necessarily of equal length can also be defined. If the time-windows for consecutive snapshots are non-overlapping it means that the end of one time-window is the beginning of the subsequent one. Formulating snapshots in this way implies that the events in each time-window are being treated as being independent of each other. However, in another context, nodes can be influenced by contacts that they had some time in the past[42,43] and in the case of information spread some nodes may be more receptive to the same information coming from multiple contacts than they are to information obtained repeatedly from the same contact. Modeling such scenarios as overlapping snapshots is one way of capturing and investigating the effect of this contact history-dependency or memory effect.

In choosing the appropriate timescale, the objective is to ensure that the resulting network is as representative and as informative as possible.[122] This has been the focus of many studies,[50,144–146] several of which show that time-window size should be considered carefully in modeling dynamical systems on networks. Liljeros et al.[144] explained that the parameter values used to simulate disease spreading in proximity data were related to the size of the time-windows. In [50] and [146], they went further in specifying how time-windows should be selected in proximity data. Another consideration when choosing the length of time-windows is their interpretation and meaning within the context of the data. In [59], the authors use HEP-TH (high energy physic theory)[147] data to investigate growth patterns exhibited in real networks over long periods. This citation network was constructed from data on papers published during January 1993 to April 2003. Each paper was represented by a node i, and if i cites another paper j, then, a direct edge is established from i to j. Given the objective of their study, i.e., to investigate how real networks evolve over time, the authors focused on annual temporal snapshots in which citations were aggregated over each year (i.e., $\ell = 1$ year). In financial systems, investigation into the long-term lending relation between banks may employ a similar approach of establishing temporal networks by aggregating bilateral trade data over long periods (e.g., month or year). However, if the aim is to understand the spread of risk given the extent of interconnections in the financial system, then, a shorter aggregation period (e.g., a day in the overnight lending data) may reflect more accurately, the loan duration which lasts a maximum

period of one day.

In addition to identifying an appropriate time window length when projecting temporal data to static network snapshots, is the matter of reducing the extent of information loss .[2] To demonstrate, we consider the adjacency matrices for a series of temporal snapshots, in which interactions between node pairs are denoted by 1 and 0 otherwise. Although we can decipher which connections are established at a given time, key information on the frequency of the interaction between each pair, at a given time, is not obvious. To incorporate this information, we would include the number of times a particular pair has been in contact during a time window as edge weight $w_{ij,t}$ (denoting the number of times node i and j have interacted with each other at time t), thus giving some insight into the diversity of the relationship in the networks. In the Worldwide Airport Network (WAN), seat capacity between airports (nodes) that are connected if a direct flight between them exists[148] or aggregate call duration between individuals[139,149]). At the same time, retaining all the data on the connections between nodes is not always necessary, hence the edges can be filtered to extract the set of relevant connections.[140,150] In [140], a filtering method was developed to extract this backbone from temporal networks by identifying significant ties — node pairs that have higher than expected interactions given their activities. In [150], the network backbone is explored within the context of information diffusion, and the extracted ties are pairs of nodes that have a higher chance of appearing in the 'diffusion trajectory', thus making it more likely for them to infect each other.

Contact dynamics and edge duration

Degree sequences contain information about links between constituents, and this essential in accessing details about the topological features of the network in general. Time-resolved data that records events (i.e., contact between nodes at a given time[2]) provides an extra layer of detail and complexity from which we can extract inherent temporal features of the network. Given the increased complexity of time-stamped data, we may elect to extract select temporal features of the network rather than all of them. This means that depending on how we construct temporal networks we may some important time-related information from the data.[1,151] One prominent temporal feature of dynamic

systems is the time interval between two consecutive events i.e., inter-event time (IET) which can be defined for either nodes or edges.[152,153]

Empirical studies, have shown that IETs are bursty[44,154,155] (i.e., events occurring rapidly between short time periods, alternating with long periods of inactivity), having a heavy-tailed distribution.[156,157] This heterogeneous characteristic of IETs, seen in various contexts,[96,99,158–160] has been described by a power-law IET distribution:

$$P(\tau) \sim \tau^{-\gamma}, \tag{2.1}$$

where γ is the power-law exponent and τ denotes IET.[161] Furthermore, we can also quantify the level of bustiness with the *burstiness parameter*[162] defined as:

$$B \equiv \frac{(\delta/\langle\tau\rangle - 1)}{(\delta/\langle\tau\rangle + 1)} = \frac{\delta - \langle\tau\rangle}{\delta + \langle\tau\rangle}, \tag{2.2}$$

where δ and $\langle\tau\rangle$ denote the standard deviation and mean of IET, respectively. The values of B span the range of (-1,1) with: $B \equiv -1$ indicating regular bustiness, $B \equiv 0$ for neutral since $\delta = \langle\tau\rangle$, and $B \equiv 1$ is as being an extremely bursty signal.[162]

Studies that simulate spreading on bursty networks find that, propagation is generally slower than it is in network with burstiness removed.[46,47] Even in instances where the network is static, as long as the heavy-tailed feature of IETs exists in the dynamical process, spreading slows down.[163] However, other studies[49,164,165] find that, burstiness can also accelerate spreading. This complex effect of bursty IETs on spreading was highlighted by Unicomb et al. who showed numerically and analytically that burstiness can create two distinct phases of slow or accelerated dynamics for epidemic and threshold models of information diffusion, and that diffusion processes are, in fact, sensitive to the IET distribution.[166]

2.3. Analogy between social networks and financial systems

2.3.1. Spreading behavior as a common concern

A primary concern in financial systems is the threat of *systemic risk* i.e., the chance that a financial system's ability to perform its core functions becomes severely impeded. Therefore, the need for

tools to quantify, signal and control financial systemic risk has been highlighted as urgent challenges among researchers across various disciplines.[73,103,126,167] Since the timescale of interaction between institutions spans a wide range with temporal resolution as high as one day [a], this has implications for the dynamics of how systemic risk emerges and unfolds in financial networks. In social networks, however, there are two distinct types of spreading dynamics that are studied extensively. First, *epidemic spreading* which shares the similarity with financial systemic risk in that the social and economic costs can be quite substantial.[168,169] Epidemics are dynamic processes in which a contagious phenomenon is transmitted from an infected to a susceptible unit; therefore, epidemic outbreaks pose significant health, social and economic risks. One may reason that as long as there is life, there is always an ongoing threat of such events and by nature of being highly pernicious, it is important to study these processes to understand them better. Studies that use epidemic models to simulate spread on social networks are focused on the objective of minimizing contagion.[170–172] In contrast, another spreading phenomenon widely studied in social networks is *influence maximization*. The objective of social influence maximization is to obtain the highest number of activated nodes at the end of a diffusive process.[79] Its application has been relevant to studies on recommendation systems,[173,174] viral marketing,[175] social media analytics[176] and rumors.[177]

As early as the 19th century, various analogies were being drawn between epidemic spreading among humans and the spread of sentiments in financial systems as a means of explaining financial contagion. Different sources of contagion, it was argued, gave rise to different manifestations of financial instability; for example, contagion generated by the spread of irrational fear precipitated bank runs during the crisis of 1797[178] while the spread of excitement (i.e., "over-confidence and unreasoning") on the part of speculators and creditors who extend credit recklessly, eventually led to widespread panic. The spread of irrational fear and/or speculative excitement were later categorized as mental contagion. The idea is that, given a closer physical proximity to other market participants (e.g. on exchange's trading floors/online), this 'contagion of the mind' or collective psychology[179,180] may amplify financial crises.[181] In the aftermath of the global financial crisis of 2007–2009, the corre-

[a] In interbank networks, banks trade overnight loans that have a maximum duration of one day, which can be less depending on the exact time that the contract was established.

spondence between social and financial networks have elucidated previously unknown stylised facts that characterize financial systems, thus creating the possibility of improving our understanding of how systemic risk emerges.[55] In the following, we discuss briefly some principles from studies of human interaction, and their early extensions to financial phenomena as a means of understanding financial instability.

Crowd psychology and physical proximity

Early studies on the spread of sentiments included that of Boris Sidis[182] who argued that as social beings, individuals are naturally susceptible to the suggestions (i.e. idea, image or movement) of others ('suggestibility'), whether voluntarily or involuntarily. An increase in the intensity of suggestibility implies that individuals tend to have a reduced sense of independent thinking which, when combined with limited movement or greater proximity to others (e.g., in crowd), may incite irrational actions such as a mob or stampede. This effect of proximity on how easily individuals are influenced in social settings, was also observe among people in urban spaces who were found to be more likely to imitate each other when they were physically close and had multiple interactions among themselves — a phenomenon known as *Tarde's Law of Close Contact*.[183] The findings from these early studies were extended to individuals in financial markets by Edward David Jones who argued that, hopes and beliefs propagate easily and fallacious beliefs are transmitted much further than in settings where individuals developed their ideas independently.[181] To Jones, exchanges (i.e., marketplaces for the trade of financial instruments) are essentially concentrated versions of Tarde's urban spaces; hence the conditions of transacting business in financial markets (e.g., stock exchanges or commodities exchanges) are ideal for the spread of collective thinking or mental contagion in the minds of market participants.

The idea long held by many economists and financial market analysts about contagion is that it emerges from irrational sentiments, and this behavior can spread even among those market participants with the most sound business judgment. Such behaviour usually arises when the data that is necessary for making independent conclusions are unavailable or inaccessible;[184–187] thus participants are more susceptible to suggestions, tips and rumors from others. In financial systems,

institutions are controlled by individuals; therefore, the interaction between institutions occur essentially among the individuals in them. This means, similar to participants in a conventional social setting, the individuals who manage financial institutions are themselves susceptible to the diffusion of market sentiments (i.e., beliefs, news, opinions etc) from one to the other. Given the inherent social underpinnings of financial systems, we can capture and investigate — via social network applications — aspects of financial systems that are not necessarily captured by conventional economic methods and models.[188]

Outside of the relationship between individuals that control financial institutions, a more conventional approach to modeling financial relationships is via graphical representation in which nodes are connected by link (or edges) that recognize the dependency between them. In contrast to face-to-face social networks, such dependencies can connect an institution (e.g. investment funds, commercial bank, central banks etc) to others without regard for geographical proximity. Although geographic proximity may not be applicable in the study of financial networks, it has been shown that, for networks in general, topological distance[107,110,112,117,189] is consequential in how instability spreads in the system. Topological distance quantifies the proximity of a node to others, and it is this measure that allows us to compare nodes in terms of their centrality or network position.[67,190] In social and financial systems, topological distance is measured along the edges formed by the dependencies between the nodes. However, the interpretation of distance is dependent on the nature of relationships; for example, in financial systems, institutions can be connected by payments or commonality in holdings of assets. In the former, the distance from node i and j could be interpreted as the extent of the interconnections that exposes j to counterparty risk from i. For studies on financial systems, a crucial point of concern, therefore, often lies in determining the institution's role in risk transmission while for social networks, one may be interested in enhancing the effectiveness of transmission (e.g. information) or reducing it (e.g. disease).

2.4. Network analysis of social systems

2.4.1. Modeling proximity relations in social networks

Proximity in face-to-face social networks

Thanks to the advanced use of communication technology in social and epidemiological research, our understanding of the link between spatial proximity and transmissibility has improved substantially. Several studies support that the transmission of pathogens via respiratory droplets, expelled during social interaction and normal bodily functions, are more likely when individuals are close to each other.[191–195] Early research on proximity networks were based on self reports[192,196] or observations in laboratories[197] that were monitored closely. In recent times, however, the collection of proximity data relies on digital technology[138,198–203] such as Bluetooth, Wi-Fi networks, and Radio Frequency Identification (RFIDs). In fact, this approach has been quite useful in approximating pairwise contact between individuals in different social settings (e.g. conferences, hospitals, households, schools/university and workplaces), with a direct link between individuals signifying that they are with a few metres [b] of each other.[138] This is the most straightforward way of visualizing social relationships because the degree of distance between individuals tend to reflect the closeness of their relationship.[203] In other words, smaller physical distance typically indicates greater familiarity, while for persons with whom we are unfamiliar, interactions tend to occur at larger distances.[203]

Proximity in social communication networks

Social networks are also based on online communities and digital communication, with interactions occurring in a virtual space. Here, direct links between pairs of individuals (e.g. bidirectional wall posts on Facebook and Twitter,[204] mobile calls,[139,205–208] email exchange[209]) represent existing relationships, despite the absence of physical proximity. Although the physical distance between individuals are not featured in this type of social tie, individuals can be influenced nonetheless via non-physical contact. In fact, an early proposition of an existing relationship between physical disorder (e.g. vacant buildings, abandoned vehicles, broken windows etc.) and crime is the broken

[b] For data collected using Radio Frequency Identification technology, in addition to being with range, a link only exists if individuals are facing each other.

window theory which explains that visible signs of incivility in neighborhoods can perpetuate disorderly and criminal behavior in others.[210] The widespread use of online communication and virtual communities have, therefore, added a whole new dimension to how we study social systems which, for a long time, was based largely on physical closeness. Due to improvements in tools of social communication, individuals can now establish and maintain friendships at much larger distances. This is important because it means that while individuals remain susceptible to infectious diseases, they are also more exposed than before to the efficient spread of social phenomena; thus having implications ranging from the effectiveness of business advertisement to the possibility of political instability due to the efficient spread of misinformation.

2.4.2. Dynamics in social networks

At the base of social networks are human beings whose engagement with each other can change quickly and frequently on timescales ranging from seconds to several years. When aggregated, these interactions cause the structure of social systems to also change rapidly and regularly. In fact, a host of systems in biology, technology and the social world exhibit this dynamical property.[211–215] While dyadic data allow us to construct social networks based on direct relationships, for any given node, we can gain insight into more complex structures by tracing the indirect ties to the neighbours of its direct neighbours.[216–219] However, without the time dimension of such connections, we remain blind to the dynamic nature of nodes and edges appearing and/or disappearing. The temporal aspects of social networks reflect the reality that individuals, and by extension the edges they form with others, are not always available as agents of transmission. This means that we can observe a rather different outcome when certain nodes and edges are present. This is one application that has motivated studies that investigate the evolution of systems to uncover the dynamical forces at play locally[67,220] and/or globally.[57,58] Other applications include enhancing our ability to predict future evolution, and to explain historical developments and/or the mechanistic understanding of network dynamics.

One of the early studies on the evolution of social networks was by Barabási and Albert who introduced the Barabási-Albert (BA) model to explain the scale-free property, seen in many real

systems,[66–68,98] and network evolution via two fundamental mechanisms: i) network expansion and ii) preferential attachment. They reason that, networks expand because new nodes join the system via links to existing nodes, and new nodes attach themselves with high probability to those that are already well connected .[67] The role of preferential attachment in the evolution of real systems are featured heavily in the literature.[221–226] However, most of these studies either assume time independence or downplay the time dependence when measuring attachment kernel.[220] To explore the validity of the time independent assumption in the rules governing how growing networks evolve, and to highlight the risk of assuming that a node's attractiveness is determined by its degree, a simple variation of the BA model (ie. k-2 model) was employed. In the k-2 model, new nodes attach to pre-existing ones in proportion to the total nodes within two steps of the target node[220] rather than proportionally to total direct neighbors. Using citation networks, Falkenberg et al. show that, although the time independent assumption is justified over short timescales, attachment kernels over longer timescales were found to be time dependent.[220] Bazzi et al. explored an alternative way to capture the relationship between network structure and temporality by considering a generative model that employs a multilayer system with interlayer dependencies. In essence, their method incorporates a *memory effect* by establishing dependency between current and subsequent layers in time.[227] By doing this, they highlighted that connectivity patterns may be related to the state of the network in another period.

The dynamic hidden-variable model has also been proposed as a more general framework for understanding network growth. In this model, each node has at a given time, a node-intrinsic property (i.e. *fitness*) which is modeled as a hidden variable. A node's fitness reflects its tendency to attract or compete for edges.[221,228] In reality, some individuals may be more skilled in socializing than others, which can have an impact on how quickly that individual makes and maintains connections with others. On the contrary, another individual may not be as sociable and, therefore, struggles with forming similar relationships. Node fitness captures such differences among persons in a social network context who are assumed to be competing for edges. Unlike a preferential attachment model in which the most connected are the most attractive, in fitness models, fitter nodes succeed those that are not as fit. The dynamic-hidden variable model has been employed in empirical systems to

understand the global dynamics of social networks.[108,229–231] Originally, the fitness model makes no distinction between total active nodes and the population of nodes in the network because it is assumed that the size of population is sufficiently large; thus making all nodes active.[55] However, if this assumption breaks down then, some nodes may exist at a given time but not active[55] which then leads to variations in population size that will ultimately impact the rate of edge formation as total active nodes increases. Recent investigations examined how the number of active nodes N and the number of edges M — as primary components with implication on global network properties — evolve over time.[57,58] In their baseline models (based on the dynamic hidden-variable model), node fitness was assumed to be uniformly distributed on the interval $[0, 1]$ because of the relative simplicity in obtaining an analytical solution.[57,58] They found that the scaling relationship $M \propto N^{\gamma}$ can have a constant exponent ($1 \leq \gamma \leq 2$), conventionally known as the *densification power law*[59,232,233] or an exponent γ that is changing with N. Both patterns emerge differently on a log-log plot of total edges against total active nodes: for a constant γ, the number of edges grows with the number of active nodes in a linear pattern; while, an increasing γ manifests as an accelerating growth in total edges.[57,58] The accelerating growth pattern emerges because of changing overall activity of nodes in the network while the conventional scaling behaviour is due to fluctuations in network population. In some networks, they observed a 'mixed-scaling' behaviour in which both patterns appear simultaneously, and the dominance of each mechanism behind the different scaling patterns was found to be switching in time.[58]

2.4.3. Contagion in social networks

Models of dynamical processes that propagate in social networks belong to one of two broad categories, either a simple[143,163,170,172,234–236] or complex[237,238] mechanism[122,239,240] (Table 2.1). The primary difference between them is that a transmission event occurs in complex contagion if there are multiple exposures. For simple contagion, however, nodes get adopted (or infected) with a fixed probability (i.e. the probability is independent of the number of exposures) once they are exposed.[240,241] Compartmental epidemic models, which categorize individuals based on their health status, belong to the class of simple contagion. Examples of these epidemic models include: susceptible-infected (SI),[143,163,170,234,242] susceptible-infected-susceptible (SIS),[234,242] susceptible-

Table 2.1: Spreading processes on social networks

Model	Class of contagion	Phenomenon	Interdependency level of contacts
Compartmental/Epidemiological model[46,49,143,172,234,252–255]	Simple	Infectious diseases	None
Generalized contagion model[42,245,256]	Complex	Infectious diseases with memory or requiring multiple exposure	Intermediate and/or variable
Threshold model[43,128,237,238,244,257–261]	Complex	Fad, rumors, influence, behavior etc.	Strong

infected-recovered (SIR).[143,234] In contrast, models of complex contagion (e.g. linear threshold model,[243–245] voter model,[246,247] generalized epidemic model[248–250]) are often used to study the propagation of behavior, ideas, and new technologies in a social context because the content entailed in these phenomena is expected to affect the nature of spreading since an individual needs to be exposed multiple times (i.e. *social reinforcement*) before adopting it.[43,122] A threshold model is one of the simplest types of complex contagion models[122] used to capture the social reinforcement mechanism at play in humans as they become exposed to opinions, ideas and knowledge which they may adopt.[238,251] In a threshold model for example, a node changes state (e.g. non-adopter to adopter) if the number[43,243,244] (or fraction[43]) of adopted neighbors exceeds a particular threshold.

2.4.4. Linear threshold model for contagion in temporal social networks

Model of social contagion are constructed with the main objective of understanding the emergence of social influence i.e. how susceptible individuals are encouraged to become an *adopter* via influence from their neighbours. Other non-social processes are also studied on social networks such as epidemic spreading for which rely generally on the use of conventional compartmental models discussed earlier (see Section 2.4.3). With conventional models of social contagion comparing social processes to that of epidemics, the similarity in certain hypotheses and assumptions across the two fields of study is quite understandable. A general assumption in these models is that the probability of an individual going from susceptible to converted grows monotonically with the number of converted neighbours.[243–245,262]

Consider an undirected network $\mathcal{G}$ with nodes representing individuals in a social network, each becoming active if it adopts an opinion and inactive otherwise; hence a node is in one of two binary states denoted by 1 and 0, respectively. An edge transmits influence between nodes j and i. For an individual i to move to an adopted state, the fraction of its neighbours must exceed its individual threshold.[243] Duncan J. Watts generalized this idea to static random networks[94] as a first approximation of the nature of cascades in real systems. In Watts classic linear threshold model on a static network, node i has a threshold $0 \leq \phi \leq 1$ its state s_i changes according to the adoption condition:

$$s_i = \begin{cases} 1 & \text{if } \frac{\sum_{j \in \mathcal{N}} s_j}{k} \geq \phi_i \\ 0 & \text{otherwise} \end{cases}, \tag{2.3}$$

meaning that i becomes active ($s_i = 1$) if a certain fraction of its neighbors are active and it remains inactive ($s_i = 0$) otherwise. A *non-adopter*[263] is faced with a binary decision with externalities[262] because it has to choose one of two alternative actions and its decision is assumed to depend explicitly on that of its neighbours. In reality, an individual may have insufficient information to make a decision or ability to evaluate the available data to make an informed decision. Of primary concern were the expected size of global cascades and the probability of such global events occurring given relatively small exogenous shocks. The main finding in this early study is that in random networks, even an infinitesimal fraction of initial adopters (seed) can lead to *global cascades* i.e., a large fraction of non-adopters are influenced. Furthermore, global cascades are relatively rare, and shocks that precipitate large cascades are often similar to those that fail to lead to global cascades.

The original version of Watts model provides a useful theoretical basis for further investigation into social influence which can be extended to treat more realistic features of human interaction. Such features include heterogeneous individual activity level[139,264–267] and the possibility of contact timings in a social setting displaying strong correlations.[43,128] Extending the classic linear threshold model to temporal social networks is, therefore, natural and this enables an investigation into the effect of certain dynamic aspects of human interaction on social contagion. In this section, we explain how the classic threshold model is adapted to empirical temporal networks in which certain

effects decline in time. While Watts considered a static network of individuals who are constantly exposed to the influence of others; in real social systems, individuals are influenced more by current exposure than older exposure because one may forget communications from the past or they may even grow irrelevant over time. Therefore, it is necessary to decide how to weight the lifetime of the interactions of an individuals.

Karimi and Holme[43] considered down-weighing the influence emanating from older contacts by integrating the contacts over a time window. In other words, they ordered the events chronologically and defined the period of influence over which an individual is susceptible to influence as a sliding window i.e., $[t-\theta,\ t)$ where θ is the distance into the past and the current time is denoted by t. Interactions outside of the current window $[t-\theta,\ t)$ are ignored and considered to have no effect on current outcomes. They simulated the spread of influence on six empirical networks: self-reported sexual contacts in a Brazilian online forum,[160] email exchange at a university,[268] face-to-face contact at a conference,[255] contacts on a Swedish dating site,[156] contact on Swedish forum for rating and discussing films.[269]

Fractional-threshold model

At a given point in time, a non-adopter converts based on the fraction f_i of its neighbors that are already adopters and this fraction is computed as:

$$f_i = \frac{\sum_{j \in c_i} s_j}{c_i}, \tag{2.4}$$

where s_j is binary (i.e., 1 for adopted and 0 otherwise) and denotes the state of i's neighbors while c_i represents number of nodes connected to i (or total neighbors). The state, s_i, of the non-adopted node is determined by the adoption condition defined as:

$$s_i = \begin{cases} 1 & \text{if } \ f_i \geq \phi_i \\ 0 & \text{otherwise.} \end{cases}, \tag{2.5}$$

where i becomes an adopter ($s_i = 1$) if the fraction of adopted neighbors exceeds a given fraction ϕ (i.e., the *fractional-threshold*). At the beginning of the process, the population of individuals are all in a non-adopted state (denoted by 0) with the exception of a randomly selected node which is

in an adopted state (denoted by 1). To remain consistent with Watts' model, Karimi and Holme[43] asserted the following specifications: i) fixed length of each time window of influence, ii) newly adopted nodes remain in state 1 for the remainder of the process, iii) cascade size Ω is the fraction of adopters in the entire population at the end of the process. However, a key difference exists in how nodes can be influenced by contacts. In the fractional-threshold model (Eq. 2.5), c_i is the number of neighbors associated with a node i for a given time window; therefore, c_i varies with each snapshot. Consequently, nodes can only be influenced by contacts within the time-window while contacts outside are irrelevant. In contrast, the static network setup gives relevance to all the contacts of a given node.

By varying the fractional-threshold ϕ for fixed time-windows, Karimi and Holme observe the effects of final cascade size. An increase in ϕ makes it is more difficult for a node to become an adopter. While the result by Watts'[244] showed that a cascade cannot be triggered for larger threshold values by a single seed, Karimi and Holme showed that including time-windows creates the possibility of a cascade to propagate for larger threshold values ϕ: in small time windows, total contacts can be small which makes it easier to attain the threshold value. In fact, for particularly small time windows in which an individual has no more than a single contact, the model is analogous to a simple spreading mechanism with a transmission event occurring with certainty if a non-adopter's only contact is with an adopter. Conversely for large enough time windows (θ), cascades are practically non-existent because an individual will have more contacts; hence a greater fraction of those contacts are necessary to attain the threshold value such that $f_i \geq \phi$ (i.e. effectively increasing the fractional-threshold ϕ). In such instances, the result resembles that of the original static network with no cascades for large thresholds.

Another key finding is that, in some temporal networks, burstiness can increase cascades when considering a threshold model. This result contrasts with findings based on disease-spreading models that showed that bursty activity slows the pace of propagation.[46] In one of the six data sets that Karimi and Holme analyzed, cascade size was higher [c] in the network that maintained the original

[c]The assumption is that a larger cascade size implied faster pace of propagation.

temporal features compared with its counterpart that was obtained by shuffling the order of contacts; thus removing burstiness. This was the conference data set for which activities are scheduled; hence, burstiness is orchestrated unlike the other data sets in which burstiness appeared more organically. The coordination of activities at conferences enables an individual to be in contact with multiple persons during a single unit of time (e.g. during lunch or coffee break). The fraction of contacts that are adopted f_i will, therefore, vary over time and this can facilitate larger cascades, particularly when the number of state 1 nodes in the system is already high.

Absolute-threshold model

Karimi and Holme introduced the absolute-threshold model as an alternative to the fractional-threshold model. For the absolute-threshold model, the number of interactions that individuals have with state 1 neighbors, defined as F_i, is the basis on which node i changes from non-adopted to adopted. The adoption condition is, therefore, simply expressed as:

$$s_i = \begin{cases} 1 & \text{if } F_i \geq \Phi_i \\ 0 & \text{otherwise.} \end{cases}, \tag{2.6}$$

which means that if the absolute number of converted neighbors F_i exceeds an absolute-threshold value Φ, then i changes to state 1, but remains as a non-adopter otherwise. The results from the absolute-threshold model indicate that the size of cascade increases with the time window size whereas the opposite effect was observed in the fractional-threshold model. In the absolute-threshold model, cascade size increases with a larger time windows because a longer window allows an individual to meet more neighbors. In the fractional-threshold model, an expanded time window lowers the fraction of neighbors that are converted via the denominator in Eq. (2.4); however, this is not the case in the absolute-threshold model. Furthermore, temporal correlations in the data sets (excluding the conference data) constrained cascade size in fractional-threshold model relative to the null models that destroyed certain temporal features. However, in the absolute-threshold model, temporal correlations enhance individuals' chances of meeting adopters; hence cascade sizes were larger than in networks with reshuffled contacts. Recall that in the fractional-threshold model, only the conference data set exhibited larger cascade sizes relative to the null models; thus highlighting

that strong temporal correlations in contact patterns can amplify spread.

2.4.5. Systemic importance in social networks

Investigations into the specific contribution of nodes and edges,[80,270,271] as processes unfold on networks, provide meaningful insights into how we can manipulate propagation based on our specific objective i.e., whether to reduce or proliferate spread. In social networks, some individuals are known to be *superspreaders* — those who are vastly more effective in influence maximization than others in the network; conversely, those who mitigate spread often constitute a completely different set known as *superblockers*.[80] Many studies on the spread of diseases use contact rates of hosts as a proxy for individual infectiousness,[272–274] and their findings support the existence of a group of high-risk nodes[273] and that 20% of cases are usually responsible for 80% of transmissions.[272,273] With the assertion that superspreading is a characteristic feature of disease propagation,[275] and an urgent need to control spread among human population, some natural questions arise: How effective is targeted vaccination in curtailing epidemics? How can intervention strategies be better formulated to manage the system as a whole?

Early studies of superspreaders include the work of Kempe et al.[79] in which the influence maximizing problem was presented as computationally difficult. Nonetheless, they introduce a greedy algorithm that yields a sub-optimal solution for a broad class of sub-modular dynamics. Subsequent works have contributed improvements with the use of tools from statistical physics.[276,277] Radicchi and Castellano[80] use an independent cascade model to find optimal *multiple* spreaders which they defined as the node set that maximizes spreading when the propagation process is initiated by all the nodes at the same time. Conversely, other studies focus on finding optimal *single* spreaders[278,279] which constitute the nodes that are most capable of maximizing spread when the process is initiated in one node at a time. Radicchi and Castellano highlight that both are different problems in that, good single influencers often share a considerable portion of the circle of influence. Initiating an outbreak in these nodes simultaneously, may lead to a final cascade size that is only vaguely larger than the sizes when each influencer is considered separately. From a regulatory perspective, optimal multiple spreaders is analogous to considering the set of banks when combined, pose a

systemic risk to the entire financial network. In fact central banks perform stress-testing by using a default cascade approach as a straightforward way to rank banks according to their systemic importance. The objective is to measure the capacity of individual banks to generate contagious effects on the system.[33] Essentially, they compute the size of the cascade of defaults when the bank in consideration is set to be the initial defaulter.[41,280] In the following section, we consider alternative approaches.

2.5. Network analysis of financial systems

2.5.1. Modeling proximity relations in financial networks

The tools of network science have proven rather advantageous in the study of financial systems evidenced by the broad range of studies that highlight how various aspects of the system can be easily represented, whether as an individual network layer or as multiple layers of interacting nodes. Here, we consider two broad types of relations categorized as *direct exposures* to lending and funding risks,[281] and *indirect exposures* via common exposures and spillovers.[281–283]

Financial network of liabilities and claims

We will provide a brief overview of a few basic concepts on the way banks[d] behave and our reliance on a basic accounting identity to assess their health (Eq. 2.7). A primary objective of banks is to maintain solvency — essentially a measure of 'good-standing' which, to some extent, can be determined from their balance sheet (Fig. 2.3). In general, the balance sheet is comprised of different assets and the quantity of each being held by the bank. Each bank makes its own decisions on the amount or type of assets, and liabilities in its portfolio; hence there is an inherent heterogeneity among banks simply on the basis of the detailed compositions of their respective balance sheets. In good times, banks are solvent i.e. having an adequate amount of assets to cover outstanding liabilities[27,34,284] and ideally, the different types of assets are funded by the appropriate type of liabilities. Many studies on solvency contagion in interbank networks consider a stylised balance

[d]Financial systems consist of banks and non-banks; however, for the sake of simplicity, we will refer broadly to institutions in the financial system whose actions affect others as *banks*.

sheet from which the following accounting identity is taken:

$$C = (A^{\mathrm{EX}} + A^{\mathrm{IB})} - (D + L^{\mathrm{EX}} + L^{\mathrm{IB}}) \tag{2.7}$$
$$C = A^{\mathrm{Total}} - L^{\mathrm{Total}}.$$

Here, a bank's capital, C is the difference between total assets (A^{Total}) and total liabilities (L^{Total}), with $C > 0$ signifying that the bank is solvent. Total assets is the sum of external assets (A^{EX}) and interbank assets (A^{IB}) while total liabilities is the sum of deposits (D), external liabilities (L^{EX}) and interbank liabilities (L^{IB}).

Interbank credit networks represent an early application of certain elements of social network analysis to financial systems. In interbank networks, banks are linked by credit contracts in which borrowers (debtors) have outstanding obligations (loans) that become payable with interest, to the respective lenders (creditors) at a certain date (maturity date). In addition to being a benchmark for short-term lending rates and a channel for monetary policy transmission, the interbank market is a source of unsecured funding that enables banks to address liquidity shortages in relation to reserve requirements stipulated by central banks. Other funding sources include repurchasing agreements that are essentially collateralized [e] loans on which interest is paid at maturity. Some studies model bilateral relationships based on unsecured[20] interbank contracts and others including Battiston et al. and Roukny et al. consider secured interbank contracts.[30,285] In the literature on financial networks, these bilateral relationships between banks are somewhat analogous to that of: sender and receiver in digital communication (e.g. online,[286] mobile,[287,288] email[59,289–291] etc.) or source (contact initiator) and target in face-to-face social networks (e.g., hospital, school, workplace etc.). Following the lending flows from one bank to the next, we recognize a sequence of balance sheets that are essentially interlocked and reflects a weighted interdependence — even in the absence of a direct connection between a given bank pair (Fig. 2.3).

The confidential nature of interbank data makes it accessible in large part only to supervisory and other authorized institutions; hence, several empirical analyses on interbank networks have been conducted based on national banking systems including Austria,[107] Brazil,[292,293] Belgium,[294]

[e] Banks are required to post a collateral prior to receiving a loan.

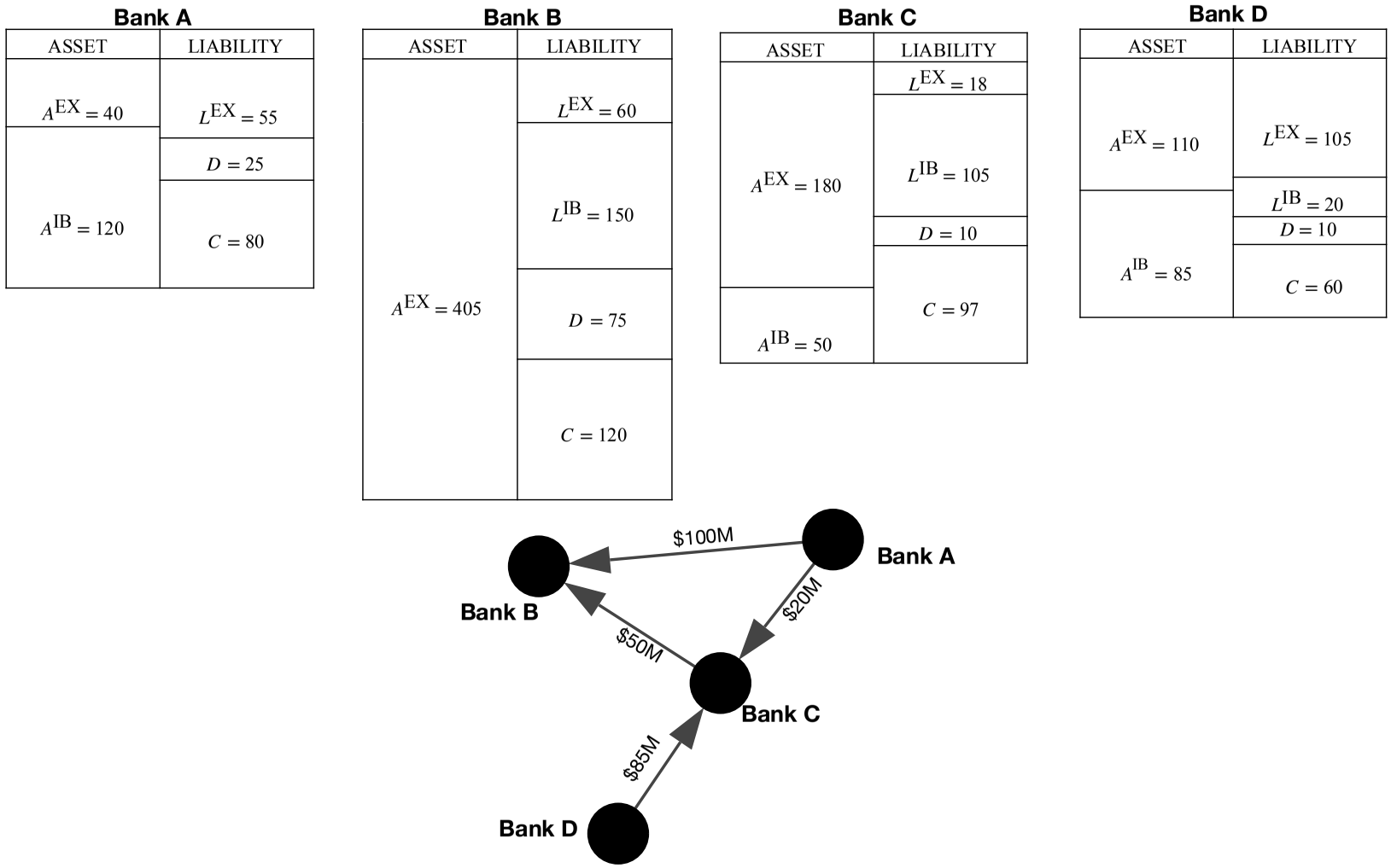

Figure 2.3: Interconnected balance sheet of four banks. In the top panel, the stylised balance sheet is comprised of external assets (A^{EX}), interbank assets (A^{IB}), deposits (D), external liabilities (L^{EX}) and interbank liabilities (L^{IB}). Bank capital (C) is the difference between total assets ($A^{\text{EX}} + A^{\text{IB}}$) and total liabilities ($D + L^{\text{EX}} + L^{\text{IB}}$). In the lower panel, outgoing edges represent a loan going from a lender to a borrower e.g. Bank A lends \$100 million to Bank B. The interconnections between banks occur because the direct neighbour of a focal bank has other neighbours that are not necessarily connected to the focal bank; thus, forming a chain of interdependencies.

Table 2.2: Empirical studies simulating contagious failures in banking networks. While interbank bilateral transactions are directly observed from e-MID or from some large value exposures outlined in financial authority's supervisory reports (SR), they are often estimated from aggregate level data provided in banks' balance sheets (BS). Bilateral interbank loans can also be extracted from settlements and transfers between banks (settlement data) by using a search algorithm that match the start of a transactions with a follow-up inclusive of interest payments in the next day.

Paper	Data period	Data type	Method	Resolution	Data source
Sheldon and Maurer[21]	1987–1995	BS	Maximum entropy	Yearly	Swiss Nat. Bank
Furfine[37]	Feb 1998–Mar 1998	Settlement data	Search algorithms	Daily	FedWire
Upper and Worms[300]	Dec 1998	BS	Maximum entropy	Yearly	Bundesbank
Wells[22]	Oct 2000–Dec 2000	BS/SR	Maximum entropy	Quarterly	Bank of England
Amundsen and Arnt[18]	Jan 2004	Settlement data	Search algorithm	Daily	Denmark Nat. Bank
Lublóy[19]	2003 (50 days)	SR	n.a.	Daily	Bank of Hungary
Elsinger et al.[39]	Sep 2002	BS	Maximum entropy	Monthly	Austrian Central Bank
Elsinger et al.[40]	Oct 2003–Dec 2003	BS	Maximum entropy	Quarterly	Bank of England
Van Lelyveld[23]	Dec 2002	BS/SR	Maximum entropy/n.a.	Yearly	De Nederlandsche Bank
Degryse and Nguyen[294]	Dec 1993–Dec 2002	BS/SR.	Maximum entropy/n.a.	Bi-Annually	Bank of Belgium
Mistrulli[38]	Jan 1989–Dec 2003	SR	n.a.	Quarterly	Bank of Italy
Imakubo and Soejima[24]	Dec 1997–Dec 2005	Settlement data	Search algorithm	Monthly	Bank of Japan-NET
Karimi and Raddant[20]	2006 and 2011	Interbank transaction	n.a.	Daily	e-MID

Colombia,[109] Germany,[295] Italy,[108,111,296] Japan,[24] Mexico,[297] Switzerland[298] and the United States of America[110,112,299] (Table 2.2). The findings in these studies that are based on bilateral relationships in financial systems, highlight some stylised facts about: the sparsity, heavy-tailed degree distributions, high-clustering, short average path length and disassortativity (i.e., the tendency for large banks to be linked to small banks). Many of these early works investigate the underlying topology, with some finding a core-periphery structure in which a subset of tightly linked banks (referred to as the *core*) exists along with a loosely connected subset of banks (referred to as the *periphery*) that is also linked to the core.

In addition to the actual relationships in the interbank market, the infrastructure surrounding transaction settlement have also been noted as a source of complexity in the system. Interbank loans are often cleared and settled bilaterally, and this may lead to a proliferation of redundant contracts that are overlapping.[301] In contrast to a central clearing system that performs a mutilateral netting of exposures, bilateral settlement of contracts can exacerbate counterparty risk (i.e., the risk that one party defaults on its obligation to the other); thus increasing the complexity and opacity of interconnections in financial systems.[301] In the aftermath of the global financial crisis, about one-fifth of over-the-counter (OTC) derivative contracts were being processed via central clearing counterparties (CCPs). Ten years on, about two-thirds[302] of these contracts were being cleared by CCPs due partly to their relative resilience during the Lehman crisis as bilateral markets dried up.[303] Given the rapid rise in usage, more research focused on the possible effects of central clearing on counterparty risk in interbank system; here we highlight two notable studies.[304,305] First, Duffie and Zhu[304] showed that average exposure to counterparty default can increase when one asset class adopts central clearing because of fewer netting opportunities across counterparties. Garrat and Zimmerman[305] extended this work by considering more realistic financial network structure, specifically large scale-free networks, to find that CCP will almost always increase expected net counterparty exposure in such systems.

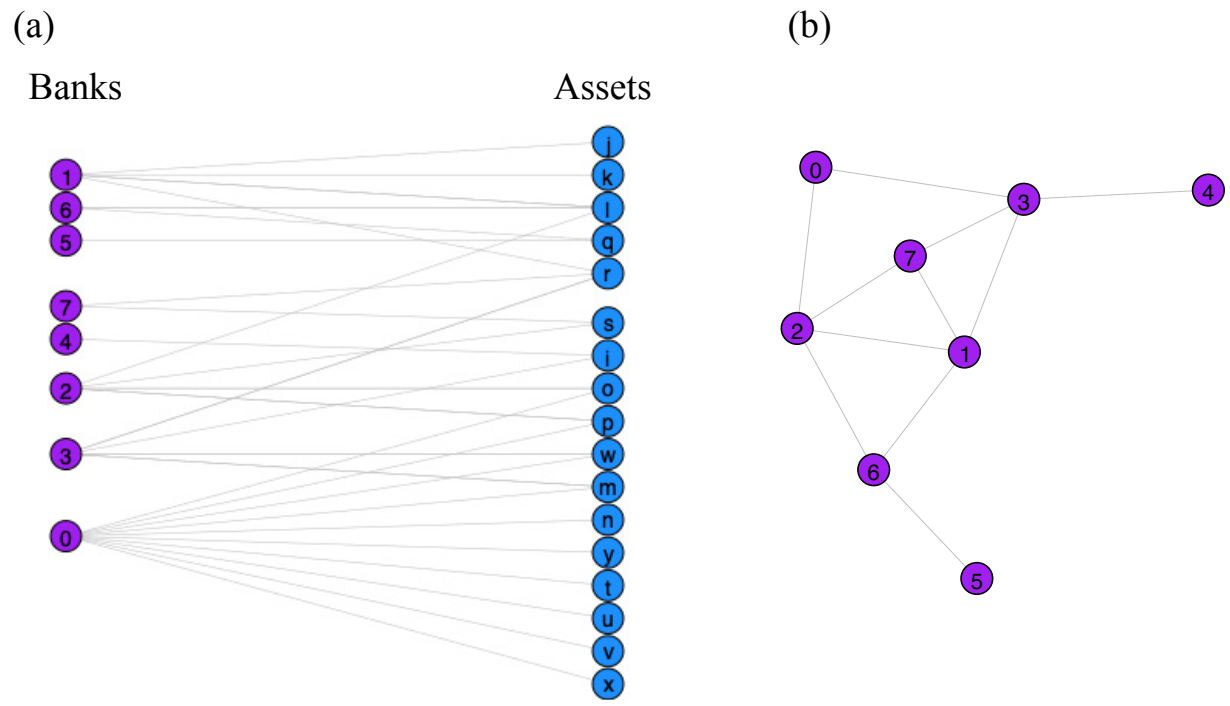

Figure 2.4: Overlapping portfolios among banks due to investing in common assets. (a) Bipartite graph of banks (purple nodes) that are linked only to the assets (blue nodes) in their investment portfolios. Multiple edges to a single asset means multiple banks have that asset in common i.e., *asset commonality*. (b) One-mode projection of the bipartite network in (a). Links exist between banks that have assets in common (i.e, common exposure to assets).

Financial network of overlapping asset portfolios and other spillovers

Banks invest surplus funds to obtain positive returns on their purchase of assets. At the same time, asset purchasing is also a means of risk diversification, with each bank's portfolio usually reflecting its appetite for risk. An overlap exists between two portfolios when banks have one or more assets in common, also referred to as *common asset holding*. In fact, many banks tend to formulate strategies which lead them to share ownership of similar assets due to various factors including, shared geography, risk appetite etc. Commonality in exposure via shared investment or ownership of assets[306] is, therefore, an indirect source of interconnectedness. It has become more evident that the ownership structure of assets is a possible source of non-fundamental risk such that it can be used to forecast fluctuations in stock price that are unrelated to fundamentals.[307,308] Furthermore, institutions with strong commonalities in investments can trigger fire sales (i.e., the

disposal of assets at heavily discounted prices) when the market encounters unexpected financial distress, often resulting in losses of a magnitude that exceeds those due to direct exposures.[39]

To capture this indirect relationship among banks, a bipartite network representation is utilized in which banks are presented as one node type and assets as another (Fig. 2.4). Generally, links between the banks are established indirectly via common exposures to asset classes (e.g. corporate loans or commercial real estate loans), and the link weights are approximated based on bank exposures.[309,310] Huang et al.[72] employ this approach in a case study of US commercial banks during the subprime crisis. The ownership fraction $s_{i,m}$ held by a bank i of an asset m is defined as the amount being held by bank i (i.e. $B_{i,m}$) as a fraction of m's total market value A_m. The proportion of m in bank i's portfolio may also be computed as $w_{i,m} = B_{i,m}/B_i$ i.e. the amount of m held by i as a fraction of i's overall asset portfolio. Another study by Gualdi et al.[311] assessed the statistical significance of an overlap between heterogeneously diversified portfolios based on similar patterns of investment. Based on this method, they constructed a validated network of financial institutions where links indicate *significant* overlap; hence, potential channels for contagion. They implemented this method on a historical database of institutional holdings for the period 1999—2013. They

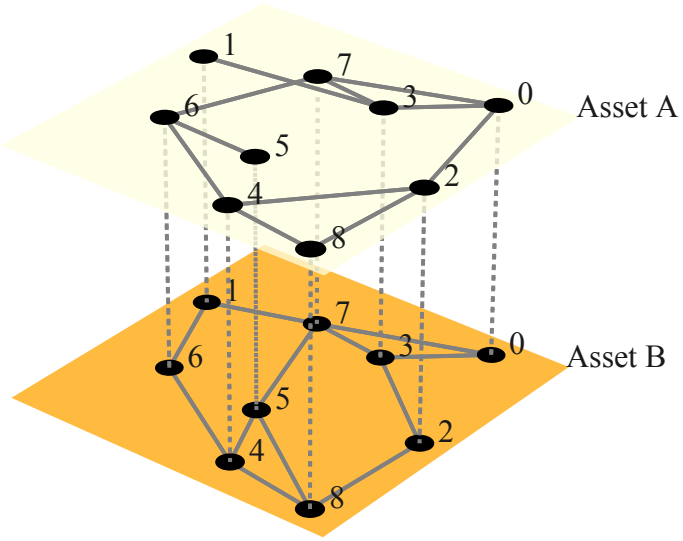

Figure 2.5: Schematic of multiple relationships between banks in different segments of a financial network. Individual layers differentiate markets for a particular type of asset and nodes represent a single bank that is acting in a particular role given a layer.

developed an algorithm which they could use to identify portfolios that amplify market trends, thus highlighting the institutions likely to experience significant losses or gains. Many other studies have also relied on a bipartite network model[312–316] which essentially provide insight into how well-balanced portfolios, in relation to other banks, can enhance the stability of the bank itself as well as the banking system as a whole.

Other indirect financial relationships can also emerge in a far more complex manner, particularly when the system is interconnected through different categories of interactions. In other words, banks interact across the various segments of the financial systems, and how they connect with other banks may be dependent on the specific segment. To elucidate the point, we draw an analogy to social networks. Our daily social interactions are multi-relational in nature, which makes it more appropriate to model them as a multi-layer network[317] if we are truly interested in the different kinds of engagements between individuals (e.g. friendship, co-worker relationship, cultural group membership etc). The types of engagement can be on the basis of relationship, activity or category, each of which can be represented as a layer. In the respective layers, the connections between nodes may differ; hence a node may not have the same neighbors given a layer that is associated with an activity, relationship type or category. Similar to social systems, banks interact and/or connect in a multi-relational financial system i.e., across different layers often in different capacities, and this engenders interdependency and inter-connectivity between otherwise disparate layers.[318,319] Layers can be differentiated in the financial system on the basis of seniority levels,[320,321] maturity,[322] asset class[323] (Fig. 2.5). Therefore, modeling financial relationship as multi-layer systems has the advantage of defining the bank-bank interaction and parallel functioning of the systems holistically and realistically.[317] A few studies[33,109,117,118,297,324–326] in the financial network literature utilize the multi-layer approach to show that some important crisis amplification effects can emerge from multi-relational linkages, and most times these effects cannot be detected or understood when restricting attention to a single layer.

2.5.2. Dynamics in banking networks

Many studies that consider the temporal aspects of financial systems have focused on understanding the dynamic structures of interbank networks.[55,113,327–329] To explore dynamical structural properties, it is essential to have access to the data on time of activity; however, such details are not always available. Based on the bilateral transaction data from e-MID, some important properties have been uncovered about the Italian interbank networks at a daily resolution. One study employed a stochastic block model to investigate which two-block organization characterized the structure of the e-MID interbank market for 2010–2014.[327,328] Their findings reveal that for most of the period, it was more likely for the network structure to be bipartite or a single-block structure. In fact, the least likely structure was a core-periphery while a modular structure was observed only a few times. An increasing bipartivity was also observed in the daily networks during 2000–2015 which was encouraged by a concurrent decline in the number of banks and edges on the daily scale,[55,327] and a strategic shift from borrower to lender by a few small banks.[327] The dynamical activity patterns that characterize the daily evolution of the e-MID interbank market are similar to that of social networks. In particular, transaction duration [f] was found to follow a power-law distribution, while the distribution interval time displayed a long-tailed pattern.[55,330] Raddant also showed daily patterns in trading activity for data between 1999 and 2010. He found that strong peaks emerged at 9:00 a.m. and 3:00 p.m. along with a relatively smaller peak at 12:30 p.m.[331] His observations were inline with previous work by Iori et al.,[111] where the daily trading patterns reflected office hours and the consistent in- and outflow of liquidity as trades are settled from the day before.

2.5.3. Contagion in financial systems

Origination of complexity in financial systems

The commoditization of financial risk has made it increasingly possible to redistribute it throughout financial markets to those (including banks) with the ability to bear it, and in exchange for higher yields. Put simply, restructuring risk by packaging, slicing and re-bundling it for sale has granted financial market participants access to new exchangeable instruments. Although the reallocation of

[f] Defined as the number of consecutive business days on which a lender and a borrower performs at least one transaction.

risk among participants presents the benefit of reducing the risk-obligation on any one participant, it also expands the chain of interconnected banks, exposing them to any repercussions from a default.[27,29,332] Based on this singular case, it is evident that financial interconnections can provide mutual insurance against risk; however, because each bank exists and operates within a network of other banks, initially localized distress can propagate to the rest of the system.[35,91,333–336] The extent of interconnectedness in financial systems makes it possible that even bad news of a moderate degree[27,337–339] can tip the system into a state of instability due to sell-offs as discussed in Section 2.5.1 combined with other reactions by banks. It should be noted that an added layer of complexity emanates from the responses of individual banks in distress situations. Despite history suggesting it is unlikely that banks will be passive during times of distress, much of the existing literature assume that banks are passive during these times. In reality, when banks have information about threats to their viability, they may strategically position themselves to improve their chances of a bailout or to acquire market share at the expense of their competitors.[340] A few studies considered bank behaviour during times of distress by incorporating responses such as liquidity hoarding by those that decline to roll over interbank loans from fear of counterparty risk[340] or those banks that shorten interbank loan duration.[341] Others also considered the behaviour of banks after distress where they may want to re-establish connections previously broken.[340]

In the lead up to the 2008 global financial crisis, banks grew in size and became increasingly interconnected at various levels within the system;[91] this engendered greater complexity as optimizing banks adapted to their environment in order to remain competitive. Complexity in financial systems refers to the increasing challenge to trace the source and location of claims and essentially risk;[91] naturally, as more banks become unable to trace risk, this can give rise to system-wide uncertainty. In social networks, complexity is due partly to the diversity of individuals and the heterogeneous responses that can be observed from exposing each individual to the same stimulus. We use another analogy in social networks where a recent study investigated the network effect among individuals given uncertainty about a disaster.[342] They found that individuals in a network setting are less inclined to make independent decisions than those who are isolated (i.e., no network effect).[342] Therefore, network effect can result in individual strategies being more alike than dissimilar in some

Table 2.3: Main channels of contagion in financial systems

Channel	Type	Source	Relationship
Solvency contagion[27,34,35,39,40,280,345]	Direct	Weak equity: low market asset value vs. debt	Interlocked balance sheets via loans, repos, derivatives etc.
Funding liquidity contagion[26,36,298,346–348]	Direct	Weak liquid reserves vs. current liabilities	Interlocked balance sheets via loans, repos, derivatives etc.
Asset fire sales[310–314,349–354]	Indirect	Mark-to-market losses on overlapping portfolios	Common assets or overlapping portfolios

systems. It is this type of dynamical complexity and absence of diversity that Haldane[91] suggests engendered the fragility that surrounded the 2008 global financial crisis.

Against this background, studies on financial systems address some crucial points in the policy discussion. First, the need for an adequate framework to identify institutions with considerable implications on the stability of the system i.e., "too-big-to-fail" and/or "too-interconnected-to-fail".[104,285] Second, the extent of data, to be disclosed by banks, that regulators deem sufficient to properly assess systemic risk.[343] Third, the appropriate actions to be undertaken by regulators given multiple equilibria. Multiple equilibria for bank values exist if the solvency of one depends on its predecessor in a cycle of sufficiently interconnected banks,[285,344] and the emergence of such a phenomenon tends to be driven by uncertainty which leads banks to lose trust in counterparties.[136] Based on conventional tools of finance and economics, it may not be immediately clear how to tackle these systemic challenges. In this section we employ the lessons from social network analysis about the effects of complexity and diversity on stability to gain insight into the dynamics of financial contagion.

Solvency contagion due to interbank linkages

Section 2.5.1 explains that in network models, a bank's solvency is determined from its capital level, if negative, the bank is assumed to be insolvent (Eq. 2.7). A bank's capital level is negatively affected when the current market price of an asset falls as it adjusts in a mark-to-market framework, or when the bank's investments fail.[284,355] From the stylised balance sheet identity in Eq. (2.7), an insolvent bank is no longer able to cover liabilities and in the absence of any intervention (e.g. government bailout), it is expected that the bank will cease operation following the necessary

insolvency proceedings. Solvency contagion is studied extensively in the financial systemic risk literature (Table 2.3) due to some highly influential works that include the pioneering study by Eisenberg and Noe,[34] later followed by Nier et al. who provided early references to techniques in network theory.[35] Since then, the work by Gai and Kapadia,[27] in which they formalized the network model of financial interdependencies based on interbank linkages, forged a new path for studying insolvency cascades in financial systems.

Eisenberg and Noe[34] were among the first to study this decades-old problem of solvency contagion; they found that the structure of financial networks play a consequential role in engendering failure among banks. This observation was consistent with findings about the dynamics of contagious phenomena on social networks.[237,238,251,257,262,356,357] Their model served as a basic characterization of solvency cascades in banking networks based on a stylised balance sheet; it therefore provided a foundation for other works on financial systemic risk.[29,332,358] The Eisenberg and Noe model simulates solvency contagion in a static financial network with banks holding nonnegative amounts of liabilities for each other, and each bank having its own operational cashflow (nonnegative). The operational cashflow and payments that a given bank receives, from its counterparties, have implications for whether the bank will default; this reflects an interdependency of liability repayments. Eisenberg and Noe reasoned that the borrowing counterparty of a given bank makes a full or partial repayment that represents an income to the lending bank; hence, the obligations of all banks should be resolved simultaneously giving due consideration to debt priority and limited liability of equity.[34] This establishes a clearing vector which contains the value of the respective interbank contracts. They proved that a unique clearing vector exists under mild *regularity*[g] condition, and they introduced an algorithm to compute this vector of equilibrium payments (i.e., a self-consistent solution when all payments are settled in the final state). Subsequent works extend the Eisenberg and Noe model to reflect more realistic aspects of real financial systems by including liquidity consideration,[314] cost of default,[359] multi-period payment system,[360] and testing the sensitivity of the original clearing vector to estimation errors.[323]

[g] A network is regular if the risk orbit (i.e., the set of nodes that are accessible from a given node i) has at least a single node with non-zero liabilities.[34]

A simpler model was introduced by Gai and Kapadia[27] in which banks are depicted as nodes and the claims and obligations between them as edges. The original model assumes a random network structure for the interbank system.[27] Investigations into the structure of real interbank systems show that they are, in fact, very different from random networks. First, studies based on the U.S. Fedwire indicate that a few big banks exist that are linked to several small ones, and small banks are themselves unlikely to connect with others of their own size; hence, real interbank networks appear to be disassortative.[361,362] Furthermore, the size of banks has also been shown to be heterogeneous, more specifically, that the ratio of bank capital to total assets was relatively smaller for large banks; thus presenting a threat to stability.[362] Nevertheless, Gai and Kapadia[27] assumed an Erdos-Renyi network consisting of N banks that randomly link to each other as borrower-lender with probability p; such that, the average number of edges is computed as $z = p(N-1)$. The network is directed, therefore, total outgoing (incoming) edges for a given bank i represents the number of loans granted to (taken from) counterparties. Bank i's capital C_i is defined as a fixed fraction of its total assets A_i^{Total}, and i grants only a fraction θ_i of its total assets as interbank loans A_i^{IB}. Bank i distributes total interbank loans evenly among its borrowers such that w_i, the value of a loan to an individual borrower is:

$$\begin{aligned} w_i &= \frac{\theta_i \times A_i^{\text{Total}}}{z_i^{(\text{out})}} \\ &= A_i^{\text{Total}} \times \frac{A_i^{\text{IB}}}{A_i^{\text{Total}}} \times \frac{1}{z_i^{(\text{out})}} \\ &= \frac{A_i^{\text{IB}}}{z_i^{\text{out}}}. \end{aligned} \tag{2.8}$$

Given that total assets $A_i^{\text{Total}} = 1$ and the interbank loan fraction θ_i is common to all banks in the Gai-Kapadia model, Eq. (2.8) implies that i's loan amount to each of its borrowers w_i will vary, among all i's, proportional to $1/z_i^{(out)}$. Note also that given $A_i^{\text{Total}} = 1$, all banks are also assumed to have the same level of capital C_i. Finally, they simulate defaults due to insolvency based on the default condition defined as:

$$\begin{aligned} C_i &\equiv \theta_i A_i^{\text{Total}} + (1-\theta) A_i^{\text{Total}} - L_i^{IB} - D_i < 0 \\ &= A_i^{\text{IB}} + A_i^{\text{EX}} - L_i^{\text{IB}} - D_i < 0. \end{aligned} \tag{2.9}$$

The Gai-Kapadia model of solvency cascades is a direct extension of Watts global cascades model,[244] which is a fundamental theory of information cascades in random social networks. In Watts' model, a non-adopted node with k degrees and m active neighbors, will become an adopter if the fraction of active neighbors m/k exceeds a fractional threshold value $\phi \in [0, 1]$ (see Section 2.4.4). The iteration of cascade dynamics begins with a small fraction ρ_0 of "seeds" (or initially active nodes). Then, at the end of the iteration, we observe the fraction of activated nodes of the entire population. This fraction is formally referred to as the cascade size denoted by ρ. Given the complex nature of bank interactions, it is more appropriate to employ a threshold model (or similar approaches that reflect complex contagion) in which nodes change state only after multiple exposure to a contagious entity. The social relationships modeled by Watts are depicted as undirected edges; however, the primary difference to be observed in modeling interbank financial relationships is the need to represent explicitly the direction in which funds flow (i.e., from lender to borrower while risk flows from borrower to lender). In other words, edge direction makes it clear that claims (i.e. assets) and obligations (i.e. liabilities) affect the balance sheet of a bank differently. Caccioli et al.[135] highlight the parallel between the threshold of Watts social contagion model and that of Gai-Kapadia when the default condition in Eq. (2.9) is rewritten as:

$$
\begin{aligned}
(1-\phi)A_i^{\mathrm{IB}} + A_i^{\mathrm{EX}} - L_i^{\mathrm{IB}} - D_i < 0 \qquad (2.10)\\
A_i^{\mathrm{IB}} - \phi A_i^{\mathrm{IB}} + A_i^{\mathrm{EX}} - L_i^{\mathrm{IB}} - D_i < 0\\
C_i < \phi A_i^{\mathrm{IB}}\\
\frac{C_i}{A_i^{\mathrm{IB}}} < \phi,
\end{aligned}
$$

where ϕ is the fraction of defaulted borrowers of bank i. It is assumed that there is zero recovery on interbank loans to such borrowers — a fairly realistic response during a crisis — because of the high degree of uncertainty around recovery rates and timings which may lead lenders to adopt the worst-case scenario. Note also in Eq. (2.10), the coefficient of A_i^{EX} is 1 which assumes that there is no sale of illiquid external assets by distressed banks.[27,362] Therefore, by varying the coefficient of A_i^{EX}, the model enables an assessment of amplification effects due to asset price interaction. Despite being simple, the model adequately reflects key elements of the complexity of bank relationships;

thus facilitating investigations into several sources of vulnerability simultaneously (e.g., sufficiency of capital buffer,[20,362] degree of network connectivity,[20,362] illiquidity of the market for failed assets, link failure instead of individual node failure[363]). Some studies have also generalized the threshold model to temporal networks[43] and to multiplex networks .[324,364,365]

The results of Gai and Kapadia's work highlight a robust-yet-fragile property of financial networks which means that, although contagion probability may be small, the system can realize catastrophic and widespread effects in the event of a problem. Subsequent studies that are consistent with this model indicate that, global cascades[244,366] can occur for a wide spectrum of network densities and threshold distributions. In the literature, global cascade refers to an event in which a small fraction of initial adopters can convert (from non-adopted to adopted) a finite fraction of an infinite-sized network (i.e, very large cascades).[244,365] We note that, while real networks are investigated quite extensively,[107,110,111] it remains unclear how the system can leverage greater connectivity to benefit from risk-sharing while reducing the adverse effects of creating more pathways to risk exposure.

Funding liquidity contagion due to interbank linkages

Similar to solvency contagion, liquidity shortage that is initially localized in one bank can spread to others across the financial network, causing a systemic liquidity problem when the bank in shortage responds by recalling its loans (or declining to renew loans) to its counterparties. One of the primary functions of the interbank market is to enable banks to manage fluctuations in liquidity by providing access to funding via interbank lending.[296,335,367] Banks use these funds to meet reserve requirements without the need to dispose of their illiquid assets. In the overnight market, borrowed funds are repaid at the beginning of the following business day; however, a bank that is facing liquidity problems may roll over their borrowings. *Funding liquidity problem* occurs when a bank is unable to raise funds at short notice by selling assets or accessing new loans.[26,368,369] Fear, lack of trust or anticipation of challenges in renewing their own short-term borrowings (i.e., rollover risk) may lead other banks to halt lending or renew loans to their own borrowers.[284] These various responses aggregate to engender chains of liquidity shortages as the initial shock reverberates through the system,[340] ultimately lowering funding supply on the interbank market. Furthermore,

Table 2.4: Theoretical studies of funding liquidity contagion in interbank networks.

Paper	Network structure	Edge generating method	No. of banks	Loss distribution	Finding
Lietner[346]	Complete	Exogenous parameters	N	Default cascade	Highly connected network structure as optimal ex-ante: Links provide mutual insurance to banks, despite it being impossible to commit formally to providing private bailouts. Banks are willing to offer bailouts if it prevents the system from breakdown.
Gai et al.[36]	Poisson, Geometric (Fat-tail)	Random	250	Liquidity hoarding	System's fragility amplified by increases complexity and concentration. Different measures can be undertaken (e.g. macroprudential policy, more stringent liquidity regulations, surcharge on banks with systemic importance) to enhance resilience.
Lenzu & Tedeschi[348]	Scale-free	Preferential attachment	150	Default cascades	Scale-free financial networks (with heterogeneity in banks' size) are more vulnerable than financial networks that have a random structure.
Lee[371]	Complete, Disconnected, Circular, Core-periphery	Exogenous parameters: reserve ratio, deposit shares, surplus funds & cross holdings	N	Liquidity shortages	Systemic liquidity shortage is highest in the core-periphery network with deficit money centre. Also, the more ill-matched [h] interbank networks have higher vulnerability to liquidity shocks.
Lux[372]	Core-periphery	Preferential attachment	50, 250	No contagion	Heterogeneous interest rates that are based on the strength of established relationships between banks may prevent the system from becoming extortionary and may also ensure that small peripheral banks survive.

spillovers could also occur as distressed banks offload large volumes of illiquid assets through fire sales; thus amplifying losses as asset prices enter a downward spiral.[313,370] While default risk in solvency contagion flow from debtors to lenders, in funding contagion, risk flows in the opposite direction via the liability side of the balance sheet i.e., from lending banks to the borrowers. In solvency contagion, knock-on defaults occur if the shock that banks encounter exceeds capital and the process stops when no additional banks default. However, with funding liquidity contagion, the shock can continue propagating until the initial liquidity need is satisfied, often via the sale of external assets.[347]

These dynamics are captured by a few theoretical frameworks shown in Table 2.4. Here we review the models used in the studies by Gai et al.[36] and Lee[371] (hereon referred to as GHM and LLM), respectively) for which an initial liquidity shock (e.g. haircut[i] or massive withdrawal by a depositor[371]) induces liquidity hoarding behavior or shortage among other banks in the system. The initially affected institution responds by hoarding liquidity via recall of short-term debt to counterparties, and this begins the liquidity contagion mechanism. Essentially, liquidity contagion models provide a mechanism to study the financial network as the system contends with illiquid banks. Both studies focus primarily on how liquidity contagion is influenced by structural characteristics of interbank networks; however, a key difference between the two approaches relates to the allowable responses by banks as they face liquidity shocks.

Liquidity hoarding in GHM. A bank that encounters liquidity shortage in the GHM, can access liquidity through repurchase agreements (or 'repo' transactions) in which banks access funding by offering collateral A^C or liquid assets A^L as security (Table 2.5). An aggregate discount (referred to as a haircut) $h \in [0, 1]$ is associated with the use of collateral assets to access liquidity funding. The haircut reflects the perception about the underlying risk of the asset; and enables lenders to hedge against complete losses if a borrower defaults. In the event that the collateral is sold, the lender may be forced to sell at a discount depending on the state of the market — for example with respect to market liquidity, information asymmetry and/or extent of default amount banks.[36] In addition

[i]Gai et al. refer to *haircut* as the difference between the loan received against a security, used as collateral, and the actual market value of the security.

Table 2.5: Stylised Balance Sheet in GHM of liquidity hoarding

<table>
<tr><th>Assets</th><th>Liabilities</th></tr>
<tr><td>Fixed Assets, A^{fixed}</td><td rowspan="2">Deposit, D</td></tr>
<tr><td>'Collateral' Assets, A^{C}</td></tr>
<tr><td>Reverse Repo, A^{RR}</td><td rowspan="2">Repo, L^{R}</td></tr>
<tr><td rowspan="2">Unsecured Interbank Assets, A^{IB}</td></tr>
<tr><td rowspan="2">Unsecured Interbank Liabilities, L^{IB}</td></tr>
<tr><td rowspan="2">Liquid Assets, A^{L}</td></tr>
<tr><td>Capital, C</td></tr>
</table>

to this aggregate haircut on collateral assets A^{C}, individual banks may be perceived differently by lenders about a borrowing bank's ability to meet its obligation, therefore, h_i represents this bank-specific haircut. Where a lender perceives a borrower to have a higher probability of default, the borrower may be offered a lower amount of funding despite a higher current market price for the collateral. Other assets which may be use by a bank that is facing a liquidity shortage includes, its reverse repo assets (A^{RR}) which are the collateralized loans to borrowing banks. Similar to the collateral assets, reverse repo assets are also subject to haircuts. Therefore, in this framework, the only assets exempted from any haircuts are liquid assets (e.g. cash and government bonds) which banks can also use as security for repo funding. Finally, banks may also rely on counterparties to provide new unsecured interbank loans L^{N}. Note that, the stylised balance sheet also consists of fixed assets A^{fixed} and interbank assets A^{IB}; however, it is assumed that banks are not able to use them to respond to liquidity shocks.

The GHM defines the liquidity condition of a given bank in the system based on a bank i that has a fraction μ_i of its counterparties withdrawing a proportion of their funding λ_i. The withdrawal by i's counterparties reflects liquidity hoarding which reduces how easily banks access funding from others. Bank i reassesses its liquidity position to find that it has lost $\lambda_i \mu_i L_i^{\text{IB}}$ in unsecured interbank liabilities L_i^{IB}. Given this loss, the liquidity condition of i is computed as:

$$A_i^{\text{L}} + (1 - h - h_i)A_i^{C} + \frac{(1 - h - h_i)}{(1 - h)} A_i^{\text{RR}} + L_i^{\text{N}} - L_i^{\text{R}} - \lambda \mu L_i^{\text{IB}} - \epsilon_i > 0, \tag{2.11}$$

where bank i is liquid if the total available liquidity is sufficient to cover the liquidity losses and existing liability. Total available liquidity is determined by the available collateral to secure repo funding plus any new borrowing (i.e., the sum of existing liquid assets A_i^{L}, collateral assets A_i^{C} and reverse repo (A_i^{RR}) which are both discounted, and new interbank borrowings L^{N}). This is matched against the sum of liquidity losses $\lambda\mu L_i^{\mathrm{IB}}$, existing repo liabilities L_i^{RR} and idiosyncratic shock $-\epsilon_i$.

To investigate the role that network structure plays in funding liquidity contagion, Gai et al.[36] began with a baseline structure defined by a Poissonian edge distribution, i.e., edges connecting banks are distributed approximately uniformly. The results from the baseline network were then assessed against that of a fat-tail (geometric) network configuration, in which concentration is expressed as a few banks being highly connected based on the number and overall value of their relationships with counterparties.[36] It is quite reasonable to compare a stylised form of the network to one that reflects the scale-free degree distribution that is often reported in several studies on interbank systems in Austria,[107] Italy,[108] US,[110] Colombia.[109] Their comparative analysis of the two network structures indicate that, the probability of a contagion is smaller and less severe given low average degrees for the concentrated (geometric) network structure. This result is consistent with findings that under random attacks, fat-tailed networks are more robust.[114,252] They also investigated further to ascertain the existence of any key differences in how the system responds to a random initial disturbance versus a targeted one. They find that a targeted shock on the most connected lender (i.e., with largest number of lending relationships) results in contagion occurring more frequently in both network configurations.[36,348] However, the frequency of such events is only slightly different from the original results in the baseline network. In contrast, contagion occurs almost with certainty in the concentrated network for a broad array of average degrees. This difference is explained by the similarity in how banks are connected under the Poisson distribution: there is relatively little difference between the most connected bank and an average bank in this network. However, in the concentrated network, banks that are highly connected are linked to a considerable fraction of others in the network.

Systemic liquidity shortage in LLM. In the LLM, Lee[347] focuses on measuring systemic liquidity

Table 2.6: Stylised Balance Sheet to model liquidity shortage in LLM[347]

Assets	**Liabilities**
Interbank Assets, A^{IB}	Interbank Liabilities, L^{IB}
Liquid External Assets, A^{QEX}	External (non-bank) Liabilities (e.g. Deposits), d
Illiquid External Assets, A^{ZEX}	Capital, C

shortage by taking account of direct and indirect liquidity shortfall in individual banks. A bank faces a direct hit to liquidity if there is a deposit withdrawal from external non-bank liabilties d. However, the links to other banks in the interbank network allow indirect or knock-on effects to be transmitted between counterparties. In contrast to the GHM, a bank that is facing liquidity shortage in LLM is restricted from borrowing new interbank loans to cope with the shock. Instead, the bank can sell available external assets starting with the most liquid assets A^{QEX}, followed by illiquid assets A^{ZEX} only if the bank is still experiencing a shortage (Table 2.6). To begin the simulation, an initial bank i is exposed to a liquidity shock to its funding that emanates from deposit withdrawals Δd_i. Bank i responds by recalling claims on counterparties and selling external liquid assets proportionally. Other assumptions about bank i's response include: (i) no short-sale of its liquid assets, (ii) liquid assets must be exhausted before liquidating illiquid assets, and (iii) new stock cannot be issued nor can the bank borrow new funds from external investor as a response to liquidity withdrawals. The second assumption follows from the notion that offloading illiquid assets prematurely is costly; while, the third assumption ensures that systemic liquidity shortage given an initial squeeze is isolated completely from effects when banks can access help from sources that are external to the system.

For a single bank i, the condition of its liquidity is determined by two components, its need for liquidity which is computed as:

$$l_i^{\text{n}} = \sum_{j \in \mathcal{N}} L_{ji}^{\text{IB}} \; + \; \Delta d_i, \tag{2.12}$$

and the total of its liquid assets computed as:

$$l_i = A_i^{\text{QEX}} \ + \ A_i^{\text{IB}}. \tag{2.13}$$

When bank i recalls interbank loans as a response to its depositors withdrawing deposits Δd_i, this action will increase the liquidity needs of other banks. Lee explains that the rippling effects are expected to continue throughout the system until external assets in the entire network falls by an amount that is commensurate with the initial withdrawals of liquidity in the system; that is:

$$\sum_i \Delta d_i \ = \ \sum_{j \in \mathcal{N}} A_i^{\text{QEX}} \ + \ A_i^{\text{ZEX}}. \tag{2.14}$$

The liquidity shortfall of any given bank is:

$$l_i^{\text{s}} \ \equiv \ \max(0, \ l_i^{\text{n}} \ - \ l_i), \tag{2.15}$$

which occurs when the bank's liquidity need exceeds its available assets. Lee aggregates the individual liquidity needs of banks based on Eq. 2.12 to obtain aggregate liquidity shortfall being faced by the system, that is:

$$\begin{aligned} \sum_{i \in \mathcal{N}} l_i^{\text{n}} \ &= \ \sum_{i \in \mathcal{N}} \left(\sum_{j \in \mathcal{N}} \Delta L_{ji}^{\text{IB}} \ + \ \Delta d_i \right) \\ &= \sum_{i \in \mathcal{N}} \sum_{j \in \mathcal{N}} \Delta L_{ji}^{\text{IB}} \ + \ \sum_{i \in \mathcal{N}} \Delta A_i^{\text{QEX}} \ + \ \sum_{i \in \mathcal{N}} \Delta A_i^{\text{ZEX}}. \end{aligned} \tag{2.16}$$

Lee shows that by comparing initial withdrawals ($\sum_i \Delta d_i$) to aggregate liquidity need (Eq. 2.16) it can be seen that the system can, in fact, have needs that are in excess of initial withdrawals.[347]

Essentially, the LLM recursively adjusts the liquidity need of each bank as a given i cancels interbank loans to cope with its own shortfall. The recursive nature of the process is due to liquidity needs of each bank increasing as other banks are liquidating interbank assets (which reduces liquidity for neighbors). This process continues until the liquidity needs of all banks are fulfilled or until banks exhaust their liquid assets. Lee introduced an algorithm to compute the overall change in liquid assets (Δl_i) exactly and efficiently by adopting a mechanism similar to that of Eisenberg and Noe[34] to solve the following fixed point equation:

$$\Delta l_i \ = \ \min \left[l_i, \ \sum_{j \in \mathcal{N}} \phi_{ij} \Delta l_j \ + \ \Delta d_i \right], \forall i \in \mathcal{N}. \tag{2.17}$$

To examine the possible determinants underlying the dynamics of liquidity shortages, Lee constructed a variety of network configurations by tuning: reserve ratio, deposit shares, surplus funds, and cross holdings. A total of six network configurations were examined; namely: complete, disconnected, circular and core-periphery. Alternative network structures were also explored in other studies,[348,372] particularly by allowing random edge formation based on the trust level that banks have in their counterparties[348] or based on some banks simply being more willing to engage in lending[372] (Table 2.4). The results from the LLM indicate that liquidity shortages of deficit banks can be mitigated by holding more asset claims on a surplus bank. The comparative analysis of the different network configurations indicates that a core-periphery structure, characterized by a deficit money center [j], engenders the highest systemic liquidity shortages. Finally, interbank networks in which banks are ill-matched exhibit greater vulnerability to liquidity shocks relative to well-matched systems. In the ill-matched scenario, deficit banks borrower only from other banks in deficit; while, two connected banks are considered to be well-matched when one is in surplus and the other in deficit.

Empirical data to study funding liquidity contagion. We highlight a few studies that extended beyond random networks or overly simplified structures of the financial system to investigate the dynamics of funding liqudity contagion.[37,298,369] Studies by Furfine[37] and Müller[298] relied, respectively, on payments data from the United States and supervisory reports on banks in Switzerland for information on bilateral exposure between banks. Both studies considered an idiosyncratic exogenous shock (i.e., the initial failure is due to some factor that is external to the system). Furfine takes the largest lender in the federal funds market as the first to fail ;[37] however Müller begins with the failure of 20% of banks that are unable to repay outstanding obligations immediately.[298] Another study used data on the banking system in France also obtained from supervisory reports on bilateral exposure.[369] Their approach differed to Furfine and Müller on the use of a common market shock, that represents correlated losses on mark-to-market assets, to analyze how the decision by banks to hoard liquidity leads to systemic liquidity shortage. For the 300 banks in the Swiss banking system, supervisory reports cover the 10 largest interbank exposures (20 for big banks).[298] The

[j] Hub banks that are connected with all other banks in the system

data set on the French banking system also consists of about 300 institutions; however, Fourel et al. consider groups at the consolidated level, ultimately examining 11 banking groups for December 31, 2011.[369] The U.S. FedWire payment data spanned the period February–March 1998. We note that, most of the empirical literature on direct contagion (i.e., solvency and funding liquidity channels) in financial networks employ an iterative (sequential) default cascade mechanism;[37,369] however a few[298,347] rely on the approach taken by Eisenberg and Noe.[34]

The simulated results from these studies agree that funding liquidity contagion is capable of inflicting considerable damage to banking systems. By overlooking distress propagation via funding liqudity shortage, systemic risk can be underestimated because losses in both solvency and liquidity channels have been shown to be of similar size.[369] In fact, illiquidity poses a greater threat in some instances relative to solvency contagion,[37] propagating to affect up to 9% of the U.S banking system if the largest federal funds borrower is no longer able to borrow. For the Swiss banking system, Múller finds that almost 90% of total assets would be affected.[298] Notwithstanding, Fourel et al. highlights ambiguous effects of liquidity hoarding by banks as a crisis response: increasing the probability of default given liquidity shortage; however the loss given a default may decrease because liquidity hoarding itself lowers a banks exposure.[369]

Contagion via external assets and fire sales

Apart from capturing banks' direct counterparty exposures, network models of financial systems also enable us to represent and study the impact of indirect connections such as common holdings of assets,[312] overlapping portfolios,[310] and linked return between portfolios[373] on stability. Shocks that propagate via the indirect channel, manifest mainly as asset fire sales[350] — meaning that a bank experiencing negative shock may sell assets as a way of returning to a leverage target.[316] In an illiquid asset market, the sale by this bank may depress prices; thus forcing others with common exposures to the asset, to deleverage as a loss response[313,316,374]

Most studies on the common exposure between banks use a bipartite network structure consisting of two node categories: banks and the assets that they invest in, and an edge can connect only nodes from different categories (Table 2.7). Empirical studies by Greenwood et al.[312] considers 90 banks

Table 2.7: Studies of overlapping portfolio as an indirect channel for financial systemic risk

Paper	Bank objective	Analysis	Data	Findings
Greenwood et al.[312]	Leverage targeting	Empirical	90 banks in E.U.	When the most leveraged banks are in possession of large values of asset classes, the banking system exhibits greater susceptibility to contagion. Dispersing volatile and illiquid assets more widely across banks can reduce fire sale spillovers.
Cont & Schaanning[375]	B/w passive & leverage targeting	Empirical	51 European banks	Spillover effects from portfolio overlap may affect the result of stress tests on banks, and also lead to heterogeneous losses on individual banks; hence such indirect effects cannot necessarily be reproduced in single-bank stress tests.
Huang et al.[72]	Passive to price changes	Empirical	U.S. banks	Their model prediction of failed banks performs well in recovering banks that FDIC reported as actual failed banks after 2007. Commercial real estate assets were identified by their model as the major culprits of 350 US bank failures between 2008 and 2011, not residential real estate.
Cifuentes et al.[314]	Risk-based capital req.	Theoretical	-	Allowing endogenous changes in prices of fire sold assets may cause an initial shock to inflict considerable damage.
Caccioli et al.[310]	Passive to price changes	Theoretical	-	The financial system experiences multiple phase transitions when there is increased diversification in the portfolios of banks: shocks do not propagate below the first due to the network being sparse; however, banks are particularly vulnerable to asset price shocks and these shocks tend to propagate between the first and second transitions. Beyond the second transition, banks are relatively more robust to devaluation of select assets.
Caccioli et al.[315]	Passive to price changes	Theoretical	-	Strong amplification of contagion, evidenced by larger number of knock-on failures, when consideration is given to counterparty risk and overlapping portfolio risk.
Caccioli et al.[316]	Passive to price changes	Empirical	U.K. banks	Simulations that ignore common asset holdings can underestimate fire sale losses considerably. Two strategies undertaken by banks were considered: one where banks maintain portfolio weights and the other where banks prefer to offload the most liquid assets first. The system always realizes a higher systemic risk given the former. However, the latter generates more spillover effects for a bank that elects to delay liquidating any of its assets when facing distress.
Levy-Carciente et al.[351]	Passive to price changes	Empirical	Venezuelan banks	Introduce a model that captures changes in the structure of the Venezuelan banking system, highlighting the sensitivity of bank portfolios to different external shocks.
Gualdi et al.[311]	-	Empirical	13-F SEC filings (Factset Ownership database)	Highlight a significant increase in the similarity of banks' holdings prior to a financial crises

in the European Union that have large exposures to the same class of assets, essentially projecting a bilateral network from a bipartite network of 90 banks linked to 42 asset classes.[312] They model fire sale spillovers via a mechanism that is prompted when a highly connected bank offloads assets. To account for the network effect of fire sales, they measured fire sale losses of the system and the susceptibility of each bank to deleveraging by others.

In modeling shock propagation dynamics on overlapping portfolio networks, a few points must be considered: the price response mechanism as banks liquidate and the banks' reaction to losses on assets (i.e., how are their portfolios readjusted to manage risk?). Regarding the first point, several models of asset fire sales employ a market impact function that assumes a linear price impact that is proportional to the volume of assets liquidated; hence a higher liquidated amount leads to higher devaluation of the asset's price. Cont and Schaanning[313] consider a more complex forms of the market impact function that considers investors being motivated to buying the asset when its prices suffers considerable devaluation. For the loss response of banks, a simple approach is to assume that banks are passive once their respective losses remain below the threshold, otherwise the bank liquidates its entire portfolio.[72,310] Caccioli et al. applied this assumption to derive results analytically for bipartite Erdös-Rényi ensemble of random networks. By using a generalized branching process they found that in a supercritical state propagation can be systemic despite an initially small exogenous shock. The branching process follows from the work of Watson and Galton who studied the probability of family names surviving across generations.[376] In epidemic spreading models, the first infected person creates a certain number of new cases where this number is obtained from a probability distribution. Each of these newly infected individuals go on to generate independently a certain number of new infections, also drawn from the same probability distribution.

The process repeats for each new set of infected individuals. If the expected number of newly infected persons (i.e., basic reproduction number) is less than 1, then the process dies with certain probability. If the expected number of newly infected persons (i.e., basic reproduction number) is less than 1, then the process dies with certain probability. It is this branching process that Caccioli

et al. generalized to account for multiple types of individuals $i \in \{1, 2, \ldots, \ldots q\}$. More specifically, this multi-type branching process focuses on the expected number of infected persons of type i that are in fact generate by a type-j individual. For each pair of individual type, a $q \times q$ matrix can be obtains with each entry being the number of infected person of type i that are produced by type j. In this specification, an on-going process will die when the largest eigenvector of the matrix is less than 1 (i.e., *subcriticality*), and if greater than 1 (i.e., *supercriticality*), then the process is expected to last indefinitely. According to Caccioli et al., banks can be differentiated on the basis of various characteristics (e.g. degrees); hence the generalized branching process outlined earlier for infected individuals could also apply to quantifying the expected number of banks of a given type i that fails due to the failure of another bank that is of type j. Caccioli et al.[310] show a phase transition consisting of a region where global cascades occur in the parameter space that is separate from another area void of such cascades. Furthermore, although diversification may reduce risk exposure of individual banks to specific assets, it does not necessarily enhance stability of the system. Huang et al. also showed that in an empirica study of U.S. commercial banks that a phenomenon exists that resembles a phase transition occurring between stable and unstable regimes.[72]

The passive response assumption on banks could be regarded as realistic if we consider that banks are responding amid a crisis, and that they have little to no time to respond in a way that staves off default. However, banks are subject to risk-management and regulatory procedures that motivate them towards optimization in reality; hence a realistic depiction of bank's behavior is one which sees them responding to changes in markets by re-balancing their portfolios. The approach by Greenwood et al.[312] considers banks being subjected to risk-management procedures; they target leverage ratios by liquidating a proportion of their assets as they experience losses.

2.5.4. Systemic importance in financial networks

Centrality and clustering measures

The systemic risk literature has highlighted that, in addition to the size of banks, the extent of their interconnections is also important. It is in this regard that the overlap between social networks and financial systems becomes even more discernible, i.e., when we aim to not only quantify the level

of interconnectedness but also identify those banks that are critical to the financial system. Policy discussions on systemic financial risk after 2008 highlighted the need to identify those banks that are analogous to superspreaders in social networks, and for consideration to be given to the system-wide importance of individual banks — a property that originates from connectivity to others or due to their scale of operation.[91,104,285] The parallel is highlighted in the approaches that are taken to evaluate banks' importance with the use of centrality measures.[377] Many studies[107,117,189] have relied on the connections between banks to find those most consequential in terms of their role in providing funding liquidity, and their vulnerability or the risk posed to the system due to their highly leveraged state. There has been some focus on formulating measures that reflect the specific features of financial systems. Against this background, some have constructed measures based on market data on banks' portfolio returns, giving consideration to contagion via fire sales[378,379] or to the presence of correlation between banks' returns.[380]

DebtRank

The DebtRank[381] measure was formulated on the basis that banking networks are not only weakened by the actualization of bank defaults. In fact, even when a default does not materialize, neighboring banks will encounter some stressful effects which reduces their ability to withstand additional strain, and this fragility will also be transmitted to their counterparties. DebtRank follows from feedback centrality[382] measures such as PageRank[383,384] which has been applied to ranking Internet pages on the worldwide web. With this type of centrality measure, networks with cycles can produce an infinite number of reverberations of the node's impact to counterparts which then reverts to itself. In such instances, may be difficult to find an economic interpretation that is measurable with practical application; however, the methodology of DebtRank addresses this challenge by focusing on exposures propagating along trails; hence links are visited only once. DebtRank considers recursively the impact of initial distress by banks, and this impact is computed as the fraction of total economic value in the network that is susceptible to that distress or default. The measure is based on a directed, weighted exposure matrix E with elements $E_{i,j}$ as the amount invested by bank i in bank j, and the individual capital buffer c_i are the elements of vector $\mathbf{c}$. The effect of bank j's default on bank i is expressed as $W_{j,i} = \min\left\{1, \frac{E_{i,j}}{c_i}\right\}$. Furthermore, the set of distressed banks is denoted

by S_f and the initial level of distress is given by $\psi \in [0,1]$ with $\psi = 1$ indicating default.

The algorithm defines two variables s and h which track the state and distress level of nodes, respectively. Nodes can be in one of three states: undistressed, distressed or inactive. The initial values $s_i(1)$ and $h_i(1)$ are $s_i(1) = D$ and $h_i(1) = \psi$, that is, if bank i belongs to the set of distressed banks; otherwise $s_i(1) = U$ and $h_i(1) = 0$. The process of updating the values of $s_i(t)$ and $h_i(t)$ occur iteratively as follows:

$$h_i(t) = min\Big\{1,\ h_i(t-1) + \sum_j W_{j,i} h_j(t-1)\Big\}, \tag{2.18}$$

$$s_i(t) = \begin{cases} D & \text{if } \ h_i(t) > 0 \ \text{ and } \ s_i(t-1) \neq I \\ I & \text{if } \ \ s_i(t-1) = D \\ s_i(t-1) & \text{otherwise,} \end{cases} \tag{2.19}$$

for all i and for $t > 2$. The first step begins with Eq. (2.5.4) where the distress level for all nodes i is updated in parallel. Here, i's current level of distress $h_i(t)$ is the based on two components: i) its distress level up to the previous time period $h_i(t-1)$ and ii) the loss impact (relative to its capital level) due to distress from j's (denoting i's neighbors). The second step considers the state of all nodes, where the current state of node i changes to distress (D) if i is not inactive and its current level of distress is positive. Eq. (2.19) also implies that in the next time period i.e., $(t+1)$, the state of node i will change to inactive (I).

Battiston et al. show that their algorithm converges in a finite number of steps T with nodes being in state U or I. The DebtRank R of the set S_f is then computed as:

$$R = \sum_j h_i(T) v_j - \sum_j (1) v_j \tag{2.20}$$

In Eq. (2.20), $v_j = \sum_k E_{j,k} / \sum_j \sum_k E_{j,k}$. Essentially, R measures the distress build-up in the system (not including initial distress), and if the set of initially distressed banks S_f contains only one bank, then R measures the stress induced by that bank on the whole system.

SinkRank

SinkRank is another measure of systemic importance in payment and/or exposure networks in which transfers between banks occur along directed edges. The sender of the payment loses access to it once the transfer is made; the receiver, however, is at liberty to transfer the funds to any bank in the system. In contrast to DebtRank which occurs along trails, the transfer process for SinkRank[61,115,385] occurs as random walks in the network; hence banks engage the same counterparty as sender and/or receiver more than once. SinkRank represents the directed, weighted payment or exposure network as an absorbing Markov process, apt for modeling liquidity dynamics in payment systems. Markov systems can be in one of any number of states, passing from one state i at time $t-1$ to another state j in a subsequent time step t based on a fixed probability p_{ij}, also referred to as a *transition probability*. The SinkRank process begins with a node which, at some point, terminates at a sink which is an absorbing node bank with no outgoing edges.[61] The method simulates the process in a payment or exposure network where transferred funds to a failed banks remain dormant (i.e. unavailable to the wider system) until the bank recovers. SinkRank determines that the systemic importance of a bank i is based on the number of steps required for a process, beginning anywhere in the system, to terminate at an absorbing node i, with higher SinkRank indicating a more central node needing fewer expected steps and greater systemic importance.

The payments between banks are represented as an $n \times n$ adjacency matrix $M = \left[s_{ij}\right]$ with elements s_{ij} representing payment edges from i to j and the weight on each edge is the value of the payment. SinkRank converts this adjacency matrix M to an $n \times n$ transition matrix P by dividing the entries in each row by their respective row sum $\sum_j s_{ij}$ to obtain $P = \left[s_{ij} / \sum_j s_{ij}\right]$. To compute the SinkRank of a node, the outgoing edges of that node are removed such that the probability of exiting that state is zero. Note that, in the absorbing state system, the states are numbered with the absorbing state displayed last in the transition matrix. The original SinkRank measure model failure of a single bank; hence the number of sinks $m = 1$. Considering node k as an absorbing

node, the transition matrix is rewritten as:

$$P_k^{\text{sink}} = \begin{bmatrix} S & T \\ 0 & I \end{bmatrix}. \tag{2.21}$$

The original transition matrix without the k-th column and row of P is denoted by an $(n-m)\times(n-m)$ matrix S, the k-th column of P (with the k-th element omitted) is denoted by an $(n-m)\times m$ vector T, the $m \times m$ identity matrix is denoted by I and an $m \times (n-m)$ row vector of zeros is denoted by the 0 entry.

Movement along the non-absorbing states is encapsulated by S; however, the time to absorption in a Markov system depends on the entries of the matrix Q obtained from $Q = (I - S)^{-1}$. A process that begins at a node i is expected to visit a node j a total of q_{ij} times before absorption. The total number of visits of the process initiated by i to all nodes in the non-absorbing states, before absorption, is computed as $\sum_i \sum_j q_{ij}$ i.e., *Sink Distance*. The SinkRank of i is then obtained by taking the inverse of its average Sink Distance:

$$\text{SinkRank} = \frac{n-1}{\sum_i \sum_j q_{ij}}. \tag{2.22}$$

2.5.5. Implications for macroprudential policy design

The application of network models to the study of financial systems can provide numerous policy insights to reduce systemic instability.[36,91,104] The acknowledgement that risk concentration played a major role in the financial meltdown of 2008 encouraged steps to formulate a post-crisis policy framework, with a need for tools to quantify interconnectedness in the system[386] and tools to identify the institutions most critical for stability.[387] In the preceding section, we addressed the latter by examining measures of systemic importance to identify banks that are most central to the operations of the entire system. For financial stability experts, measuring interconnectedness is one aspect of the puzzle, the other is tracing the potential paths for contagion as a way of improving how micro- and macro-prudential policies are formulated. Early versions of stress testing focused on measuring the impact that a severe but plausible negative economic shock has on the capital level of banks.[387] The post-crisis move towards macroprudential stress tests, however, aimed at

expanding the supervisory perspective to the entire system to incorporate: i) the interaction among banks during stressful times, and ii) the mechanisms that can amplify an exogenous shock which may then lead to the realization of large losses.[282,283] In other words, macroprudential policies extend beyond minimizing idiosyncratic risks from individual banks to a much broader objective of reducing the potential for financial network spillovers.[91] In the following sections, we examine some macroprudential policy concerns that have been simulated in the literature that use network models to investigate financial systemic risk.

Regulating capital levels

Capital ratio is the amount of capital held by a bank as a percentage of risk-weighted assets. To limit the occurrence of insolvency among banks, regulators implement capital requirements on banks by stipulating that this ratio is to be maintained above a given threshold. To safe guard the system as a whole, it was proposed that higher regulatory requirements be levied on banks with the capacity to destabilize the system due to their size and connectivity.[104]

Bluhm et al.[388] simulated increasingly strict capital requirements in an interbank network in three stages. The first stage considered low capital requirements, for which they find that interbank lending is extensive and occurs among banks that realize high returns on non-liquid assets. However, as interbank lending increases, so does interest rates which favors highly profitable banks that borrow considerable amounts. At this stage, Bluhm et al.[388] describes the system as being in a *robust-yet-fragile* state. This means, given a medium-sized shock to one of the highly leveraged banks, fractional amounts of the shock is transmitted to each of its lenders; thus allowing the lenders to bear their respective losses and avoid default. However, a large shock to one of these lending banks will lead to the default of a substantial fraction of banks in the network.

They then simulated a gradual increase in the capital requirement, to find that the scope for leveraging declined which subsequently lowered the demand for interbank loans, and consequently the interest rate on them. The reduced interest rate on interbank loans induced more banks to borrow because their non-liquid asset returns were now higher than that of the interbank market. Bluhm et al.[388] explains that, at this stage the interbank market has more borrowers and fewer

creditors; hence, the network is in a more fragile state because there is a smaller number of creditors to share the effects of a shock from a single borrower. Finally, for a capital requirement above 7 percent, interbank activity and investment in non-liquid assets experienced declines, which produced an inefficient network with monotonically decreasing systemic risk. In essence, their result indicates systemic risk evolves in a bell-shaped pattern as capital requirement increases gradually.

Although capital requirements have been shown to have the ability to keep bank insolvency in check,[20,35,388] its interaction with the mark-to-market accounting of banks' balance sheet can cause endogenous amplification of an initial shock. Cifuentes et al.[314] investigated this possibility and find that an initial decline in the value of a bank's assets will induce asset disposal. If the demand for the asset is perfectly elastic, then market price may not be affected; otherwise, selling the asset leads to a lower market price. Once the price has been updated, the bank may find that they no longer meet the minimum capital requirement; thus inducing additional asset disposal. Following from the previous round, the market price of the asset may be lowered even further and so on. The study, therefore, highlights that it is quite possible to generate undesirable spillover effects that far exceed the initial shock when an externally imposed solvency constraint on capital is combined with mark-to-market accounting of banks' balance sheet.

Regulating liquidity levels

Liquidity requirements stipulate that banks should maintain a minimum liquidity ratio i.e, the amount of liquid assets held by banks in relation to their short-term liabilities. The motivation behind liquidity requirements is the idea that they can mitigate systemic effects that emanate from funding liquidity challenges that may be amplified via fire sales.[104] The simulation exercises by Gai and Kapadia[36] discussed in Section 2.5.3 indicate that, a liquidity requirement that targets large banks more effectively reduces the probability and size of contagion compared with a uniform increase in the requirement on all banks. Subsequent studies[389] share similar findings that liquidity requirements have the ability to reduce overall systemic risk and the contribution of individual banks to aggregate risk. Aldasoro and Faia[390] raised liquidity requirement for systemically important banks (SIBs) while reducing the requirement for others in the system. The SIBs responded by

increasing liquidity through the sale of interbank assets and non-liquid assets, which means lower risk of contagion. However, the other banks have room to increase liquidity in the system which compensates for any shortage emanating from higher liquidity requirements on the SIBs. This balancing act serves to maintain the assurance of liquidity in the interbank market. Under difference conditions, however, stability comes at the cost of efficiency in the system, even to the point of making the system more fragile.

To investigate this, one study[390] conducted a policy experiment in which 'phase-in' increases in banks' liquidity ratios were shown have unintended consequence for system-wide fragility. This can occur when the policy requirements is applied to banks equally, despite them having different portfolios. From the outset, some institutions may have funding that is less stable and/or more exposure to risk on asset returns. Increasing liquidity ratio can lead these banks to liquidate their assets prematurely, as they attempt to meet the stricter requirement. This liquidation places downward pressure on asset prices which causes other banks to suffer balance sheet losses. If depositors of the affected banks respond via bank runs, the system may suffer a further decline in liquidity and induce more asset fire sales. As discussed earlier, applying liquidity requirement according to systemic importance is one way to maximize the beneficial aspects of the policy, resulting in lower systemic risk while on the flip side, it also minimizes those that could be harmful.

2.6. Future challenges

We have provided an overview of various tools and methods from network science in general, and more specifically social network analysis, that can be applied to further understand certain challenges faced by authorities in managing financial systems. The rapid pace of development in both fields of study is due partly to the interdisciplinary nature of network science, which means that at the moment there may be several tools being developed to advance our current knowledge about them. We have highlighted that similar to social networks, it is crucial that the health of the global financial system is maintained to avoid detrimental social and economic consequences. It is, therefore, critical that we continue working to develop better ways of identifying and regulating systemically important institutions. Although several regulatory measures exist that have been shown to be effective in

maintaining stability, there is still the need to formulate policies in a way that reduces reckless risk-taking among institutions.[33] Moreover, the introduction of new technology, for example the growing popularity of digital currency, may be an added source of complexity in the system. It may be worthwhile to investigate how these developments may challenge the state of financial systems. We have also discussed that a key advantage of employing network models in financial network analysis is the ability to capture and represent aspects of the system that are usually ignored in conventional approaches in economics and finance. However, room remains for more realistic models of financial networks that incorporate the temporal dimension of the relationships between institutions into the analysis. This is expected to promote effective real-time monitoring of financial systems which support early-warning signals of distress. Of course, such steps rely heavily on the availability of more real-time data to research. Another area for improvement is that of stress-testing performed by financial authorities. Battistion and Jaramillo[391] have highlighted a need for other channels of contagion to be included in the supervisory stress-testing of several financial authorities. They explained that for many, the solvency channel is included in the analysis; however, the channels of funding liquidity and common assets are usually missing. Improvements in these areas will hopefully facilitate early-detection mechanisms and/or strengthen our response to occasional failures.

CHAPTER 3

The diurnal evolution of financial systemic risk

Shaunette T. Ferguson[1], Sadamori Kojaku[2], and Teruyoshi Kobayashi[1,3]

1 Graduate School of Economics, Kobe University, Kobe 657-8501, Japan

2 Luddy School of Informatics, Computing and Engineering, Indiana University, Bloomington 47408, United States of America

3 Center for Computational Social Science, Kobe University, Kobe 657-8501, Japan

Abstract

Interbank markets facilitate banks in managing liquidity via bilateral funds exchanges, but an adverse initial local shock can spark a catastrophic series of events that cripples the entire system. Temporal interaction patterns on spreading dynamics in social networks have been explored in several studies. However social networks often feature interacting entities that are active intermittently, while in interbank networks, credit contracts have set expiration dates which makes the duration of bank interactions dependent on when loans are initiated. Here, we model banks' interactions using overnight bilateral trade data (i.e., with maximum duration of a day) and assess contagion effects from one initially defaulted bank given the robust pattern in trade timings. Before controlling for network size, banks appear to face the highest risk around the time the market opens. As in many real-world systems, interbank networks have finite size which we correct for to find that there is no significant difference in systemic risk among the time categories. However, we investigate why mean systemic risk is slightly higher in networks close to end-of-day to find that the accessibility of initial risk increases at this time.

3.1. Introduction

In interbank markets, banks establish borrowing and lending relationships to insure against liquidity shocks. Although interbank transactions can serve as a means of risk diversification for individual banks, they may also establish paths to financial contagion that could spread throughout the entire system.[27,29,30,126,135,392] Each borrowing bank exposes its direct creditors to counterparty risk. If the borrowing bank fails to repay the loan amount in full at maturity, the lending bank incurs a financial loss. In the worst case, the bank defaults, which in turn creates another financial distress to other banks, leading to a global cascade of defaults, known as systemic risk.[135,393]

The systemic risk hinges on the structure of networks and how it evolves in time. Simple structural features such as the number of edges and degree of banks have profound impact on the size of cascade.[27,394,395] Temporality of network structure also influences spreading phenomena such as infectious diseases, opinions and rumors.[2,3,42,43] In the context of the overnight market, most studies examined the systemic risk from daily to quarterly scales by aggregating trades at different times into a single network.[19,20,22,24,37–40,294] While such aggregation is often necessarily due to the unavailability of data and also helps reduce the fluctuations in network structure, it neglects a critical feature of the overnight market: the duration of interbank relationships can be shorter than a day. For example, it is possible that cascade occurs in the aggregated networks but does not in practice if there is no direct lenders at the time of default. It has not been clear whether the short duration of relationships facilitates or reduces the contagious risk in the interbank networks.

Here, we compare contagious risk at intraday time scale with the risk from daily aggregated networks using high-resolution transaction data from the Italian interbank market (e-MID). We show that a widespread measure for systemic risk has a strong bias arising from the number of banks in networks. This bias is problematic particularly for the analysis at intraday time scale, where the size of the network largely fluctuates in time. We address this bias problem by comparing the risk for the networks of a similar size. While the biased measure for systemic risk displays the highest peak in the morning, we find an opposite result after controlling the network size effect, i.e., the risk is the highest in the evening.

We explore the question of what gives rise to the high risk in the evening using null models for networks and time series. Our results suggest that although systemic risk is well explained by degree distribution and the bursty nature of trade in the market, they do not fully explain the high risk. Rather, the high risk in the evening can be explained by the increasing number of banks being exposed to risk.

We highlight the need to observe the short duration (i.e., up to a maximum of one day) of interbank relationships in assessing systemic risk because a bank can default at any time prior to the actual maturity of the loan and, our results indicate that at different point, the level of risk is higher. We also demonstrate that the conventional measure of systemic risk (i.e., the fraction of banks to default), presents a critical limitation due to differences in network size, thus resulting in inconsistent initial risk at different times. In fact, this is a common concern for empirical studies on systemic risk and, more generally, cascading behavior on networks.[36,244,321,366,396] We address this network size bias to facilitate a comparison of systemic risk between the intraday networks. Finally, we postulate that both the distance and, the fraction of lenders linked to the initial defaulter influence higher risk.

3.2. Data

3.2.1. Italian interbank network

We use a data set on bilateral interbank transactions conducted through the e-MID platform. The e-MID is the Italian electronic market for interbank deposits and loans founded by e-MID SIM S.p.A based in Milan, Italy. Our data set consists of transactions for $3,922$ business days between 2000–2015 with banks trading mostly between 9:00–17:30. We retrieved the euro-denominated contracts with an overnight maturity, which constitutes 86% of all $1,192,738$ transactions. In the e-MID market, banks can initiate a contract at any time during a day to meet liquidity requirements, and the overnight contracts must be settled the following day.

3.2.2. Intraday networks

We model interconnectedness between banks as a network, where nodes represent banks, and a directed edge from i to j represents a lending–borrowing relationship between lender i and borrower

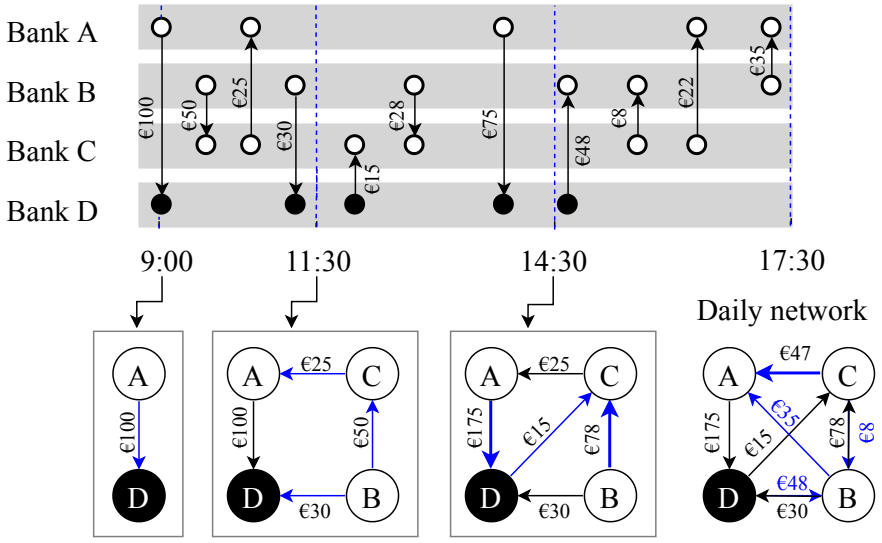

Figure 3.1: Schematic of intraday networks. Outgoing and incoming edges represent lending and borrowing activity, respectively. Bank D (black circle) is the initial defaulter realized at each point in time and the remaining banks (white circles) are initialized as solvent in the corresponding time bin. The lower panel illustrates the corresponding intraday networks, i.e., cumulative networks up to given time intervals, in which edge weights represent the sum of traded volume. The width of edges indicate the amount traded between two banks.

j. Before the market opens, there is no transaction between banks, i.e., the network is empty. When a new transaction is made between lender i and borrower j, an edge from i to j is added to the network, i.e., the edge is weighted by the amount of funds transacted between the banks since the opening of the market (see Fig. 3.1 for a schematic). The network thus grows over time in a monotonic manner, and the network that emerges at the market closing time captures all the transactions that were performed on that day.

All overnight loans must be repaid via an external automatic settlement service, closing out all loan contracts between banks from the previous day. Therefore, when the market reopens, our data set captures only new trades between banks. We analyze the intra-day temporal network at every interval of 15 minutes between 9:00 and 17:30, where 97% of transaction events take place. We refer to the networks between 9:00 and 17:30 as intra-day networks, and that at 17:30 as the inter-day network for the day.

Fig. 3.2a shows that the fraction of trades, in terms of both number and amount in 15-minute

Table 3.1: Banks' stylized balance sheet.

Assets	Liabilities
External assets (A^{EX})	Deposits (D)
Interbank assets (A^{IB})	Interbank liabilities (L)
	Capital (C)

snapshots averaged over all business days, displays a bimodal pattern, where the first peak and the second peak emerge around 9:30 and 15:00–17:00, respectively. For intraday networks, we observe a superlinear scaling relationship between the numbers of active nodes N and edges M, i.e., $M \propto N^{\beta}$, with exponent $\beta = 1.65$, which is higher than that reported for interday networks[55] (Fig. 3.2b). The burstiness parameter B[205] based on the inter-event times of intraday transactions is 0.48, which indeed indicates a bursty activity pattern in the Italian overnight market.

3.3. Model of default cascades on intraday networks

3.3.1. Balance-sheet structure

We simulate a dynamical process of cascading bank failures under the worst case scenario; defaulted banks fail to meet all of their debt obligations. Specifically, we consider a short-run response of lending banks to the failure of borrowing banks, where the lenders have to resort to covering their losses by reducing their own capital. This allows us to follow the convention in the literature on financial systemic risk, where insolvency is a criterion for a bank failure. A bank is solvent if and only if it retains a positive amount of capital (Table 3.1):

$$C = A^{\mathrm{EX}} + A^{\mathrm{IB}} - D - L \geq 0, \tag{3.1}$$

where C is the bank capital, A^{EX} and A^{IB} respectively denote the bank's external assets (e.g., government bonds, stocks and other securities) and interbank credits, and D and L denote retail deposits and interbank liabilities, respectively.

To study default cascades on interbank networks, C needs to be set at a hypothetical value since the e-MID data set does not contain information on bank capital. Here, we assume that a bank's capital is correlated with its trade volume. Specifically, a bank's capital is given by a fraction $\bar{r}$ ($= 0.08$) of the average daily traded volume, denoted by $\mathrm{TV} \equiv \bar{A}^{\mathrm{IB}} + \bar{L}$, where $\bar{A}^{\mathrm{IB}}$ and $\bar{L}$

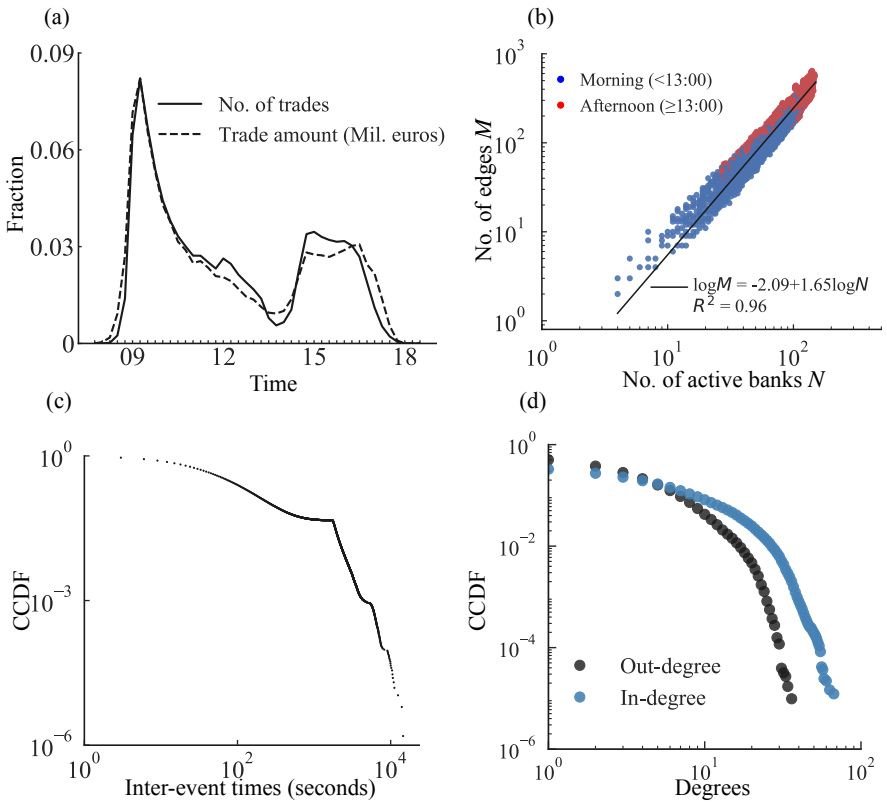

Figure 3.2: Diurnal trading activity. (a) Fraction of trade count (solid) and trade volume (dashed) in a day, averaged over business days during 2000–2015 (3,922 business days). (b) Superlinear scaling relationship for networks between 2002–2015. Each dot represents a 15-minute time interval of a day. Blue and red dots indicate morning ($<$ 13:00) and afternoon ($\geq$ 13:00), respectively. Solid line corresponds to a log-linear regression estimated by the ordinary least squares. (c) Complementary cumulative distribution function (CCDF) for inter-event times of trades. Inter-event times are computed as total seconds that elapsed between two consecutive trades. The burstiness parameter B^{205} is 0.48, which suggests that the transactions pattern is indeed bursty. (d) Complementary cumulative distribution function (CCDF) for degrees. The networks are inhomegeneous in degrees i.e., most banks have only a few out-going (in-coming) edges but few banks have large numbers of out-going (in-coming) edges. These plots highlight that trading activity have a diurnal pattern, and these activities occur in bursts among banks with heterogeneous degrees. These influence the network structure over time and may have implications on the evolution of systemic risk.

denote the daily average of interbank lending and borrowing, respectively. However, determining a persistent state variable such as bank capital from the most recent trading volume would not be appropriate because banks' trading activity can be intermittent (i.e., there can be a long period of no trade). Therefore, we use the average value for TV over the past 12 months in computing the (hypothetical) bank capital. If banks have no recorded transaction over the past 12-month period,

we compute their individual capital level as follows: Given the observed TV in the current month, we first estimate a pseudo average daily TV for the preceding 12 months by exploiting the estimated positive relationship between TV in the current month and the average TV in the preceding 12 months using the data for the banks that traded over the past 12 months (Fig. 3.B.1). Then, the bank's capital is given by a fraction $\bar{r}$ of the pseudo TV. It should be noted that our simulation period now ranges from 2002 to 2015 (3,585 business days) because the preceding 12 months are used for the estimation of capital levels. We assume that the bank capital is constant for a month.

3.3.2. Simulating default cascades

We investigate the level of systemic risk by quantifying the impact that a bank default has on the entire interbank market. To do this, we simulate the spreading process using a threshold model.[27,366,397] In this simulation, we first select a borrower at random as an initial defaulter. Then, we compute the losses caused by the initial defaulter on its lenders. The lenders default if their capital is insufficient to cover the losses they face from the borrower. The newly defaulted banks may in turn inflict losses on their lenders, causing additional defaults. Note that exposure to a defaulted bank may not cause the exposed banks to become insolvent. However, it reduces the banks' capital at least to some extent, making those banks more vulnerable to default. The default cascade continues until no new bank defaults.

Our cascade model has three assumptions. First, the set of initial defaulters (i.e., seed set) consists only of banks that have engaged in at least one transaction as a borrower. This is because the risk of default flows from a borrower to a lender. Second, we assume that all lenders to a defaulted bank lose their loans entirely i.e., a recovery rate of 0%.[27] Although in practice a portion of losses could be recovered immediately following the default of a bank, a high degree of uncertainty about the amount that can be recovered and when this will be possible lead a presumption of total loss of their loans by creditors. Third, failed banks are not allowed to recover (i.e., become solvent subsequent to a state of default) because we study default cascades over a short timescale.

3.3.3. Measuring systemic risk

We quantify how likely it is for a bank to fail given an initial defaulter. Therefore, we want to capture the system-wide effect of a single defaulted bank on the network so we adopt a conventional measure of systemic as the fraction of defaulters at the end of a cascade;[27,280,321] if an initial defaulter i causes a cascade that results in N_i^{f} failed banks, the risk originating from bank i denoted by f_i, is defined as

$$f_i \equiv \frac{N_i^{\mathrm{f}} - 1}{N - 1}, \tag{3.2}$$

where N is the number of banks in the network, excluding isolated banks. We note that we subtract one in both the numerator and the denominator to exclude the initial defaulter, i.e., the bank that defaults due to some exogenous factors. Risk f_i depends on which bank is selected as the initial defaulter. Assuming that every bank has an equal chance of being an initial defaulter, we compute the average systemic risk by

$$f \equiv \frac{1}{|\mathcal{B}|} \sum_{i \in \mathcal{B}} f_i, \tag{3.3}$$

where $\mathcal{B}$ denotes the set of borrowers (i.e., the set of initial defaulters). In general, systemic risk measure f quantifies the vulnerability of the interbank network to the default risk from one borrowing bank.

3.4. Results

3.4.1. Diurnal pattern of systemic risk

Since the global financial crisis, the number of participating banks,[398] trading volume[399] and the number of transactions[398,399] in the Italian interbank overnight market have declined considerably. While no single causal factor has been identified, other events have transpired in the post-crisis period that could have mutually contributed to the persistence downward trend highlighted in some studies[20,331,398,399] including the European Debt Crisis and the considerable expansionary monetary policies employed by the European Central Bank. To exclude the possible impact of such disruptive changes, we segment trade data into three periods prior to, in the midst of and posterior to the global financial crisis.

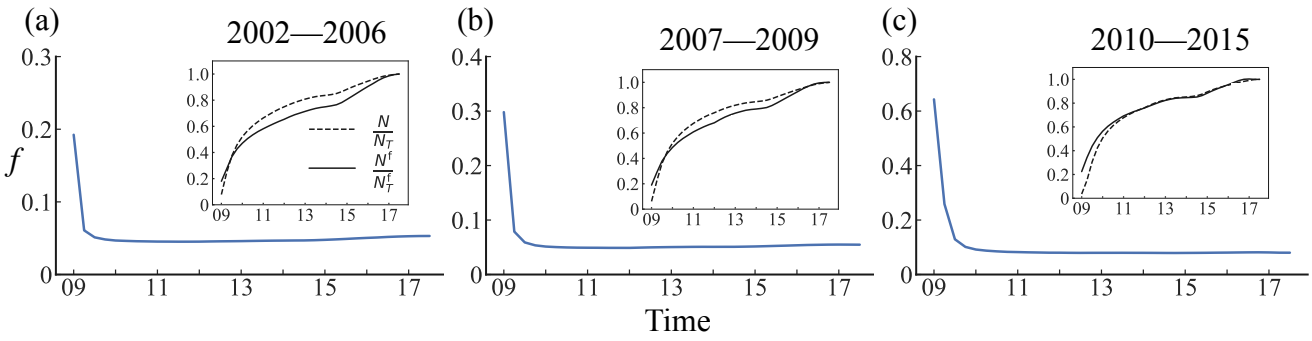

Figure 3.3: Systemic risk f measured at the intra-day time scale. We split the data set into three subsets, namely (a) before the global financial crisis, (b) during the crisis, and (c) the post crisis periods. Then, for each period, we compute f averaged over all business days. *Insets:* Despite an almost constant f after 10:00, the evolution of active banks N and failed banks N^{f} (normalized by their respective daily volumes) increase in time as they approach the maximum value of 1 at the end of the day. This suggests the possible impact of changing network size. N_T and N_T^{f} are the numbers of active banks and defaulted banks in the daily network, respectively.

In all three periods, systemic risk f (Eq. 3.3) is highest around 9:00 but then decreases rapidly within an hour (Fig. 3.3). This peak in risk is at least three times higher than the risk estimated from the daily aggregated network. We examine further, why a higher level of systemic risk emerges in the morning?

The interbank network grows monotonically from a characteristically small size as the market opens until it achieves the size of the daily network at the end of day (Fig. 3.3, *inset*). This systematic growth in the network size is crucial in the evaluation of systemic risk because, risk f is strongly anti-correlated with network size, i.e., the number of active banks, N (Spearman correlation, $\rho = -0.67$; Fig. 3.4a). This leads to a question of whether the high risk in the morning is attributed to the network structure or to the small network size.

We control for the network size by comparing the risk f of networks of a similar size. Specifically, we group the networks into three groups based on the network size, i.e., $25 \leq N < 50$, $50 \leq N < 75$, $75 \leq N < 100$, which accounts for the 70% (approximately $20,000$ networks) of all networks in the data set. Then, for networks in each group, we compare the risk f across four time categories: Early-morning (<11:00), Mid-morning (11:00–12:59), Afternoon (13:00–14:59), and Evening (≥15:00). Note that we exclude excessively small or large networks (i.e., $N < 25$ and $100 \leq N$) from the

analysis because we did not have the sufficient number of such networks for this comparison.

Overall, systemic risk f tends to increase with respect to time, as indicated by the increasing median of risk f (Fig. 3.4b). Regarding median risk, evening networks have up to 50% higher f than that of morning networks (Fig. 3.4b, *middle*). The distribution of risk f for the evening is significantly higher than that for the morning under the significance level of 5% (Fig. 3.G.1; Table 3.H.1).

In sum, the interbank network faces the highest systemic risk in terms of f in the morning (Fig. 3.3), which, however, is due to the nature of the risk measure f, i.e., f is inherently high when the network is small (Fig. 3.4a). By controlling for the network size, the evening network turns out to be the riskiest during the day. The conventional measure of systemic risk is, therefore, sensitive to network size and this emphasizes that the dynamic components of the metric e.g., changing network size, should be controlled to enable meaningful comparison of risk in different periods. Eliminating the difference in network size allows us to focus on other network characteristics that are affecting risk differently in each period. While the results highlight that evening networks are the riskiest, cascades that occur in early periods are not necessarily innocuous. This is because banks have full information about themselves but not about their counterparties or other banks which means that, an otherwise small early-morning cascade in the overnight market could be amplified, resulting in system-wide effects (e.g., credit freezes) when the remaining solvent banks withdraw from the market to avoid being exposed to further risk.

3.4.2. Position of the initial defaulter on systemic risk

Why is the evening network riskier than that of the morning? We approach the question by focusing on two processes that may facilitate the cascade of defaults in the interbank networks, namely the timing of trades and network structure. The various mechanisms that underlie occurrences of network cascades are complex, however, some features of cascades can be explained by network topology.[244] For financial networks, understanding their structure can elucidate how shocks that are initially localized can proliferate within the system via interconnections.[20,27] Another mechanism that can affect spreading phenomena is the temporal structure which can be obtained from the event times, in fact, heterogeneous distribution of inter-event times has been shown to facilitate

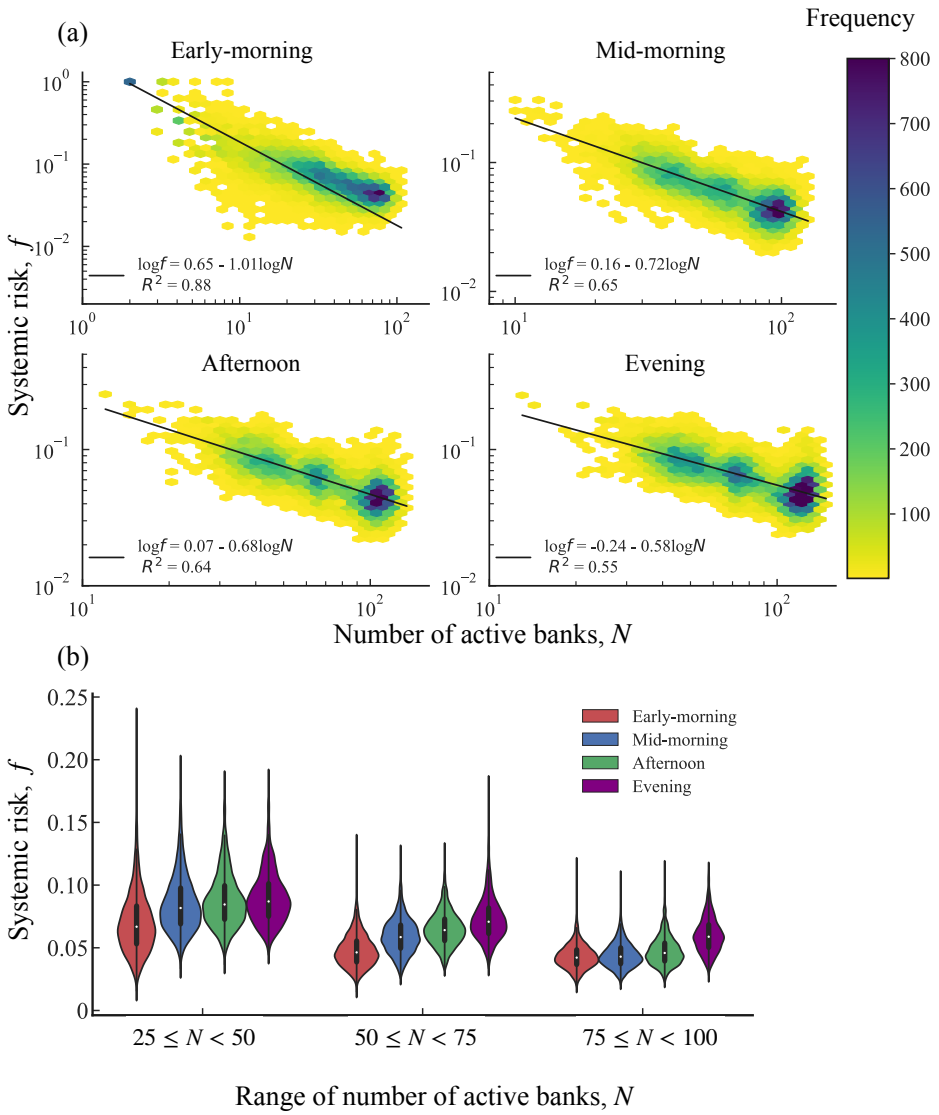

Figure 3.4: Systemic risk for networks in different time periods. (a) Joint distribution of systemic risk and network size for time categories: *Early-morning* (<11:00), *Mid-morning* (11:00–12:59), *Afternoon* (13:00–14:59) and *Evening* (≥15:00). The solid line denotes a log-linear regression of the relationship between f and N. For all time categories, the systemic risk f has a strong anti-correlation with the network size as indicated by larger $R^2 \geq 0.55$. (b) To control for the strong correlation, we compare the risk of the network of a similar size. The risk in the evening is up to 1.5 times higher than that for the morning. The distributions of f in later times are significantly higher at the 5% significance level (Kolmogorov-Smirnov test).

propagation in some cases[400,401] but hinder it in others.[46,163,164,402–404] To control for the network size effect, we focus on the networks with size $75 \leq N < 100$ in each of the four periods (Early-morning, Mid-morning, Afternoon and Evening). Also, a bank fails if and only if it is first exposed

to risk, hence, we measure the initial defaulter's ability to reach the rest of the network (via a directed path) and then note the size of the set of banks at risk expressed as a fraction of all active banks (i.e., the reachable fraction).

As a proxy of the initial defaulter's ability to reach susceptible banks via a directed path (i.e., the initial defaulter's '*reachability*'), we use the geodesic distance d_{ji}. A bank is more likely to be exposed to risk if it is close to the initial defaulter. Therefore, we conjecture that systemic risk increases if the initial defaulter is in close proximity to many banks in the network. As a measure of the initial defaulter's proximity to other banks, we use the geodesic distance, a simple widespread measure of network proximity. Note that, default risk flows in the opposite direction to the original direction of an edge.

To investigate the effect of network distance on cascade size, we first test whether a bank is more likely to default the closer it is to the initial defaulter. Based on the Fig. 3.5a it is reasonable to expect that a shorter distance to the initial defaulter may increase a bank's chances of a default. As shown in Fig. 3.5a, most banks that have defaulted are in fact, directly connected with the initial defaulter (i.e., $d = 1$). To confirm, we calculate the likelihood of default at a given distance d, by first grouping banks by the distance and computing the fraction of the defaulters within each group, or equivalently the probability of default given a distance. Therefore, for each distance group, we compute the default probability for all networks and then take the average. We find that there is virtually no difference in the likelihood of the default with respect to the distance from the initial defaulter (Fig. 3.5b).

We also consider that, a bank is exposed to risk *only if* it is reachable from the initial defaulter, which implies that cascade size is inherently constrained by the number of reachable banks from the initial defaulter. Therefore, one reason for the high risk for the evening network is because more banks are reachable from the initial defaulter in the evening than in the morning. To test this hypothesis, we compute the fraction of banks that can be reached by the initial defaulter (via a directed path) i.e., the reachable fraction of banks, conditioned on $75 \leq N \leq 99$ to control for the network size effect. The fraction of reachable banks increases in time which suggests that more

banks are exposed to initial risk in later networks (Fig. 3.5c, *blue boxes*). Moreover, this pattern in the reachable fraction is followed closely by systemic risk f (Fig. 3.5c, *red circles*). We note that the reachable cluster reflects the worse-case where all banks default once exposed to initial risk. Systemic risk, therefore, cannot exceed this limit because without a directed path between the initial defaulter and other banks, risk will not propagate.

3.4.3. Effect of network structure and temporal correlations on systemic risk

While we have focused on the impact of network size and the reachability of initial defaulters on risk, it is possible that other inherent heterogeneity in the interbank networks has a greater impact on systemic risk. For example, the distribution of the degree (i.e., the number of edges emanating from a node) and the strength (i.e., the sum of the weights on edges emanating from a node) predict well the systemic risk in networks.[394] Meanwhile, the timing of events affect the frequency of transactions and this can either impede[402,404] or facilitate cascades.[42,49] We find that the interbank networks are heterogeneous in terms of the degree and strength distributions (Fig. 3.2d), and the timing of trading events (Fig. 3.2c). These observations lead us to ask whether heterogeneity in degree, strength and trading activities explain the diurnal pattern in systemic risk f. We investigate the extent of the effects by employing three null models as follows. Each null model randomizes the original networks while maintaining the degree (i.e., in-/out-) of each bank, the order of trade events, or the time on trade events. For each reference model, we generate 100 realizations.

Network structure

We employ the *enhanced configuration model* (ECM) as a null model that preserves the degree and strength distributions. The ECM is built based on the maximum entropy approach.[405] Consider a directed and weighted network represented as the weighted adjacency matrix $\boldsymbol{W} = (W_{ij})$, where W_{ij} is the weight of the edge from node i to node j. In the ECM, one samples a randomized network, denoted by $\tilde{\boldsymbol{W}}$, from a probability distribution P over all networks composed of the same set of nodes with the original network. One finds the probability P by maximizing the entropy — a quantity that measures the randomness — with constraints on the expected degree and strength

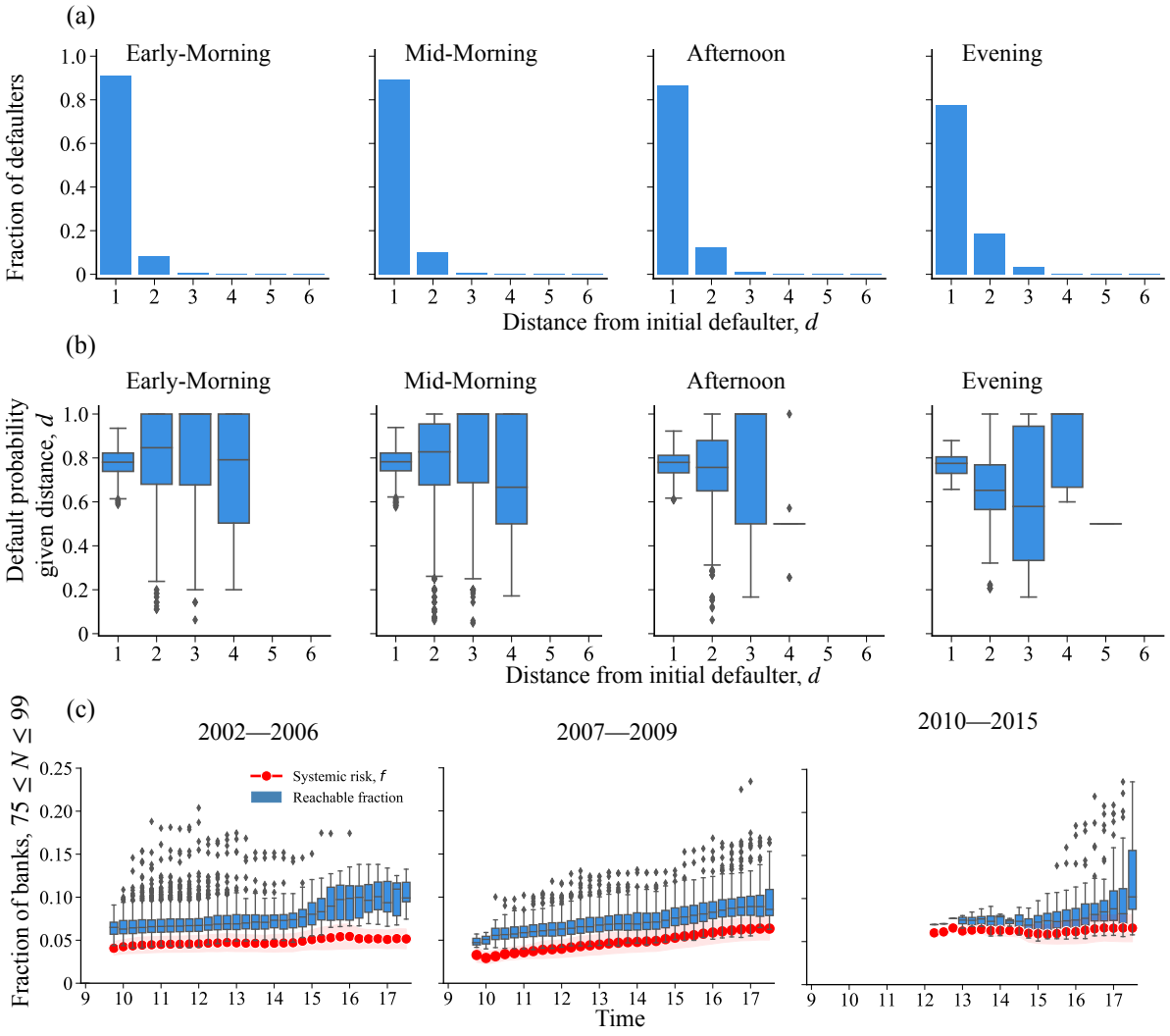

Figure 3.5: Reachable fraction as an approximation of systemic risk, f. (a-b) Intraday networks during 2002–2006. (a) Fraction of defaulters at distance d from the initial defaulter. (b) Fraction of defaulters among banks at distance d from the initial defaulter. (c) Fraction of banks that are reachable by the initial defaulter. Systemic risk is close to the reachable fraction of active banks which is effectively an upper bound for f. For a-c, the average is taken over all networks with size $75 \leq N < 100$. The figures for 2007–2009 and 2010–2015 that correspond to a-b are shown in Fig. 3.E.1 and Fig. 3.F.1

of each node to be equal to those for the original network, i.e.,

$$\max_{P} \; -\int P(\tilde{\boldsymbol{W}}) \ln P(\tilde{\boldsymbol{W}}) d\tilde{\boldsymbol{W}}, \tag{3.4}$$

subject to

$$d_i^{\pm}(\boldsymbol{W}) = \int d_i^{\pm}(\tilde{\boldsymbol{W}}) P(\tilde{\boldsymbol{W}}) \mathrm{d}\tilde{\boldsymbol{W}}, \quad i = 1, 2, \ldots, N, \tag{3.5}$$

$$s_i^{\pm}(\boldsymbol{W}) = \int s_i^{\pm}(\tilde{\boldsymbol{W}}) P(\tilde{\boldsymbol{W}}) \mathrm{d}\tilde{\boldsymbol{W}}, \quad i = 1, 2, \ldots, N, \tag{3.6}$$

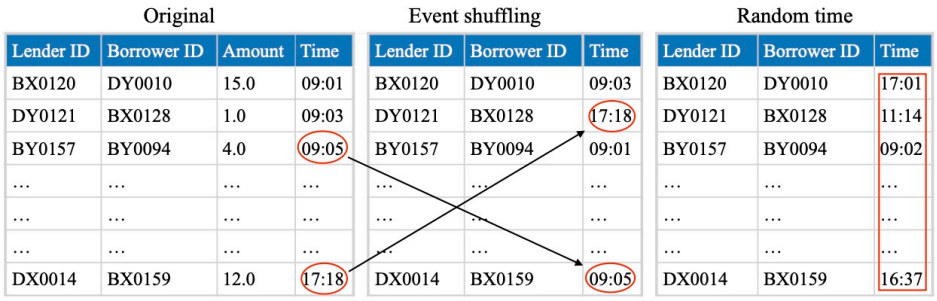

Figure 3.6: Schematic of reference null models that eliminate temporal structure. Event shuffling (ES) assigns a time which is selected randomly from the set of original event times, to each transaction. Random time (RT) method ignores the original transaction times on trades within a day and repeatedly selects times between 9:00–17:30 uniformly at random until all trades for that day have been assigned a time.

where $d_i^+(\boldsymbol{W}) = \sum_j h(W_{ij})$ and $d_i^-(\boldsymbol{W}) = \sum_j h(W_{ji})$ are the out-degree and in-degree of node i for $\boldsymbol{W}$, respectively, and $h(x) = 1$ if $x > 0$, and $h(x) = 0$ otherwise. $s_i^+(\boldsymbol{W}) = \sum_j W_{ij}$ and $s_i^-(\boldsymbol{W}) = \sum_j W_{ji}$ are the out-strength and in-strength of node i for $\boldsymbol{W}$, respectively. See Section 3.A in Supplementary Information (SI) for details.

Systemic risk for the random networks follows a similar diurnal rhythm observed for the original network, with a difference in that the magnitude of f at its peak is lower (Fig. 3.7a). The lower peak in f is partly attributed to the fragmentation of random networks into many disconnected components, which particularly occurs when the network is small. If the network is large, systemic risk is well predicted by the degree and strength distribution which is inline with previous studies.[394]

Trade timings and other temporal correlations

The long-tailed distribution of inter-event times highlight the bursty nature of trades in the interbank data set (Fig. 3.2c) which can mitigate or facilitate spreading behaviour. Here, we use two reference models to determine how f is impacted by the order and timings of trades.

Event shuffling(ES): First, we consider event shuffling (ES) which randomly permutes the original timestamps on trading events for a single day (Fig. 3.6, *middle*). This method retains the number of events and the total traded amount for a bank pair while shuffling the times for all trading events. In other words, ES can produce a different network at each time during a day but the same network

as the original at closing time (i.e., daily network).

In the ES model, we find a marked peak of risk f in the morning (Fig. 3.7, *middle*) which is attributed to the small network size at this time. As is the case for the original network, the morning network is the smallest in the ES model (Fig. 3.C.1, *middle*). Although, the inter-event timing between consecutive trades in the ES model is the same as the original data (i.e., ES preserves the original timestamps), heterogeneity in inter-event times for single links are interrupted. ES therefore allows us to test whether risk f is explained solely by this type of heterogeneity in timing between trades. Since we still observe a peak in risk around 9:00 in the ES model, we conclude that despite a lower f, systemic risk is not solely influenced by heterogeneous inter-event times. Notwithstanding, maximum intraday f in ES is not only lower than that of original networks, but it is comparable with risk in the daily ES network (Fig. 3.D.1).

Random time(RT): In addition to the order of events, we further randomize the timing of events. To this end, we distribute the timestamps of events uniformly at random between 9:00–17:30 in each day (Fig. 3.6, *right*). RT networks display a similar diurnal pattern as original networks; however, the magnitude of f at 9:00 is noticeably lower (Fig. 3.7c). In the RT model, trades are distributed more uniformly across time bins, disrupting the the timing between trades for individual banks hence Lenders (borrowers) accumulate losses (obligations/debt) more slowly. In other words, burstiness of bank interaction in the original networks facilitates the spread of contagion, which is consistent with previous studies .[42,49] Up to a certain period, the RT model creates networks that are less bursty in trade activities than original networks. The randomization method maintains daily activities within the original daily time window of trades (i.e., 9:00–17:30). However, due to the finite size of the daily networks, the bursty activity pattern observed in original networks re-emerges towards market closing time. In fact, by 12:00 the original network size is reclaimed in all the null models (i.e., 80% of daily network size) (Fig. 3.7, *inset* a-c). This highlights why, despite a lower peak in RT networks at 9:00, f is comparable with the original networks in subsequent periods. Furthermore, this also implies that the features that give rise to expanding reachable fraction in the evening (Section 3.4.2) are not interrupted by RT.

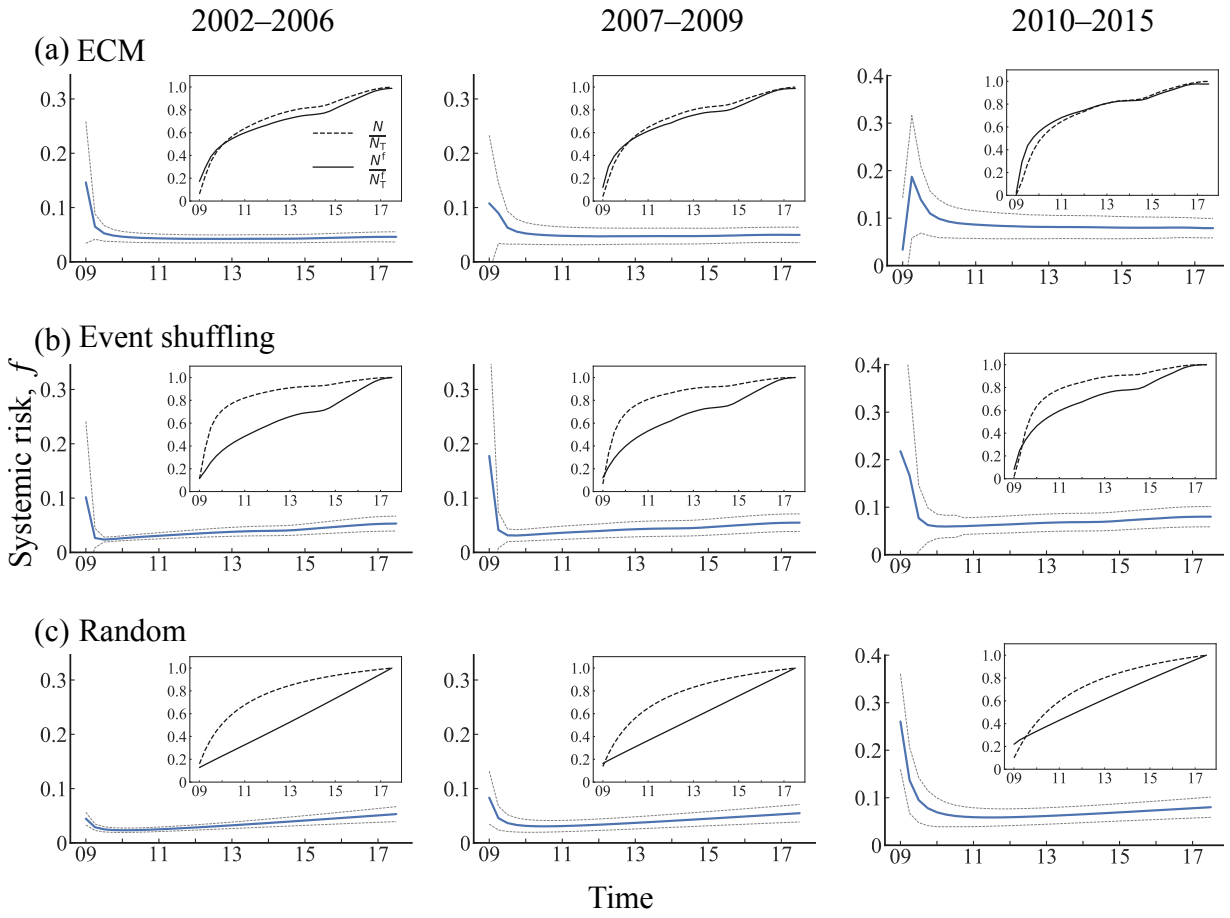

Figure 3.7: Diurnal pattern of systemic risk in the three reference models. (a) Enhanced configuration model which rewires the edges while maintaining the average in-/out-degree and average in-/out-strength of banks in the interbank network. (b) Event shuffling (ES) model randomly shuffles the order of trades. (c) Random time (RT) model distributes the timings of trades uniformly at random. *Insets:* N_T and N_T^{f} respectively show how the numbers of active banks and defaulted banks change during the daily time window.

3.5. Discussion

Our analysis reveals a diurnal pattern of risk propagation, in which the market experiences the highest risk in the morning but relatively lower risk in most of the remaining time. We investigated the role played by some inherent features of the interbank network: market size, accessibility of initial risk and bursty trading.

Although we demonstrated a strong correlation between risk and network size, it is not exactly clear why smaller networks are riskier. It could be argued that in small networks sufficient banks are not

yet active to enable the risk-sharing benefits often associated with financial networks. Systemic risk has a strong dependence on the network size, making it difficult to compare the risk of networks of different sizes. In fact, systemic risk for the morning networks is considerably larger than that of the evening for most days. However, if we compare the network of a similar size, we find that evening networks are indeed riskier. Our result call for correcting the network size effect so that we can correctly measure the impact of risk.

From the null models, we also find that although the degree distribution explains the level of systemic risk in interbank networks to some degree, it does not explain why risk is slightly higher in networks closer to market closing time. Even in destroying the order and timing of trades, the original diurnal pattern of systemic risk is not disrupted. However, when we compare networks of the same size, we find that close to market opening time, most banks that default have a direct lending relationship with the initial defaulter while in later times, the group of banks that are accessible to the initial defaulter expands in time. This means that more banks become exposed to risk in networks near market closing time.

Despite focusing on systemic risk generated by random initial shocks, risk can also originate from targeted initial defaults on the basis of nodes' position in the network or their characteristic of being net borrowers (net lenders). This can be addressed in future research on temporal interbank networks to understand how risk is impacted by the dynamism of node properties. We also suggest further investigation into whether the likelihood of a default differs between direct and indirect lenders to the initial defaulter since, a higher risk among indirect lenders may partly explain the tendency for systemic risk to be higher in the evening than in the morning. Furthermore, we restricted certain bank responses given a default such as, allowing lenders to suffer complete loss of loans to defaulters and preventing the sale of assets by lenders to offset losses. These assumptions could exaggerate systemic risk (i.e., representing the worse-case) because in reality, banks will respond to reduce the impact of a loss. However, we elected to focus on banks' short-run reactions because some responses — such as recouping a portion of defaulted loans — could be infeasible and time-consuming.

By taking a dynamic modelling approach to systemic risk analysis in interbank networks, we illustrate that the system is more fragile at different times in a day. Interbank vulnerability is underpinned by the simultaneous interaction of banks' activity pattern and network architecture that entails market size and banks' interdependencies. In many ways, current policies aimed at maintaining stability in financial systems rely on information almost entirely about the architecture of the network. However, incorporating temporal characteristics highlights that, while market size affects risk at different times, when markets are the same size; high interconnectedness of risk between banks drives the system's fragility. The dimension of time in systemic risk analysis reflects more realistically, the setup of the interbank system and it can provide useful insights into how regulators can monitor and, to some extent, anticipate growing risk to guide the most appropriate responses that ensure stability.

Appendix

3.A. Enhanced configuration model

We show how we solve the entropy maximization problem defined by Eqs. 3.4, 3.5 and 3.6. One rewrites the constrained entropy maximization problem as an unconstrained maximization problem using the Lagrangian, which is given by

$$\begin{aligned}\mathcal{J} = &-\int P(\tilde{\boldsymbol{W}}) \ln P(\tilde{\boldsymbol{W}}) \mathrm{d}\tilde{\boldsymbol{W}} \\ &+ \sum_i \alpha_i^+ \left[\int d_i^+(\tilde{\boldsymbol{W}}) P(\tilde{\boldsymbol{W}}) \mathrm{d}\tilde{\boldsymbol{W}} - d_i^+(\boldsymbol{W}) \right] + \sum_i \alpha_i^- \left[\int d_i^-(\tilde{\boldsymbol{W}}) P(\tilde{\boldsymbol{W}}) \mathrm{d}\tilde{\boldsymbol{W}} - d_i^-(\boldsymbol{W}) \right] \\ &+ \sum_i \beta_i^+ \left[\int s_i^+(\tilde{\boldsymbol{W}}) P(\tilde{\boldsymbol{W}}) \mathrm{d}\tilde{\boldsymbol{W}} - s_i^+(\boldsymbol{W}) \right] + \sum_i \beta_i^- \left[\int s_i^-(\tilde{\boldsymbol{W}}) P(\tilde{\boldsymbol{W}}) \mathrm{d}\tilde{\boldsymbol{W}} - s_i^-(\boldsymbol{W}) \right] \\ &+ \gamma \left[\int P(\tilde{\boldsymbol{W}}) \mathrm{d}\tilde{\boldsymbol{W}} - 1 \right], \end{aligned} \tag{3.7}$$

where $\alpha_i^{\pm}$, $\beta_i^{\pm}$ $(i = 1, 2, \ldots, N^{\mathrm{a}})$ and γ are the Lagrange multipliers. By taking the functional derivative with respect to $P(\tilde{\boldsymbol{W}})$, we have

$$\frac{\partial \mathcal{J}}{\partial P} = -\ln P(\tilde{\boldsymbol{W}}) + \sum_i \alpha_i^+ d_i^+(\tilde{\boldsymbol{W}}) + \sum_i \alpha_i^- d_i^-(\tilde{\boldsymbol{W}}) + \sum_i \beta_i^+ s_i^+(\tilde{\boldsymbol{W}}) + \sum_i \beta_i^- s_i^-(\tilde{\boldsymbol{W}}) + \gamma + \text{constant}. \tag{3.8}$$

Solving $\partial \mathcal{J} / \partial P = 0$ with respect to $P(\tilde{\boldsymbol{W}})$ and setting γ such that $\int P(\tilde{\boldsymbol{W}}) \mathrm{d}\tilde{\boldsymbol{W}} = 1$ lead to the enhanced configuration model (ECM):[406]

$$P\left(\tilde{\boldsymbol{W}}\boldsymbol{\theta}\right) = \frac{1}{C\left(\boldsymbol{\theta}\right)} \exp\left[\sum_i \left(\alpha_i^+ d_i^+(\tilde{\boldsymbol{W}}) + \alpha_i^- d_i^-(\tilde{\boldsymbol{W}}) + \beta_i^+ s_i^+(\tilde{\boldsymbol{W}}) + \beta_i^- s_i^-(\tilde{\boldsymbol{W}}) \right) \right], \tag{3.9}$$

where $\boldsymbol{\theta} = (\alpha_i^+, \alpha_i^-, \beta_i^+, \beta_i^-)_i$ is the parameters for the ECM, and $C\left(\boldsymbol{\theta}\right)$ is the normalization constant. We rewrite $d_i^{\pm}$ and $s_i^{\pm}$ using $\tilde{W}_{ij}$, which yields

$$P(\tilde{\boldsymbol{W}}|\boldsymbol{\theta}) = \frac{1}{C(\boldsymbol{\theta})} \prod_i \prod_j \exp\left[(\alpha_i^+ + \alpha_j^-) h(\tilde{W}_{ij}) + (\beta_i^+ + \beta_j^-) \tilde{W}_{ij} \right]. \tag{3.10}$$

We find $\boldsymbol{\theta}$ by fitting $P(\tilde{\boldsymbol{W}}\boldsymbol{\theta})$ to the original network, $\boldsymbol{W}$, using the maximum likelihood estimation.[406] In other words, we seek $\boldsymbol{\theta}$ by maximizing the log-likelihood $\ln P(\boldsymbol{W}\boldsymbol{\theta})$. In the original paper on the ECM,[406] the authors employed a root finding algorithm. Here we employ a gradient descent algorithm, which is computationally less expensive than the root finding algorithm. Note

that the gradient descent algorithm will find the global maximum of $\ln P(\boldsymbol{W}|\boldsymbol{\theta})$ because $\ln P(\boldsymbol{W}|\boldsymbol{\theta})$ is a concave function with respect to $\boldsymbol{\theta}$.

The gradients for the log-likelihood with respect to $\boldsymbol{\theta}$ are given by

$$\frac{\partial \ln P\left(\boldsymbol{W}\boldsymbol{\theta}\right)}{\partial \alpha_i^{\pm}} = d_i^{\pm}(\boldsymbol{W}) - \mathbb{E}_{P(\tilde{\boldsymbol{W}}\boldsymbol{\theta})}\left[d_i^{\pm}(\tilde{\boldsymbol{W}})\right], \tag{3.11}$$

$$\frac{\partial \ln P\left(\boldsymbol{W}\boldsymbol{\theta}\right)}{\partial \beta_i^{\pm}} = s_i^{\pm}(\boldsymbol{W}) - \mathbb{E}_{P(\tilde{\boldsymbol{W}}\boldsymbol{\theta})}\left[s_i^{\pm}(\tilde{\boldsymbol{W}})\right], \tag{3.12}$$

where $\mathbb{E}_{P(\tilde{\boldsymbol{W}}|\boldsymbol{\theta})}\left[\tilde{x}\right]$ is the expected value for a random variable $\tilde{x}$ under probability distribution $P(\tilde{\boldsymbol{W}}|\boldsymbol{\theta})$.

The gradients involve the expectation $\mathbb{E}_{P(\tilde{\boldsymbol{W}}\boldsymbol{\theta})}\left[d_i^{\pm}(\tilde{\boldsymbol{W}})\right]$ and $\mathbb{E}_{P(\tilde{\boldsymbol{W}}\boldsymbol{\theta})}\left[s_i^{\pm}(\tilde{\boldsymbol{W}})\right]$,which we derive as follows. With the ECM, the weight of edge (i,j) is independent of that for other edges (k,ℓ). Therefore, the normalized constant $C(\boldsymbol{\theta})$ is the product of the normalization constants for each node pair, i.e.,

$$C(\boldsymbol{\theta}) = \prod_i \prod_j C_{ij}(\theta_i, \theta_j), \tag{3.13}$$

where $C_{ij}(\theta_i,\theta_j)$ is the normalization constant for node pair (i,j), and $\theta_i = (\alpha_i^+, \alpha_i^-, \beta_i^+\beta_i^-)$. The pairwise normalization constant $C_{ij}(\theta_i,\theta_j)$ is given by

$$\begin{aligned} C_{ij}(\theta_i,\theta_j) &= \sum_{w=0}^{\infty} \exp\left[(\alpha_i^+ + \alpha_j^-)h(W_{ij}) + (\beta_i^+ + \beta_j^-)W_{ij}\right] \\ &= 1 + \exp\left(\alpha_i^+ + \alpha_j^-\right) \sum_{w=1}^{\infty} \exp\left[\left(\beta_i^+ + \beta_j^-\right) w\right]. \end{aligned} \tag{3.14}$$

Substituting Eqs. (3.13) and (3.14) into Eq. (3.10), we have

$$\begin{aligned} P(\boldsymbol{W}|\boldsymbol{\theta}) &= \prod_i \prod_j \frac{1}{C_{ij}(\theta_i,\theta_j)} \exp\left[(\alpha_i^+ + \alpha_j^-)h(W_{ij}) + (\beta_i^+ + \beta_j^-)W_{ij}\right] \\ &= \prod_i \prod_j \frac{\exp\left[(\alpha_i^+ + \alpha_j^-)h(W_{ij}) + (\beta_i^+ + \beta_j^-)W_{ij}\right]}{1 + \exp\left(\alpha_i^+ + \alpha_j^-\right) \sum_{w=1}^{\infty} \exp\left[\left(\beta_i^+ + \beta_j^-\right) w\right]} \\ &= \prod_i \prod_j \frac{\exp\left[\left(\alpha_i^+ + \alpha_j^-\right) h(W_{ij})\right] \exp\left[\left(\beta_i^+ + \beta_j^-\right) W_{ij}\right] \left[1 - \exp\left(\beta_i^+ + \beta_j^-\right)\right]}{1 - \exp\left(\beta_i^+ + \beta_j^-\right) + \exp\left(\alpha_i^+ + \alpha_j^-\right) \exp\left(\beta_i^+ + \beta_j^-\right)}. \end{aligned} \tag{3.15}$$

The expected value for $h(W_{ij})$ under $P(\boldsymbol{W}|\boldsymbol{\theta})$ is given by

$$\begin{aligned}\mathbb{E}_{P(\tilde{\boldsymbol{W}}|\boldsymbol{\theta})}\left[h\left(\tilde{W}_{ij}\right)\right] &= 1 - \frac{1-\exp(\beta_i^+ + \beta_j^-)}{1-\exp\left(\beta_i^+ + \beta_j^-\right) + \exp\left(\alpha_i^+ + \alpha_j^-\right)\exp\left(\beta_i^+ + \beta_j^-\right)} \\ &= \frac{\exp\left(\alpha_i^+ + \alpha_j^-\right)\exp\left(\beta_i^+ + \beta_j^-\right)}{1-\exp\left(\beta_i^+ + \beta_j^-\right) + \exp\left(\alpha_i^+ + \alpha_j^-\right)\exp\left(\beta_i^+ + \beta_j^-\right)}. \end{aligned} \tag{3.16}$$

Note that we have exploited relationship $\mathbb{E}_{P(\tilde{\boldsymbol{W}}|\boldsymbol{\theta})}[h(\tilde{W}_{ij})] = P\left(h(W_{ij})=1\right) = 1 - P\left(h(W_{ij})=0\right)$. The expected value for the weight W_{ij} under $P(\boldsymbol{W}|\boldsymbol{\theta})$ is given by

$$\mathbb{E}_{P(\boldsymbol{W}|\boldsymbol{\theta})}\left[\tilde{W}_{ij}\right] = \mathbb{E}_{P(\tilde{\boldsymbol{W}}|\boldsymbol{\theta})}\left[h\left(\tilde{W}_{ij}\right)\right]\sum_{w=1}^{\infty} w\left[1-\exp\left(\beta_i^+ + \beta_j^-\right)\right]\exp\left(\beta_i^+ + \beta_j^-\right)^{w-1}. \tag{3.17}$$

Note that $\sum_{w=1}^{\infty} w\left[1-\exp\left(\beta_i^+ + \beta_j^-\right)\right]\exp\left(\beta_i^+ + \beta_j^-\right)^{w-1}$ is equivalent to the mean of the geometric probability distribution with success probability $1-\exp\left(\beta_i^+ + \beta_j^-\right)$. The mean with success probability p for the geometric distribution is given by $1/p$. Therefore, we have

$$\mathbb{E}_{P(\boldsymbol{W}|\boldsymbol{\theta})}\left[\tilde{W}_{ij}\right] = \frac{\mathbb{E}_{P(\tilde{\boldsymbol{W}}|\boldsymbol{\theta})}\left[h\left(\tilde{W}_{ij}\right)\right]}{1-\exp\left(\beta_i^+ + \beta_j^-\right)}. \tag{3.18}$$

One obtains the gradients (i.e., Eqs. (3.11) and (3.12)) using the expected values for $h(W_{ij})$ and W_{ij}, which are given by Eqs. (3.16) and (3.18).

Gradient descent algorithms has a learning rate (i.e., step size) as a hyper-parameter which controls the amount of changes in the parameter values at each iteration. To determine the learning rate, we use the ADAptive Moment estimation (ADAM),[407] which adjusts the learning rate based on the current and previous gradients at each iteration. We set parameters for the ADAM as $\beta_1 = 0.9$, $\beta_2 = 0.999$ and $\eta = 10^{-3}$.

3.B. In

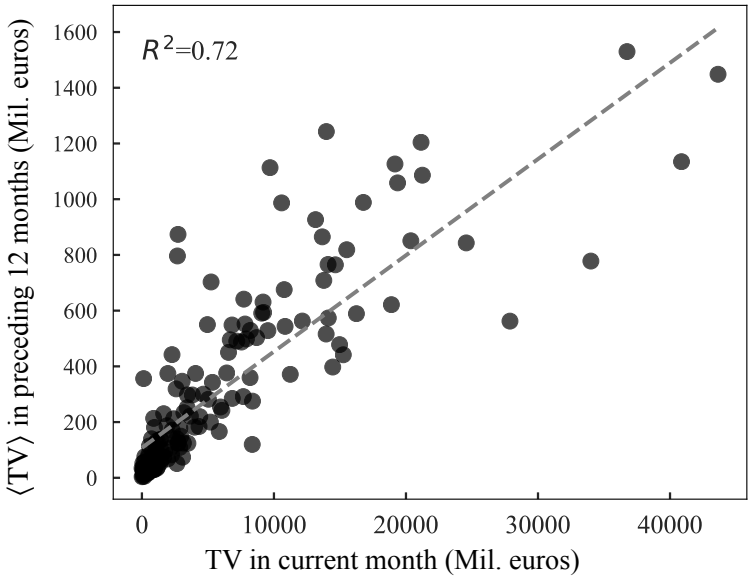

Figure 3.B.1: Daily traded volume averaged over the previous 12-month period against the total traded volume in the current month. For banks with no trade volume (TV) data from the previous one year, we impute the average daily TV from the estimated line (dashed), given the total TV in the current month.

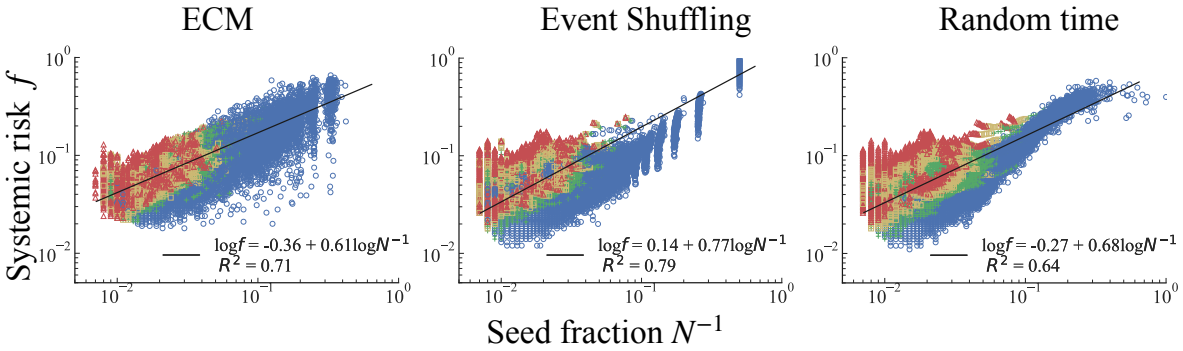

Figure 3.C.1: Relationship between intraday systemic risk and the fraction of initial defaulters in time-randomizing models.

3.D. Interday systemic risk and maximum intraday systemic risk

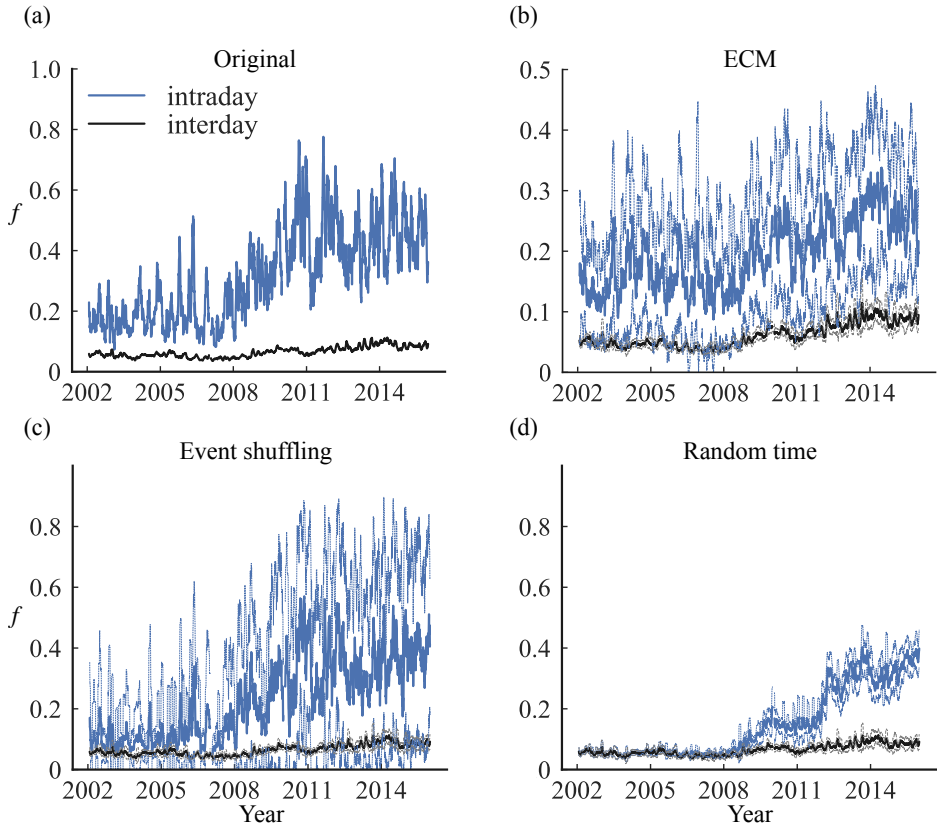

Figure 3.D.1: Interday systemic risk and maximum intraday systemic risk. (a) The empirical data set is compared with (b) ECM that randomly rewires edges in the network while preserving in-/out-degree and in-/out-strength, (c) the ES model that randomly shuffles the order of transactions, and (d) the RT model that randomly assigns the timing of trade uniformly. We compare the 20-day moving average of systemic risk in intraday networks with that of the daily aggregated networks. Maximum intraday risk (solid blue) is higher than the risk of contagious default on the aggregated daily networks (solid black). The dotted line indicate the standard deviation.

3.

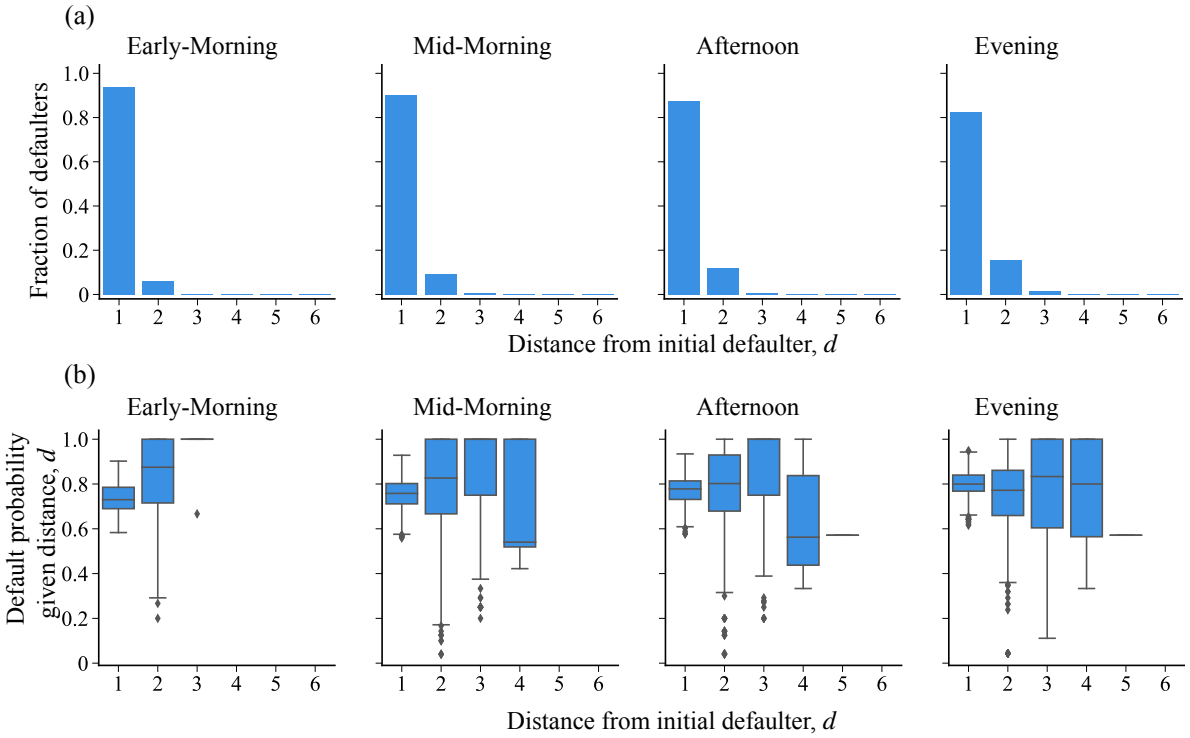

Figure 3.E.1: Reachable fraction as an approximation of systemic risk, f. (a-b) Intraday networks during 2007–2009. (a) Fraction of defaulters at distance d from the initial defaulter. (b) Fraction of defaulters among banks at distance d from the initial defaulter. For a-b, the average is taken over all networks with size $75 \leq N < 100$.

3.

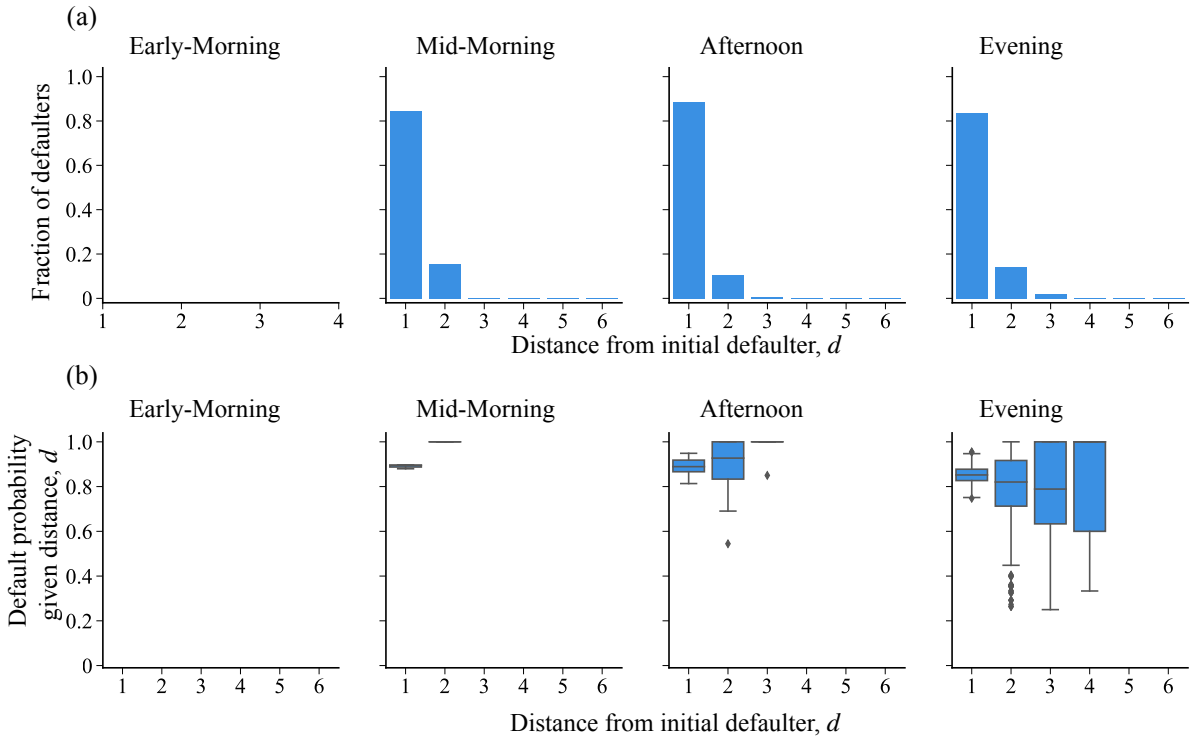

Figure 3.F.1: Reachable fraction as an approximation of systemic risk, f. (a-b) Intraday networks during 2010–2015. (a) Fraction of defaulters at distance d from the initial defaulter. (b) Fraction of defaulters among banks at distance d from the initial defaulter. For a-b, the average is taken over all networks with size $75 \leq N < 100$.

3.G. Distribution of systemic risk in networks for temporal category

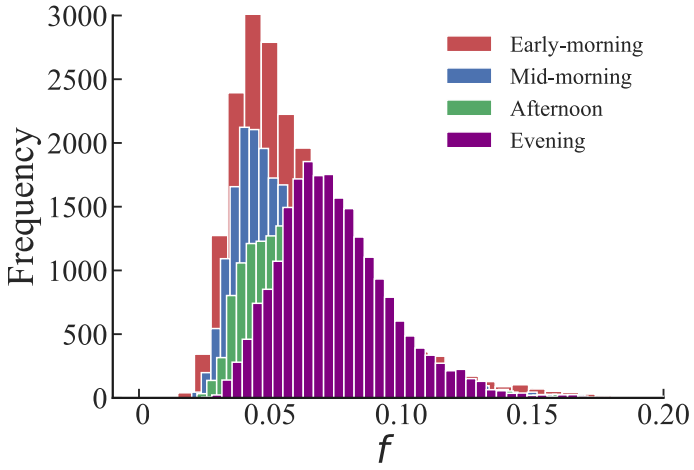

Figure 3.G.1: Distribution of f in networks corresponding to each temporal category. The analysis is restricted to the range in which the four periods share the same network size By doing this we eliminate the disturbance arising from differences in levels of initial risk. From the distributions, we can conclude that Evening networks tend to generate higher systemic risk than at any other period.

3.H. Comparing risk in Early-morning to later periods given range of networks size

Periods	25–50	50–75	75–100
Mid-morning	0.0	0.0	$5.89 \times 10^{-}5$
Afternoon	0.0	0.0	$3.58 \times 10^{-}48$
Evening	0.0	0.0	0.0

Table 3.H.1: KS test comparing samples of systemic risk f in Early-morning with f in later periods given a range of networks size. For each period: H_0:Distribution of f in Early-morning = Distribution of f in later period (e.g., Evening), H_A: Distribution from Early-morning > Distribution of f in later period (e.g., Evening). At the 5% significance level we reject the null hypothesis and conclude that the empirical CDF is larger for Early-morning than for each of the later periods. This means, the probability density function for Early-morning systemic risk is skewed to the left relative to the other periods (Fig. 3.4b).

CHAPTER 4

Identifying the temporal dynamics of densification and sparsification in human contact networks

Shaunette T. Ferguson[1], and Teruyoshi Kobayashi[2,3]

1 Graduate School of Economics, Kobe University, Kobe, Japan

2 Department of Economics, Kobe University, Kobe, Japan

3 Center for Computational Social Science, Kobe University, Kobe, Japan

Abstract

Temporal social networks of human interactions are preponderant in understanding the fundamental patterns of human behavior. In these networks, interactions occur locally between individuals (i.e., nodes) who connect with each other at different times, culminating into a complex system-wide web that has a dynamic composition. Dynamic behavior in networks occurs not only locally but also at the global level, as systems expand or shrink due either to: changes in the size of node population or variations in the chance of a connection between two nodes. Here, we propose a numerical maximum-likelihood method to estimate population size and the probability of two nodes connecting at any given point in time. An advantage of the method is that it relies only on aggregate quantities, which are easy to access and free from privacy issues. Our approach enables us to identify the simultaneous (rather than the asynchronous) contribution of each mechanism in the densification and sparsification of human contacts, providing a better understanding of how humans collectively construct and deconstruct social networks.

4.1. Introduction

Individuals are interacting in unprecedented ways due to advancements in communication technology, which has granted access to human contact data in a variety of social contexts (e.g., mobile calls,[139,205–208] texts,[408,409] email,[209] face-to-face[8,140,255,410,411]). Our understanding of fundamental human behavioral patterns have benefited considerably from these rich data sources in which individuals (i.e., nodes) establish and break existing connections (i.e., edges) with each other, thus driving the evolution of a complex network structure. To capture the dynamics of these systems in which the contacts between nodes occur intermittently, social networks are often modeled using a temporal representation.[16,412]

In social systems, contacts tend to occur periodically because individuals have a choice on how and when to engage with others; hence, at a given point in time, the number of active nodes (N) and the number of edges (M) in the system are changing. Furthermore, many empirical networks exhibit a relationship between total edges and network size that is consistent with a densification scaling property:[55,59,232] $M \propto N^{\gamma}$ with $\gamma > 1$, in which aggregate edges increase superlinearly in network size. In temporal social networks, this dynamical property between N and M is influenced either by i) fluctuations in population size,[57–59] ii) changing probability of node connection,[57] or iii) both.[58] Given a fixed connection probability and changing size of population, the conventional superlinear scaling emerges i.e., $M \propto N^{\gamma}$ with $\gamma > 1$.[57] Conversely, for constant population size and varying connection probability, M exhibits an accelerating growth pattern.[57]

However, many human contact networks exhibit a dynamical N-M relationship that is a mixture of the two behaviors, each appearing either as a growth in M along a straight line or an increasing M along an upward sloping trajectory on log-log scale.[57,58] This type of mixed densification scaling usually appears when individuals are free to enter and exit the system, and opportunities to connect are clearly defined (e.g., during lunch in a work setting) or activities are strictly regulated by a schedule (e.g., events at a conference). At a conference, for instance, it is expected that attendees will limit socialization during times designated for a keynote talk because they are attentive to the speaker. During coffee break, in contrast, they are free to interact with others. The emergence of a

mixed scaling relationship in temporal social networks suggests that the mechanism that describes the dynamical growth of M in N may be alternating occasionally.[58] From this standpoint, a Markov regime-switching model[413,414] is employed in a previous study to estimate the probability that the dynamical source of densification and sparsification is attributed either to changing population size *or* fluctuating intensity in activity level at a given time.[58]

Here, we develop an alternative approach to identify the extent to which changing population and connection probability concurrently influence the dynamics of densification and sparsification in human contact networks. The proposed method, based on numerical likelihood functions, enables the simultaneous estimation of population size (= # active nodes + # isolated nodes) and connection probability in different social networks using a series of (N, M) observations, each corresponding to a given temporal snapshot. By taking this approach, we can gain insight not only into the independent contribution of the two mechanisms but also into how their co-movement influences the emergence of a mixed scaling. While contact lists (or event sequences) usually allow us to observe the number of active individuals who made at least one contact, the number of inactive individuals who were present but have never interacted (i.e., isolated nodes) is often unknown. Our approach also provides an estimate for the number of isolated nodes by relying only on the total numbers of active nodes and edges at a given point in time.

4.2. Methods

4.2.1. Data

We use the following four temporal human-contact networks collected by the SocioPatterns collaboration:[137]

- **Hospital**[415]: Contacts between patients, nurses and doctors at a hospital in Lyon, France on December 7, 2010.
- **Workplace**[416]: Contacts between employees at an office building in France on June 27, 2015.
- **IC2S2-17**[417]: Contacts between conference attendees at the International Conference on Computational Social Science 2017 at GESIS in Cologne, Germany on July 11, 2017.

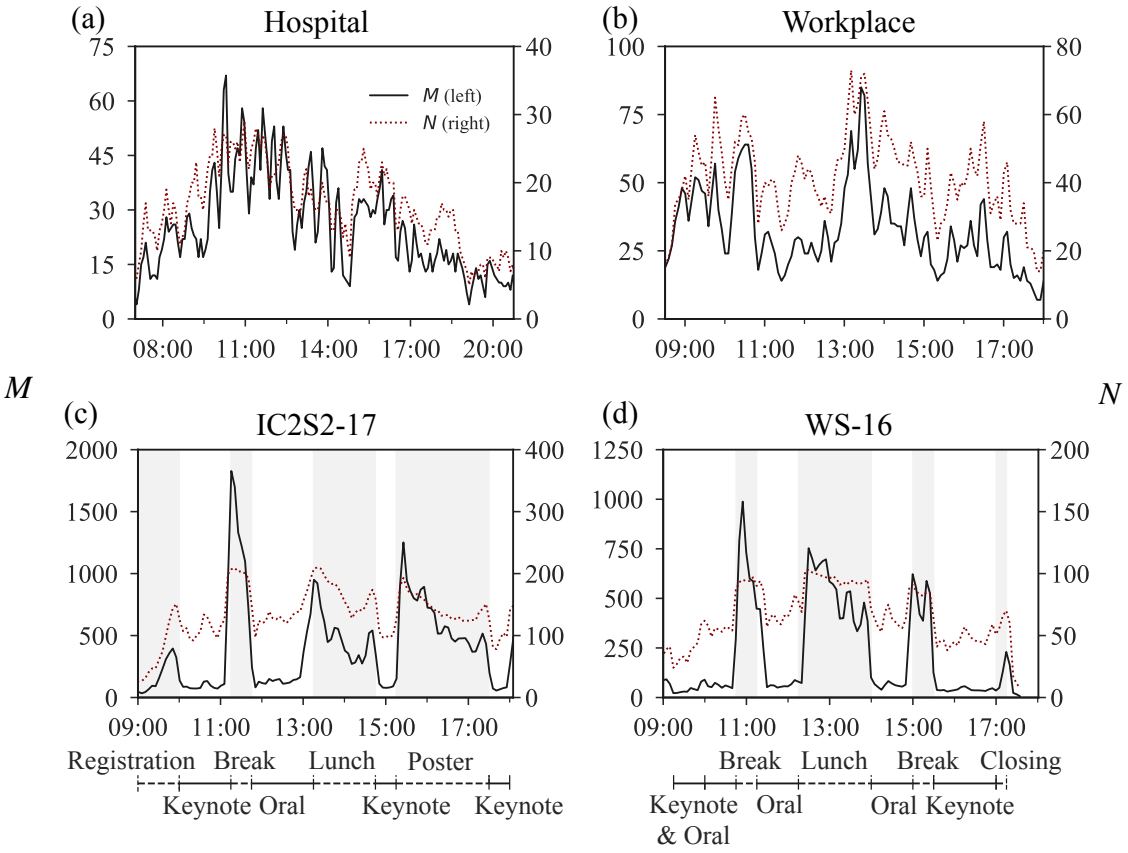

Figure 4.2.1: Evolution of number of edges M and active nodes N in face-to-face networks. The following days are shown for each data set: (a) Hospital on December 7, 2010, (b) Workplace on June 27, 2015, (c) IC2S2-17 on July 11, 2017 and (d) WS-16 on December 1, 2016. Timeline below panels c and d identify time windows for scheduled events. Gray shading highlights unrestricted sessions i.e., registration, break, lunch, poster session and closing remarks.

- **WS-16**[417]: Contacts between participants at the Computational Social Science Winter Symposium 2016 at GESIS in Cologne, Germany on December 1, 2016.

For each data set, interaction between individuals occurs in a physical location, and Radio Frequency Identification (RFID) sensors detect a contact when one person is within 1.5 meters of another.[415–417] Contacts are recorded at 20-second intervals. Such high-resolution data have been frequently used to discover temporal patterns in human behavior[3,16,138,154] or to explore how infectious diseases spread through human contacts.[194,418,419]

We take advantage of the time-resolved data to explore the temporal dynamics of densification

and sparsification in the data sets, by converting them to temporal networks with unweighted and undirected edges. We segment a data set into a snapshot sequence (i.e., a series of networks that are ordered in time[420]), which we construct as sliding time windows. A time window has a duration of 10 minutes and consecutive windows have a 5-minute overlap between them. Then, we connect two nodes if they have at least one contact within the time window, and we extend this to all other time windows to obtain a sequence of snapshots. A node is considered to be active if we detect that it is involved in one or more contact events for a given network snapshot. The numbers of active nodes and edges in a snapshot are denoted by N and M, respectively. The observed N and M are shown in Fig. 4.2.1 (See Fig. 4.A.1 in Supplementary Information for different days).

4.2.2. Estimation

Dynamic hidden-variable model

To explore the densification and sparsification dynamics in temporal networks, we employ a hidden-variable (or a fitness) model with a temporal dimension.[57,58,229,230] The probability that two nodes i and j are connected in time interval $[t, t+\Delta t]$ (henceforth, we refer to as time interval t) is given by

$$p_{ij,t} = 1 - e^{-\kappa_t a_i a_j}, \quad i,j = 1,\ldots,N_{\mathrm{p},t},\ t = 1,\ldots,T, \tag{4.1}$$

where a_i is node i's intrinsic activity level and is assumed to be uniformly distributed on $[0,1]$. Note that the dynamical source of networks is decomposed into two factors: $N_{\mathrm{p},t}$ and κ_t. In time interval t, the overall activity of nodes is captured by $\kappa_t > 0$, which encapsulates changing activity levels due to prespecified schedule, circadian rhythm, etc., while the total number of nodes (i.e., combined sum of active and inactive nodes) is denoted by $N_{\mathrm{p},t}$. It should be noted that the number of active individuals N, at a given time, can be directly observed from contact lists, but the potential number of individuals (i.e., population) in a system is not usually known because contact events naturally exclude non-interacting individuals. Due to the lack of information on population, it is generally not obvious to what extent variations in N and M could be explained by changes in population or activity. Our model takes into account the two possible factors, population and overall activity level, in explaining the observed behaviors of N and M, which cause densification and sparsification

of temporal networks.

As an alternative to the connecting probability in Eq. (4.1), we also show the results for the following specification:

$$p_{ij,t} = \kappa_t a_i a_j, \quad i,j = 1,\ldots,N_{\mathrm{p},t}, t = 1,\ldots,T. \tag{4.2}$$

This specification is employed in previous studies,[57,58] and we confirm that the essential results do not change compared to the baseline model based on Eq. (4.1).

Numerical maximum-likelihood estimation

We estimate the parameters $(\kappa_t, N_{\mathrm{p},t})$ for a given (N_t, M_t) in time interval t, using a numerical maximum-likelihood method. Let $\Theta_\kappa \equiv \left\{\kappa^{(1)},\ldots,\kappa^{(L_\kappa)}\right\}$ and $\Theta_{\mathrm{p}} \equiv \left\{N_{\mathrm{p}}^{(1)},\ldots,N_{\mathrm{p}}^{(L_{\mathrm{p}})}\right\}$ be the sets of all possible values for κ and N_{p}, respectively. The Cartesian product of two sets Θ_κ and Θ_{p} is given as

$$\Theta = \left\{(\kappa, N_{\mathrm{p}}) | \kappa \in \Theta_\kappa, N_{\mathrm{p}} \in \Theta_{\mathrm{p}}\right\}. \tag{4.3}$$

We define $\boldsymbol{\theta}^\ell \in \Theta$ as the ℓ-th element of the set Θ for $\ell = 1,\ldots,|\Theta|$, where $|\Theta| = L_\kappa L_{\mathrm{p}}$ is the cardinality of Θ, i.e., the total number of combinations (κ, N_{p}).

Our maximum-likelihood estimation proceeds as follows:

1. For a given $\boldsymbol{\theta}^\ell$, generate an unweighted and undirected network based on probabilities $\{p_{ij}\}$ for $i > j$. By repeating the network generation S times, one can obtain a sequence of combinations $\left\{\left(N^{(s)}, M^{(s)}\right)\right\}_{s=1}^{S}$, where $N^{(s)}$ and $M^{(s)}$ respectively denote the number of active nodes and the number of edges observed in the s-th simulation. We set $S = 10^4$.

2. Count the number of appearances of each unique combination in $\left\{\left(N^{(s)}, M^{(s)}\right)\right\}_{s=1}^{S}$ and express as a fraction of the number of runs S to get the joint distribution $f_\ell(N, M|\boldsymbol{\theta}^\ell)$, i.e., the likelihood function for a given $\boldsymbol{\theta}^\ell$.

3. Repeat steps 1 and 2 to obtain a set of likelihood functions $\left\{f_\ell(N, M|\boldsymbol{\theta}^\ell)\right\}_{\ell=1}^{|\Theta|}$.

4. Select $\ell = \ell^* (\leq |\Theta|)$ such that $f_{\ell^*}(N_t, M_t|\boldsymbol{\theta}^{\ell^*})$ yields the highest probability for a given

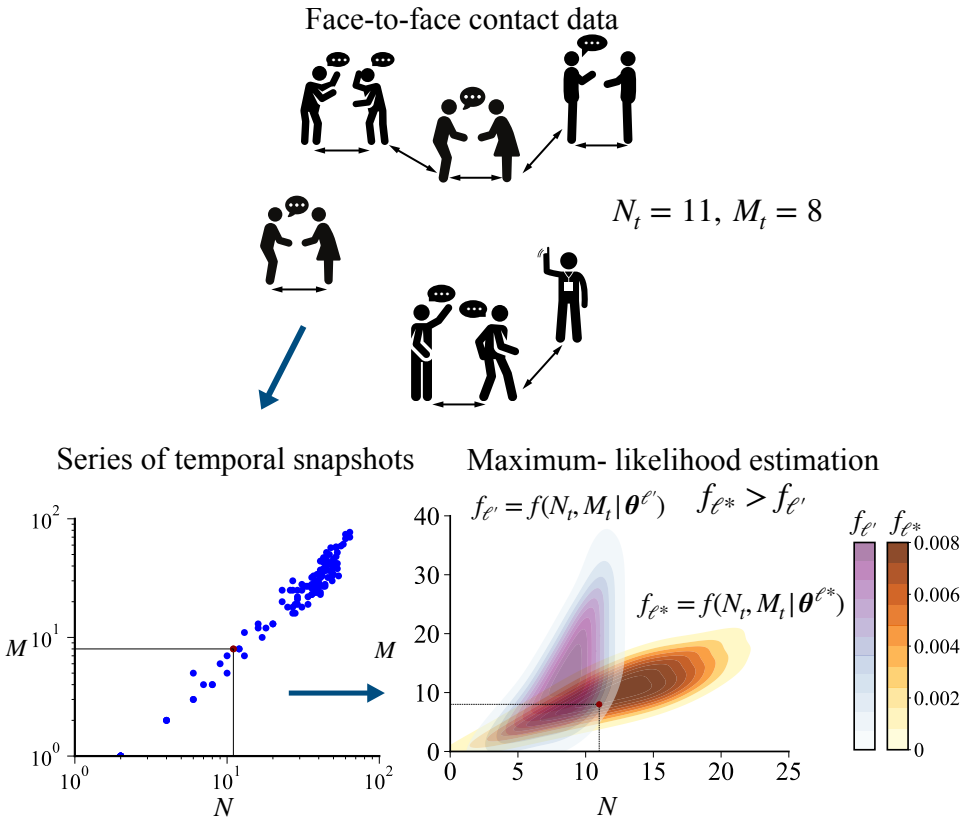

Figure 4.2.2: Schematic of maximum-likelihood estimation of κ and $N_{\rm p}$. The top panel shows contact data that gives a combination (N_t, M_t). The sequence $\{(N_t, M_t)\}_{t=1}^{T}$ is plotted in the N-M space, in which a particular combination of $(11, 8)$ is highlighted in red (bottom left). The joint distributions of (N, M), or likelihood functions, are generated using the hidden-variable model for different combinations of $(\kappa, N_{\rm p}) = \boldsymbol{\theta}$, with each indexed by ℓ' and ℓ^* (bottom right). A likelihood function gives the probability of observing a network with N nodes and M edges, for a given combination of $(\kappa, N_{\rm p})$. The maximum-likelihood estimators, denoted by $\widehat{\kappa}_t$ and $\widehat{N}_{{\rm p},t}$, are given by a combination of κ and $N_{\rm p}$ associated with the maximum-likelihood function $f_{\ell^*} = f(N_t, M_t|\boldsymbol{\theta}^{\ell^*})$.

empirical observation (N_t, M_t). The maximum-likelihood estimators $\widehat{\kappa}_t$ and $\widehat{N}_{{\rm p},t}$ are thus given by

$$\left(\widehat{\kappa}_t, \widehat{N}_{{\rm p},t}\right) = \boldsymbol{\theta}^{\ell^*}, \tag{4.4}$$

where $\ell^* = \arg\max_\ell\ f_\ell(N_t, M_t|\boldsymbol{\theta}^\ell)$.

5. Repeat steps 1–4 for all time intervals $t = 1, \ldots, T$.

A schematic of the estimation method is presented in Fig. 4.2.2.

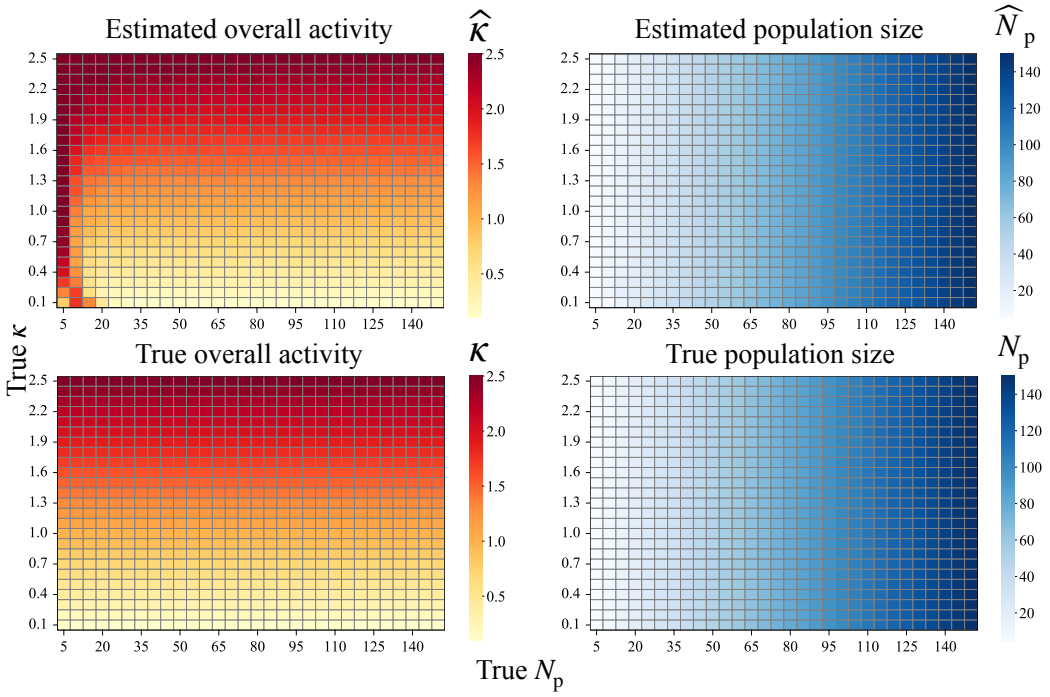

Figure 4.2.3: Validation of the maximum-likelihood estimation method. The upper panels show estimated overall activity level $\widehat{\kappa}$ and population size $\widehat{N}_{\mathrm{p}}$, given the respective true values of N_{p} ranging from 5 to 150 (incremented by 5) and κ ranging from 0.1 to 2.5 (incremented by 0.1). The performance of the maximum-likelihood estimators are respectively assessed against the true overall activity κ and true population size N_{p} shown in the lower panels. The estimates $\widehat{N}_{\mathrm{p}}$ and $\widehat{\kappa}$ are obtained based on Eq. (4.1).

4.2.3. Validation Analysis

We perform a validation analysis to assess the accuracy of our numerical maximum-likelihood method in estimating the model parameters. For each combination of the true values (N_{p}, κ), we generate synthetic networks based on the baseline model (Eq. 4.1) and apply the estimation method to obtain $\widehat{N}_{\mathrm{p}}$ and $\widehat{\kappa}$. Then we take the average of the respective estimated values over 1,000 runs.

Based on the comparison of estimated values with their respective true values, the maximum-likelihood estimators perform well in recovering the true population size and overall activity (Fig. 4.2.3). It should be noted, however, that $\widehat{\kappa}$ is sensitive to small values of the true population size (i.e., $N_{\mathrm{p}} \leq 50$), in that $\widehat{\kappa}$ overestimates true κ (Fig. 4.2.3, *left*). For larger population sizes (e.g.,

$N_{\mathrm{p}} > 50$), the performance of the estimation method improves considerably, with deviations, if any, being much smaller. The reason for the low accuracy when N_{p} is small is that our method relies on N and M to identify the most likely combination of the model parameters; a particular combination (N, M) does not necessarily have a one-to-one correspondence with a particular (κ, N_{p})-combination especially when the network is small, thereby making it possible to see large deviations as exhibited in Fig. 4.2.3 (*left*). We also show another validation in which one of the two parameters is fixed (Fig. 4.B.1).

4.3. Results

4.3.1. Evolution of κ and N_{p} in temporal social networks

Estimation results for N_{p} and κ are shown in Figs. 4.3.1 and 4.3.2, respectively. Fluctuating $\widehat{N}_{\mathrm{p},t}$ and $\widehat{\kappa}_t$ in the four data sets indicate that, quite often, both are changing simultaneously. Similar findings are seen in other days for the model based on Eq. (4.1) (Figs. 4.C.1 and 4.D.1) and also for the alternative probability based on Eq. (4.2) (Figs. 4.E.1–4.H.1).

A source of these shifts in κ and N_{p} would be stemming from situational conditions that may affect human behavior in each location. One example is a pre-specified schedule in an academic conference that rules the behavior of participants.[58,421–423] For the IC2S2-17 and WS-16 data, we can compare the shifts in the estimated values with the official programs that are available publicly.[424,425] In contrast, a strict schedule of activities is not stipulated in the Hospital and Workplace data, thus precluding a similar kind of assessment.

Dynamic behavior of estimated population size $\widehat{N}_{\mathrm{p},t}$.

Fluctuations of $\widehat{N}_{\mathrm{p},t}$ in Hospital and Workplace (Figs. 4.3.1a and b) stands in contrast to that of IC2S2-17 and WS-16 (Figs. 4.3.1c and d), in which $\widehat{N}_{\mathrm{p},t}$ exhibits more systematic variations. Prior to the first keynote talk of IC2S2-17, $\widehat{N}_{\mathrm{p},t}$ increases steadily as expected during a period when participants are arriving at the venue; however, it declines during poster session (Figs. 4.3.1c). The poster session precedes the final keynote talk; hence the decline in population size (Fig. 4.3.1c after 15:00) may reflect the exit of participants who, based on the subsequent rise in $\widehat{N}_{\mathrm{p},t}$ shortly after (Fig. 4.3.1c, 17:00), reconvene for the keynote speech (Fig. 4.3.1c, 17:30). In WS-16, the

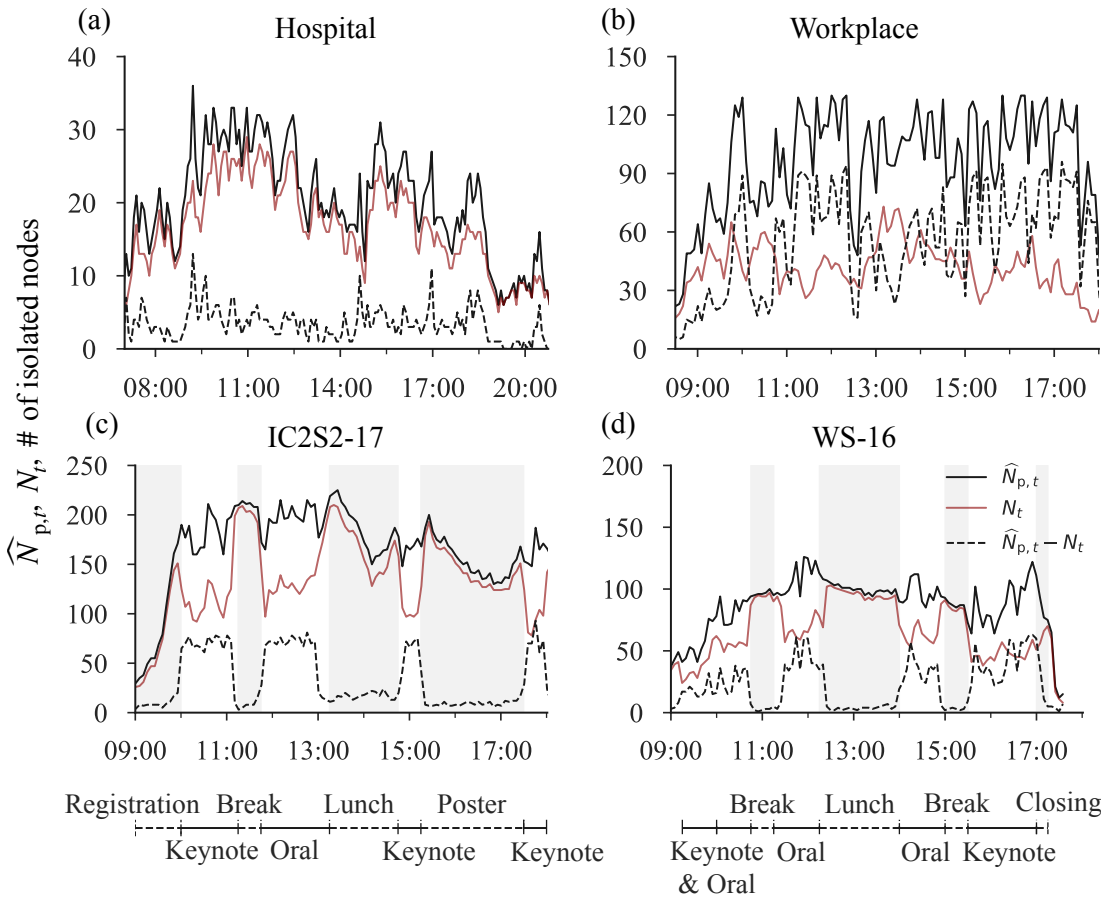

Figure 4.3.1: Estimated size of network population, $\widehat{N}_{\mathrm{p},t}$, number of active persons, N_t, and total isolated nodes, $\widehat{N}_{\mathrm{p},t} - N_t$ for (a) Hospital, (b) Workplace, (c) IC2S2-17, and (d) WS-16. Timelines at the bottom identify time windows for conference schedule. Gray shading highlights unrestricted sessions i.e., registration, break, lunch, poster session and closing remarks.

population size is also high during oral and keynote sessions and a noticeable decline is seen during the closing remarks, which is the final event of the day (Fig. 4.3.1d, 17:00). In Fig. 4.C.1d, WS-16 has a similar schedule to that of IC2S2-17 (Fig. 4.3.1c) and similar movements in $\widehat{N}_{\mathrm{p},t}$, which grows during registration but subsides during poster session before increasing again prior to the start of the final keynote speech.

In most of the data sets, total active individuals N_t follows closely the population size, which is the maximum possible value of nodes that can be active at a given time (i.e, $N_t \leq N_{\mathrm{p},t}$). From the estimated population size, we can compute the number of resting nodes as $\widehat{N}_{\mathrm{p},t} - N_t$ (Fig. 4.3.1, broken line). Resting nodes reflect a realistic but generally unobservable feature of dynamic networks,

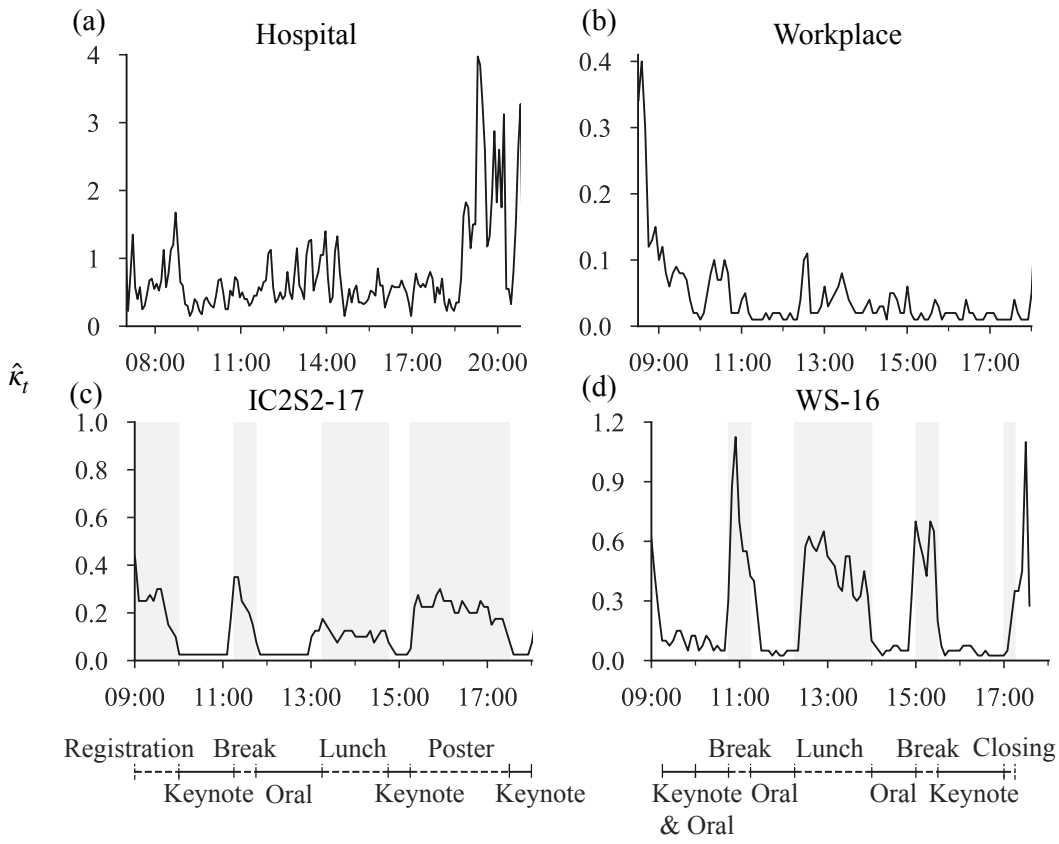

Figure 4.3.2: Estimated overall activity level, $\widehat{\kappa}_t$. (a) Hospital, (b) Workplace, (c) IC2S2-17, and (d) WS-16. Timelines at the bottom identify time windows for conference schedule. Gray shading highlights unrestricted sessions i.e., registration, break, lunch, poster session and closing remarks.

that of isolated individuals who are not in direct contact with any other individual in the system.[57] In conference data, total isolated nodes exhibit a systematic correspondence with activities; few individuals are isolated during registration, break, lunch, and poster session, while elevated levels are seen for keynote talks and oral sessions (Figs. 4.3.1c and d, broken line). In Hospital data, total isolated nodes is fairly small (close to zero in many instances); however, this is not unnatural in such high-contact environments where hospital staff are frequently engaging each other and/or attending to patients (Fig. 4.3.1a, broken line). In contrast, the number of isolated nodes in Workplace data is generally high, up to three times N_t (Fig. 4.3.1b).

Dynamic behavior of estimated overall activity $\widehat{\kappa}_t$

The estimated activity parameter, $\widehat{\kappa}_t$, is high during unrestricted sessions at both conferences, signaling intense interactions between participants (Figs. 4.3.2c and d, shading). However, during keynote talks and oral sessions, $\widehat{\kappa}_t$ fluctuates around much smaller values. This suggests that attendees have a greater chance of making contact with each other during registration, coffee break, lunch and poster session than during the oral sessions. Although $\widehat{\kappa}_t$ declines and remains very low for the duration of keynote talks and oral sessions, our method still detects slight variations, suggesting that $\widehat{N}_{\mathrm{p},t}$ is not the only dynamical parameter at play. Fig. 4.F.1 shows estimated overall activity for the same days based on an alternative probability, Eq. (4.2).

In contrast, $\widehat{\kappa}_t$ changes erratically in Hospital and Workplace data. A discernible pattern that corresponds with coordination in movement or activity, as seen in conference data, is not exhibited (Figs. 4.3.2a and b). Nevertheless, for Hospital data, $\widehat{\kappa}_t$ is highest at the end of the day (Fig. 4.3.2a) when there is also a diminution in population size (Fig. 4.3.1a), while for Workplace data, $\widehat{\kappa}_t$ is highest at the beginning of the day (Fig. 4.3.2b) when $\widehat{N}_{\mathrm{p},t}$ is increasing (Fig. 4.3.1b). At these times, the behaviors of N and M reflect the dual impact of a sharp rise in $\widehat{\kappa}_t$ as individuals leave the Hospital network (thereby reducing $\widehat{N}_{\mathrm{p},t}$) or individuals in Workplace join the system (thereby increasing $\widehat{N}_{\mathrm{p},t}$).

4.3.2. Time-varying contribution of N_{p} and κ to the emergence of densification scaling

We now examine the dynamical relationship between the number of active nodes N and the number of edges M in empirical data to identify the source of densification scaling in social networks. Figs. 4.3.3 and 4.3.4 demonstrate the relationship between N and M based on a series of temporal snapshots for each data set, and the respective color scales denote changing levels of population size $\widehat{N}_{\mathrm{p},t}$ and overall activity $\widehat{\kappa}_t$. All data sets exhibit a superlinear scaling, or "densification power law",[59,233] i.e., M grows in N more than proportionally. This behavior is also evident in other days which we analyzed for each data set (Figs. 4.I.1–4.J.1). However, the scaling pattern emerges as a mixture of two distinct behaviors;[57,58] the straight-line scaling pattern indicates a constant exponent $\gamma > 1$ of $M \propto N^{\gamma}$, and it emerges for small to intermediate values of N. However, for larger values

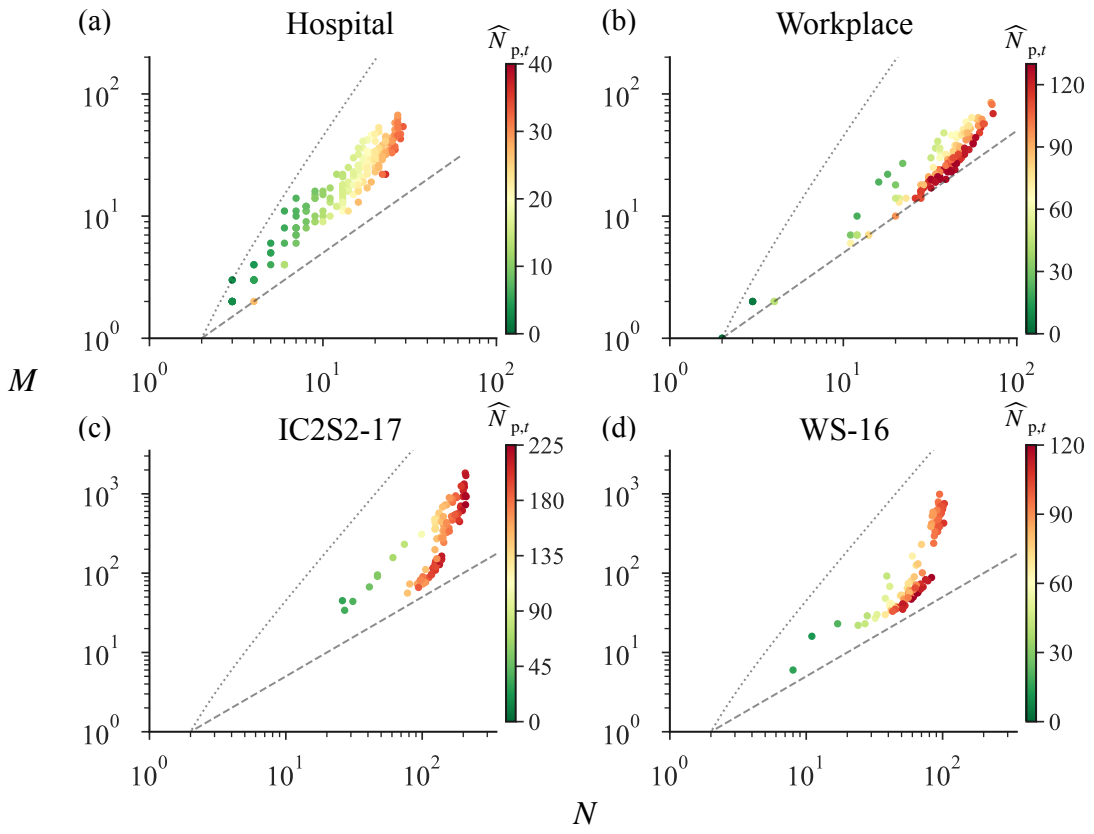

Figure 4.3.3: Densification scaling and changes in estimated population size in face-to-face networks. N-M scaling plots are shown for (a) Hospital on December 7, 2010 (b) Workplace on June 27, 2015 (c) IC2S2-17 on July 11, 2017 and (d) WS-16 on December 1, 2016. Each dot represents a snapshot of the network and colors denote estimated population size $\widehat{N}_{p,t}$ based on the respective color bar. Gray dashed and dotted lines show theoretical lower ($M = N/2$) and upper ($M = N(N-1)/2$) bounds. Estimates are based on Eq. (4.1).

of N, total edges M grows along an upward bending trajectory, implying an accelerating growth of M in N. The two patterns are easily distinguished in the conference networks but to a lesser extent in Hospital and Workplace data.

In all data sets, a linear pattern tends to emerge within a specific range of values for population size $\widehat{N}_{p,t}$ and activity level $\widehat{\kappa}_t$. Population size gradually expands from small to moderate values and, along with this, N_t is also increasing (Fig. 4.3.3). At the same time, activity level is high in small networks with the number of edges M at its upper bound $N(N-1)/2$ in some instances, implying that a considerable proportion of the individuals present are engaged (Figs. 4.3.4a and

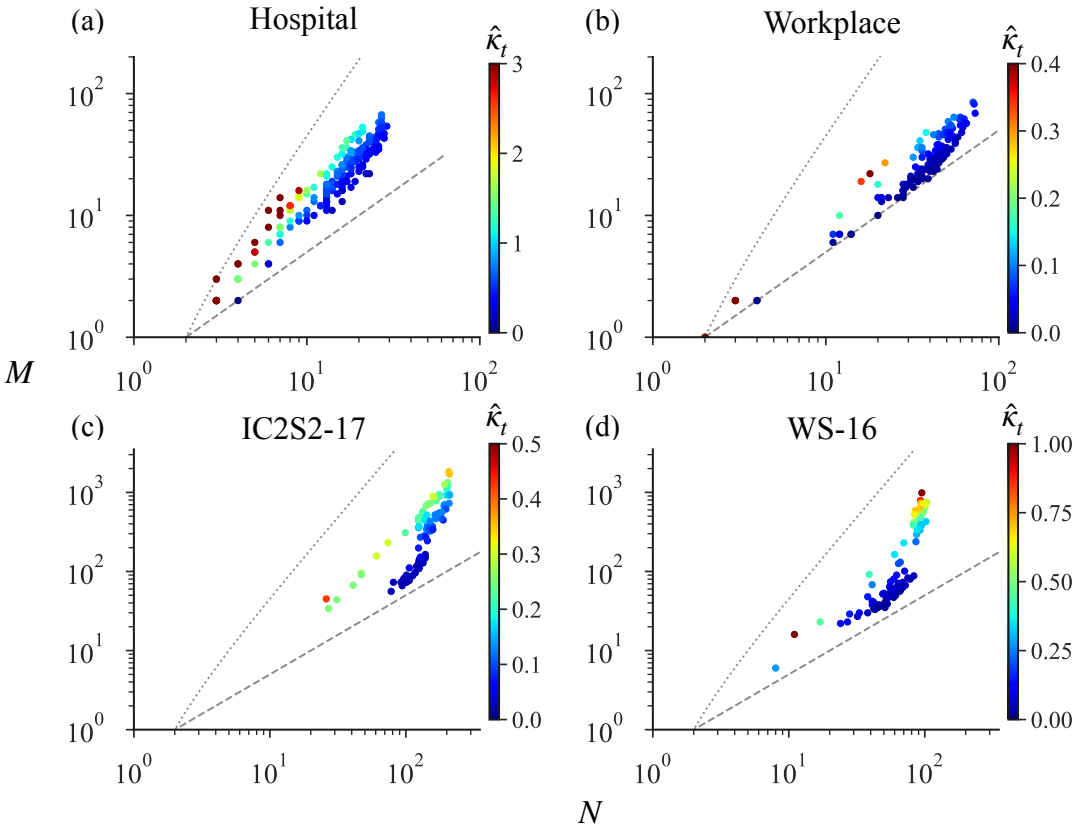

Figure 4.3.4: Densification scaling and changes in overall activity $\widehat{\kappa}_t$ in face-to-face networks. See the caption of Fig. 4.3.3 for details.

4.J.1a, c–d). However, as the population grows, activity level declines rapidly and M continues to grow at a constant rate (e.g. Fig. 4.3.4a blue-green-yellow transition). During this phase, therefore, the dynamics between M and N are dominated by the gradual expansion of $\widehat{N}_{\mathrm{p},t}$ which allows more and more individuals to become active.

Given that population size of face-to-face networks is finite, $\widehat{N}_{\mathrm{p},t}$ will eventually become constant but M may continue to grow as the number of active nodes N gradually approaches $\widehat{N}_{\mathrm{p},t}$, yielding an upward bending slope towards M's upper bound $N(N-1)/2$ (dotted line in Figs. 4.3.3 and 4.3.4). The plots for IC2S2-17 and WS-16 in Figs. 4.3.3 and 4.3.4 suggest that this accelerating growth in M occurs as $\hat{\kappa}$ increases while $\widehat{N}_{\mathrm{p},t}$ remains high and relatively constant. As the number of active individuals N gets closer to $\widehat{N}_{\mathrm{p},t}$, few isolated nodes (if any) remain, thus resulting in denser networks in which M is almost at the maximum number of edges that can exist between active nodes.

To enable these previously isolated individuals to make at least one connection, overall activity level increases, and this drives the continued growth in aggregate edges. We also show in Supplementary Information the corresponding figures based on the alternative probability of connection in Eq (4.2), and the results are consistent with that of the baseline model (Figs. 4.K.1–4.N.1).

4.4. Discussion

In this study, we proposed a method to identify the driving force of the dynamical relationship between total active nodes N and total edges M in temporal networks. Changes in population size N_{p} and overall activity κ have both been identified as the mechanisms behind this dynamical relationship, each contributing to the emergence of different densification scaling patterns. Our main contribution is a numerical maximum-likelihood method that is able to estimate simultaneously, population size N_{p} and activity rhythm κ at given times, extending previous works in which one parameter is estimated by assuming the other is constant.[57,58] We found that changes in the mechanisms of densification and sparsification reflect explicit periodic transitions in networks that have rigid time constraints. Furthermore, our findings remain consistent with previous studies which explain the emergence of a constant scaling exponent as the result of an increasing population size, while the accelerated growth pattern is being impelled by intensification of overall activity.

Although we have focused on social temporal networks in face-to-face contexts, the method is adaptable to practically any dynamical system that can be modeled as a time-varying network of nodes and edges. This is one advantage of our method because of the accessibility of N and M in most networks without having privacy issues. Of course, there are some limitations which need to be addressed in future research. Firstly, we employed a dynamic hidden variable model in generating networks, in which each node is randomly linked to another based on their individual activity. This means that although the model can reproduce the global quantities of N and M, more realistic structural features that are known to exist in social networks (e.g. community structure, triads) are absent in generated networks. However, our focus in this work is to understand the variation in these global quantities of networks which does not require knowledge of structural properties. Our method also facilitates the use of network generating models that incorporate such properties

observed in empirical networks.

Secondly, we assume that the distribution of node fitness (i.e., intrinsic activity of a node) in the network generating model is uniform. Although an empirical fitness distribution is preferred, the challenge exists in obtaining the individual activity level of nodes that are part of the population but are dormant (i.e., having no edges). Such nodes are generally not observable, because they are not explicitly stated as nodes that have interacted with others in the contact data set.

The relevance of this work lies in the simplicity of the method for understanding the dynamical relationship between fundamental global quantities of temporal networks, and the adaptability of our method to include more realistic features of empirical networks. The dynamics of network growth and shrinkage is central to how systems work, and it would also be one crucial factor in how information and infectious diseases spread in networks. Given the pervasiveness of complex systems and our reliance on them in our daily lives, greater understanding of the dynamics of networks would improve how we interact with, and even control such systems.

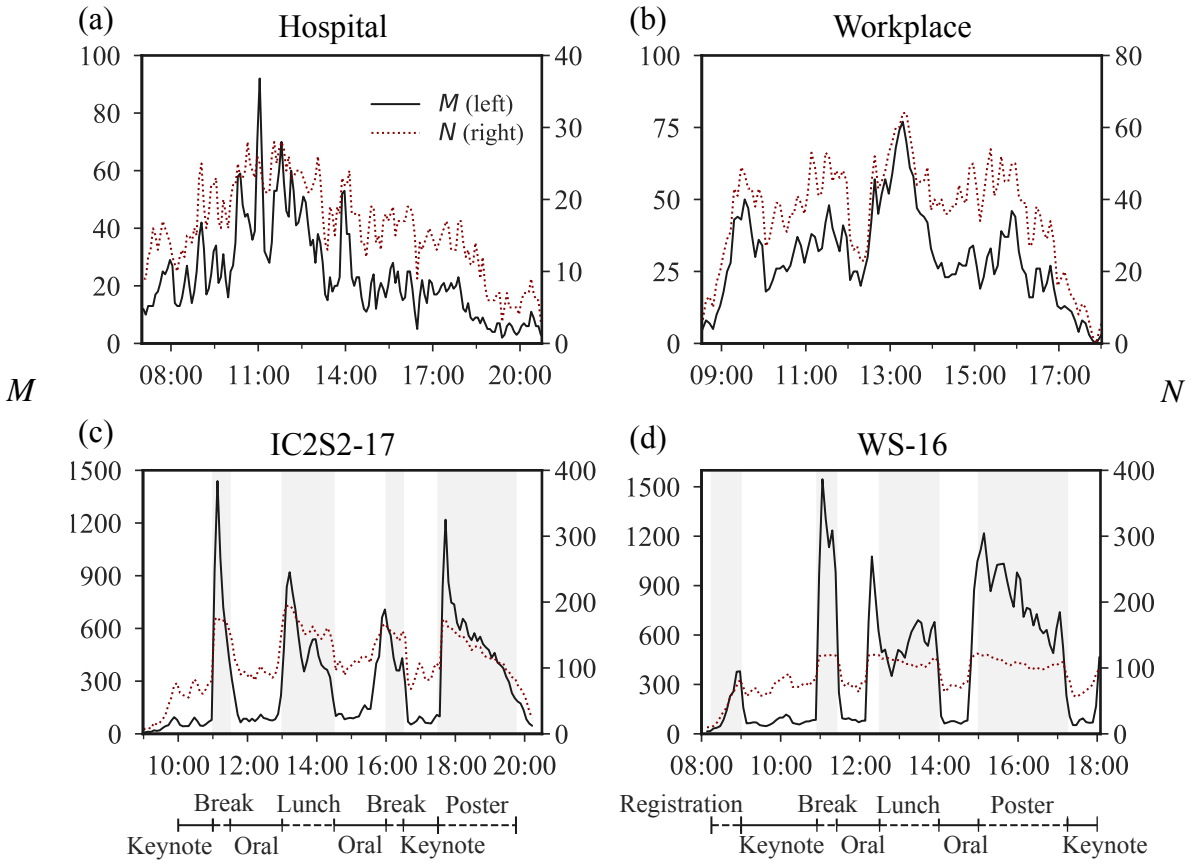

Figure 4.A.1: Evolution of total active edges M and total active nodes N in face-to-face networks. The following days are shown for each data set: (a) Hospital on December 8, 2010, (b) Workplace on June 28, 2015, (c) IC2S2-17 on July 12, 2017 and (d) WS-16 on November 30, 2016. Timeline below conference data ((c) IC2S2-17 and (d) WS-16) identify time windows for scheduled events. Gray shading highlights unrestricted sessions i.e., registration, break, lunch and poster session.

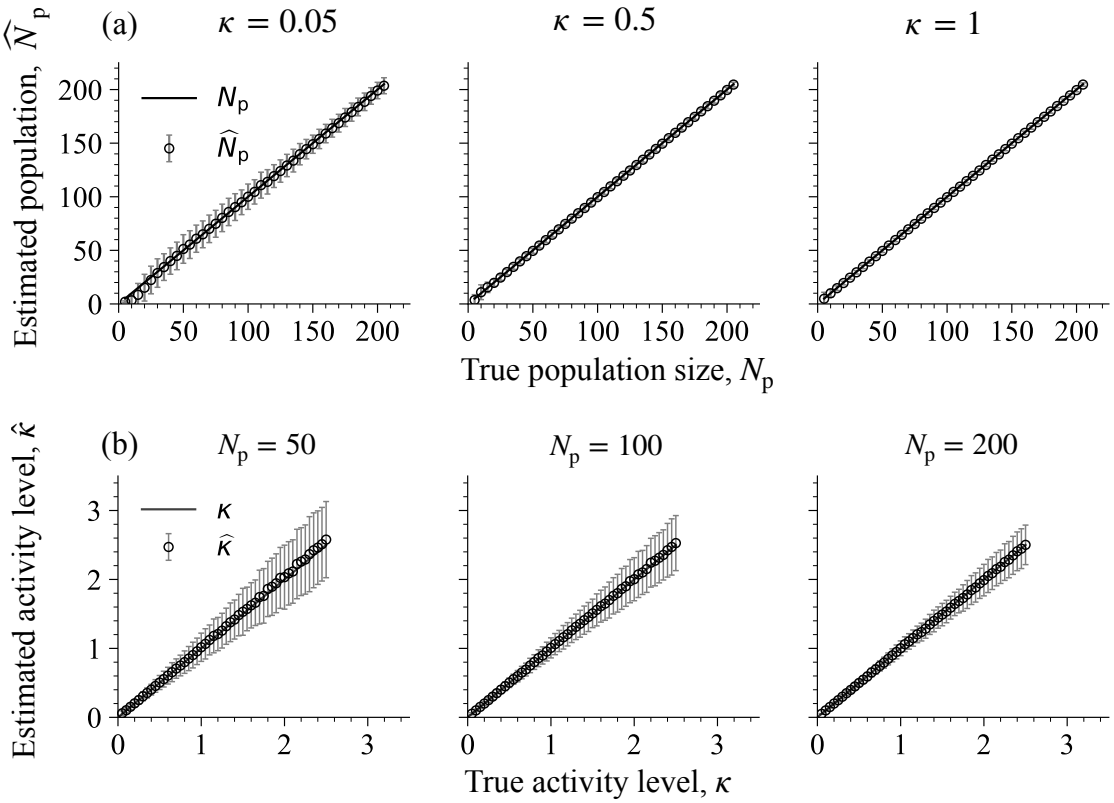

Figure 4.B.1: Validation of the maximum-likelihood estimation method. (a) Estimation of N_{p} for N_{p} ranging from 5 to 200 (incremented by 5) given $\kappa = 0.05$, $\kappa = 0.5$ and $\kappa = 1$. (b) Estimation of κ for κ ranging from 0.05 to 2.5 (incremented by 0.05) given $N_{\mathrm{p}} = 50$, $N_{\mathrm{p}} = 100$ and $N_{\mathrm{p}} = 200$. The estimates $\widehat{N}_{\mathrm{p},t}$ and $\widehat{\kappa}_t$ are obtained from the model with probability of a connection between two nodes i and j given by Eq. (4.1). Errors bars represent one standard deviation and they are computed over 1,000 runs.

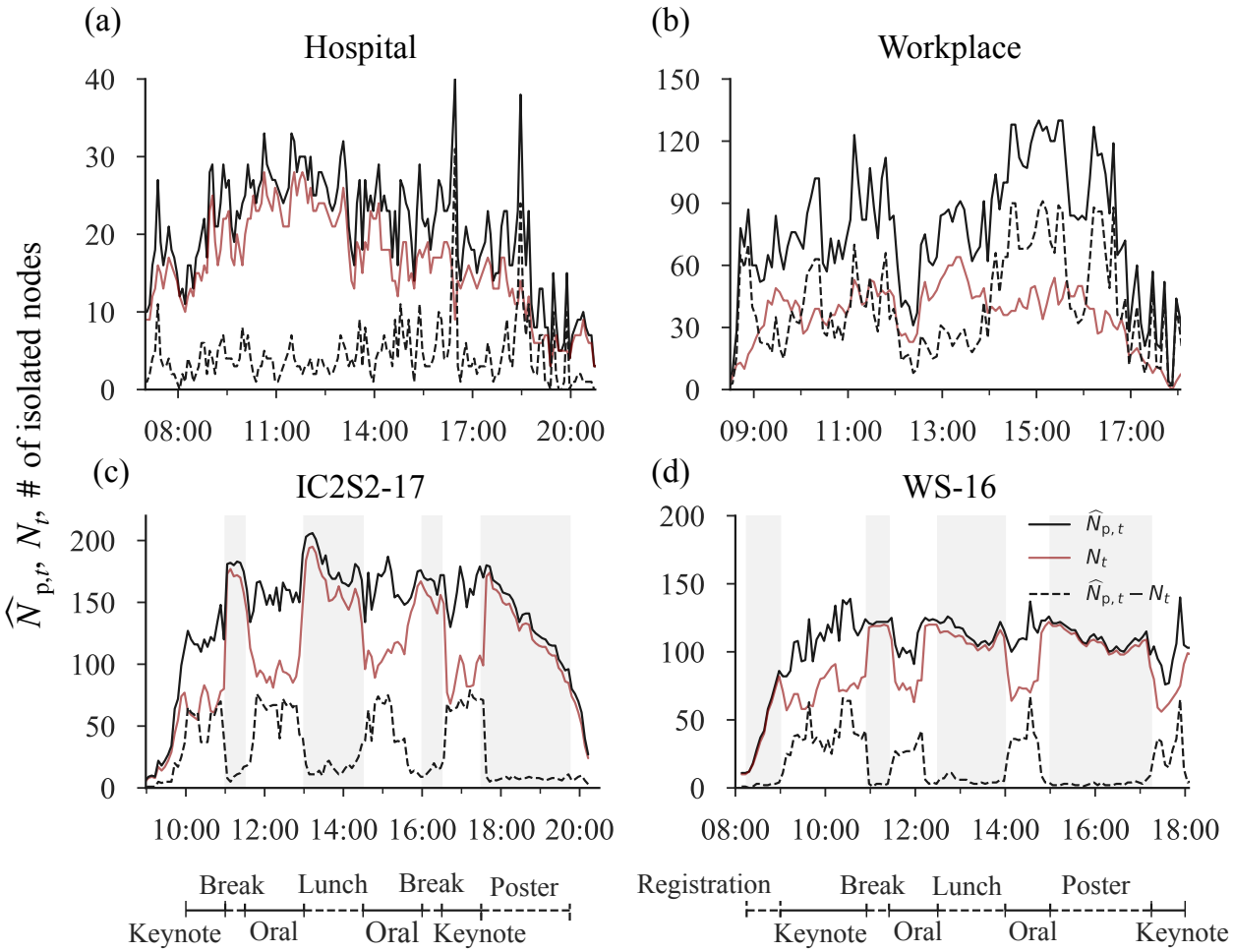

Figure 4.C.1: Shifts in estimated population size $\widehat{N}_{\mathrm{p},t}$, number of active persons N_t and total isolated nodes $\widehat{N}_{\mathrm{p},t} - N_t$ in face-to-face networks. The following days are shown for each data set: (a) Hospital on December 8, 2010 (b) Workplace on June 28, 2015 (c) IC2S2-17 on July 12, 2017 and (d) WS-16 on November 30, 2016. Timelines below conference data, in panels (c) and (d), identify time windows for scheduled events. Gray shading highlights unrestricted sessions i.e., registration, break, lunch and poster session. Estimates of $N_{\mathrm{p},t}$ are based on the model with probability $p_{ij,t} = 1 - e^{-\kappa a_i a_j}$ from Eq. (4.1).

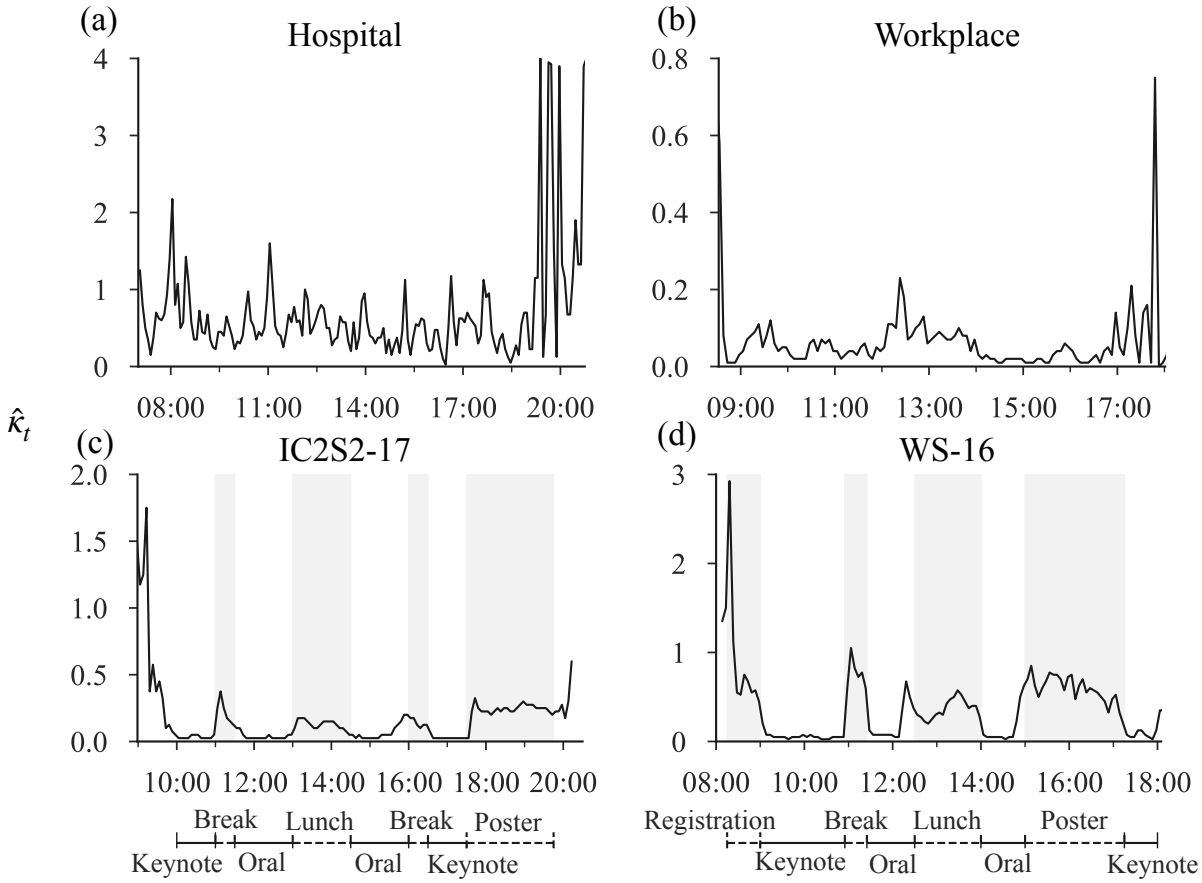

Figure 4.D.1: Changes in estimated overall activity $\widehat{\kappa}_t$ in face-to-face networks. The following days are shown for each data set: (a) Hospital on December 8, 2010 (b) Workplace on June 28, 2015 (c) IC2S2-17 on July 12, 2017 and (d) WS-16 on November 30, 2016. Timelines below conference data (c) IC2S2-17 and (d) WS-16 identify time windows for scheduled events. Gray shading highlights unrestricted sessions i.e., registration, break, lunch and poster session. Estimates of $\widehat{\kappa}_t$ are based on the model with probability $p_{ij,t} = 1 - e^{-\kappa a_i a_j}$ from Eq. (4.1).

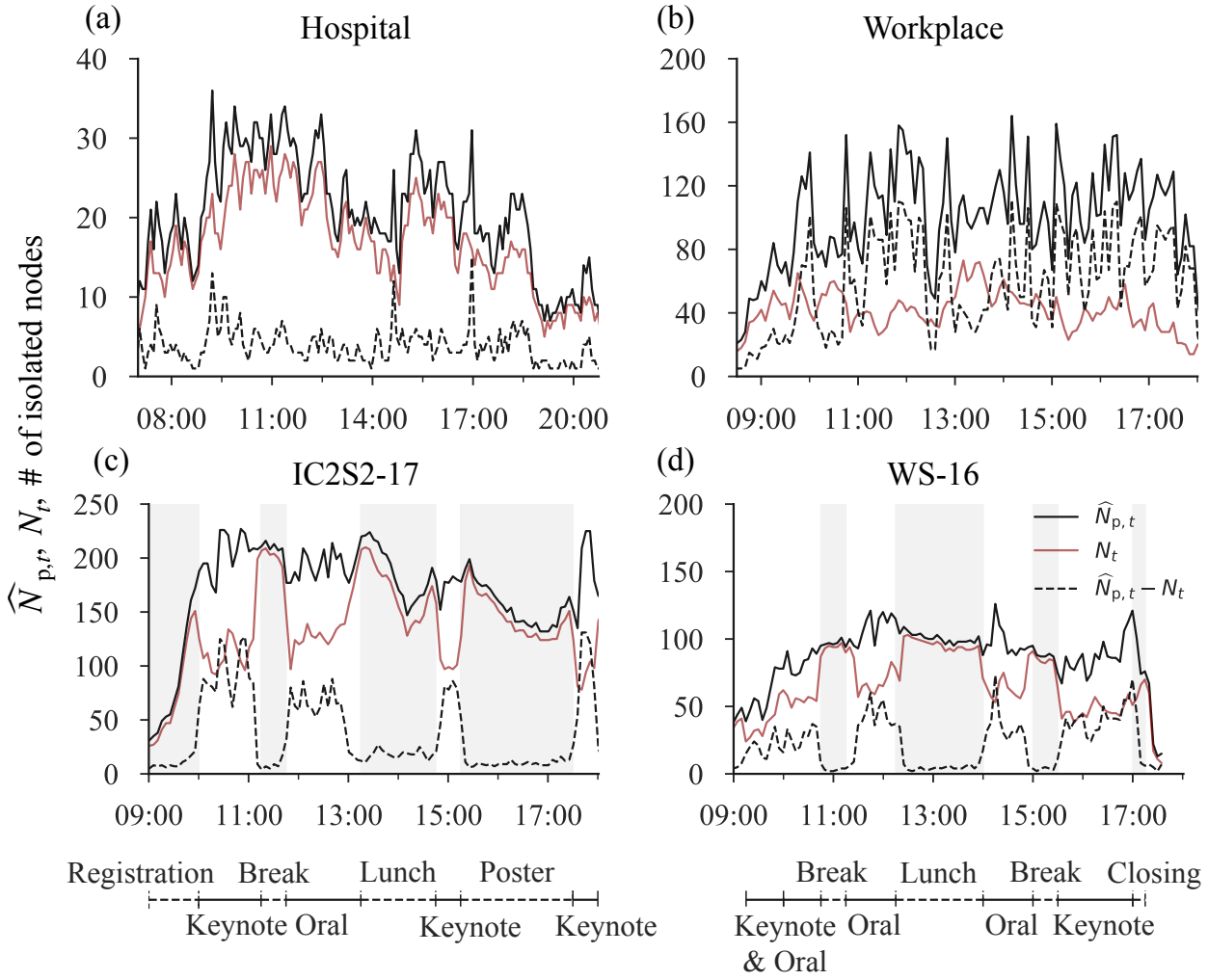

Figure 4.E.1: Shifts in estimated population size $\widehat{N}_{\mathrm{p},t}$, number of active persons N_t and total isolated nodes $\widehat{N}_{\mathrm{p},t} - N_t$ in face-to-face networks. The following days are shown for each data set: (a) Hospital on December 7, 2010 (b) Workplace on June 27, 2015 (c) IC2S2-17 on July 11, 2017 and (d) WS-16 on December 1, 2016. Timelines below conference data (c) IC2S2-17 and (d) WS-16 identify time windows for scheduled events. Gray shading highlights unrestricted sessions i.e., registration, break, lunch, poster session and closing remarks. Estimates of $N_{\mathrm{p},t}$ are based on the model with probability $p_{ij,t} = \kappa a_i a_j$ from Eq. (4.2).

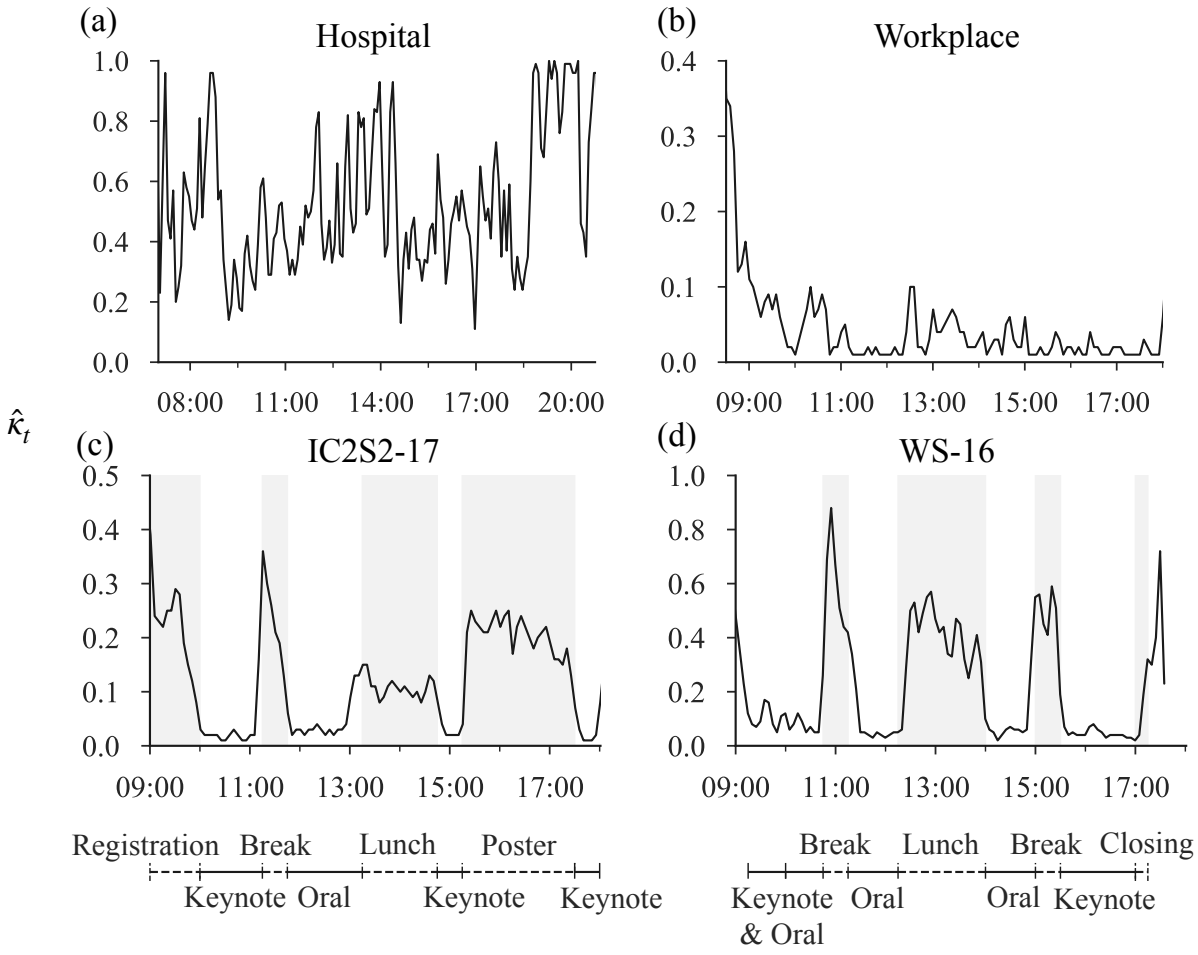

Figure 4.F.1: Changes in estimated overall activity $\widehat{\kappa}_t$ in face-to-face networks. The following days are shown for each data set: (a) Hospital on December 7, 2010 (b) Workplace on June 27, 2015 (c) IC2S2-17 on July 11, 2017 and (d) WS-16 on December 1, 2016. Timelines below conference data (c) IC2S2-17 and (d) WS-16 identify time windows for scheduled events. Gray shading highlights unrestricted sessions i.e., registration, break, lunch, poster session and closing remarks. Estimates of $\widehat{\kappa}_t$ are based on the model with probability $p_{ij,t} = \kappa a_i a_j$ from Eq. (4.2).

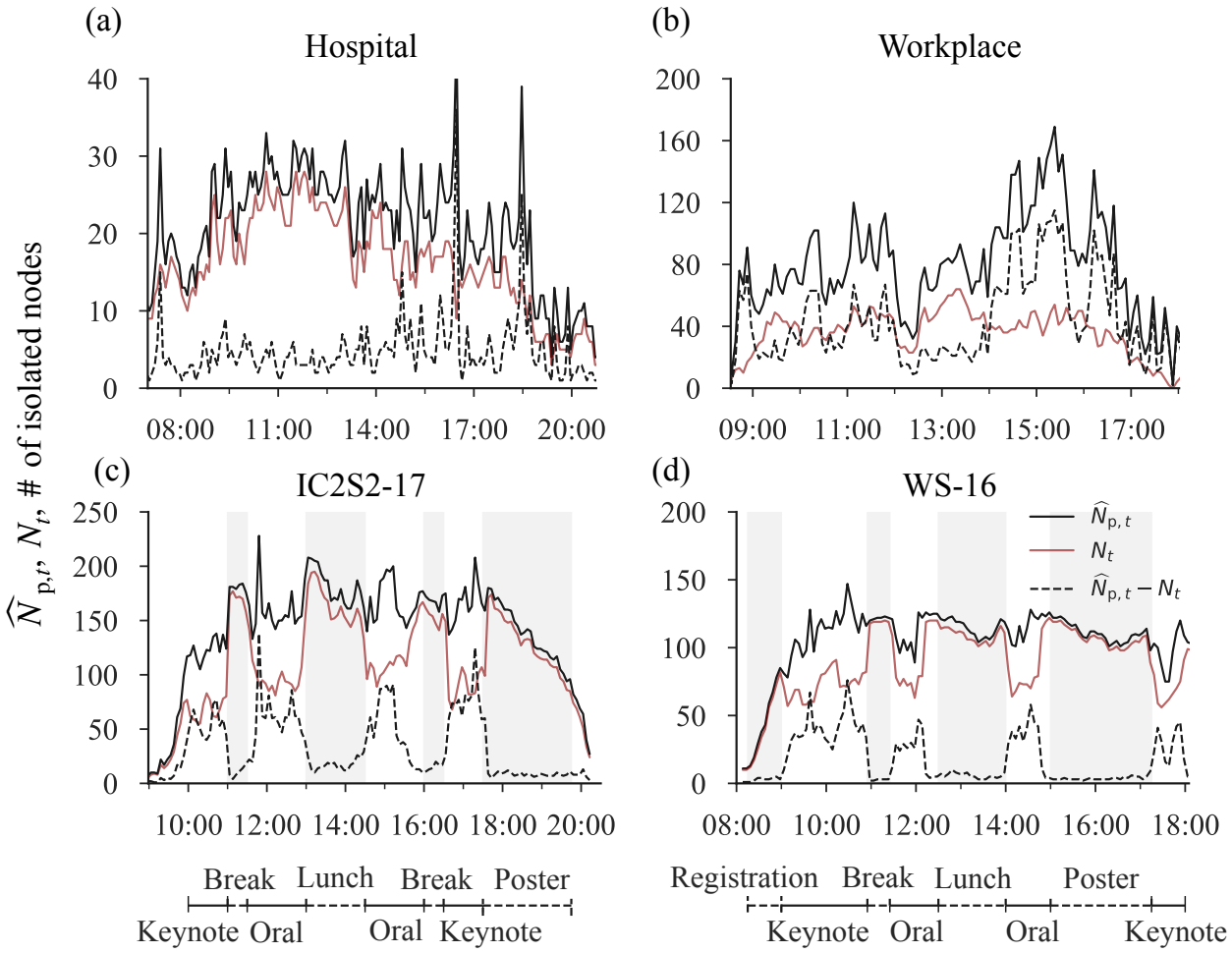

Figure 4.G.1: Shifts in estimated size of population $\widehat{N}_{\mathrm{p},t}$, number of active persons N_t and total isolated nodes $\widehat{N}_{\mathrm{p},t} - N_t$ in face-to-face networks. The following days are shown for each data set: (a) Hospital on December 8, 2010 (b) Workplace on June 28, 2015 (c) IC2S2-17 on July 12, 2017 and (d) WS-16 on November 30, 2016. Timelines below conference data (c) IC2S2-17 and (d) WS-16 identify time windows for scheduled events. Gray shading highlights unrestricted sessions i.e., registration, break, lunch and poster session. Estimates of $N_{\mathrm{p},t}$ are based on the model with probability $p_{ij,t} = \kappa a_i a_j$ from Eq. (4.2).

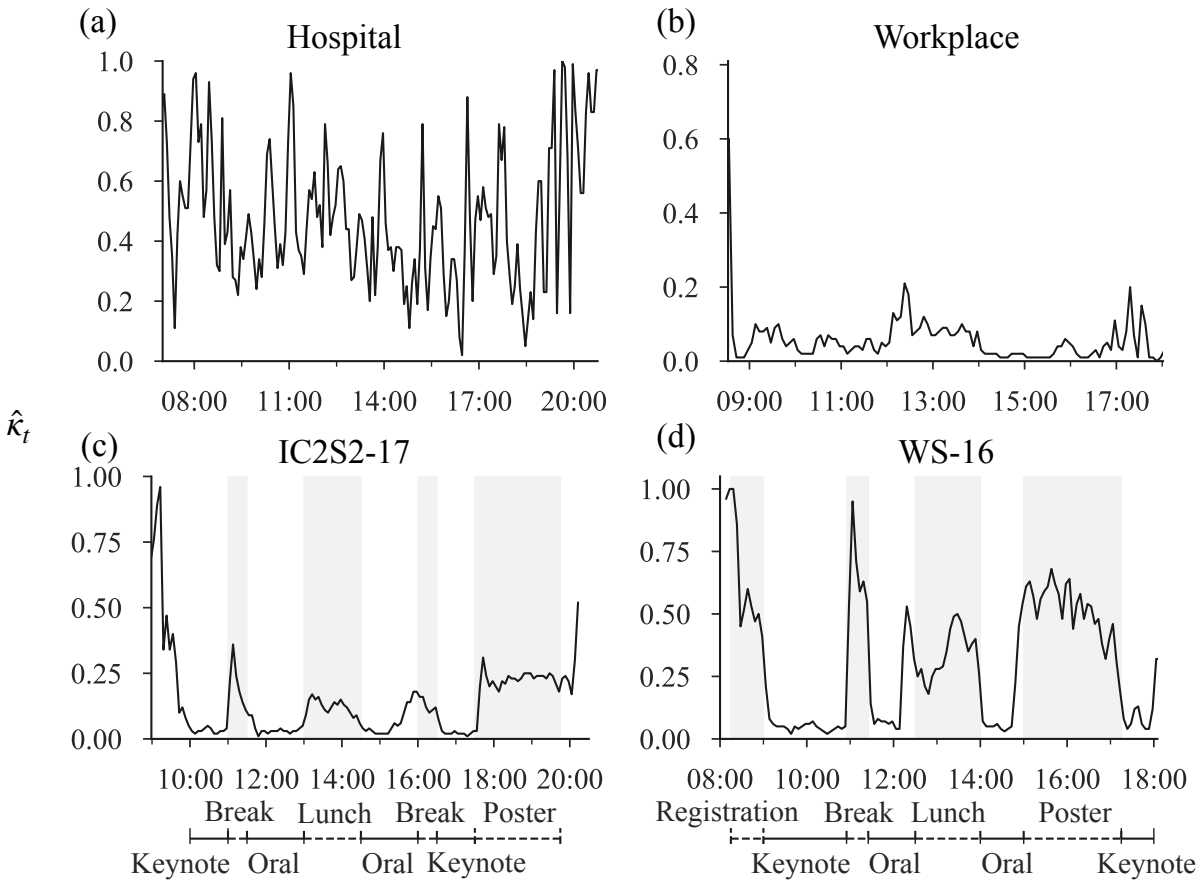

Figure 4.H.1: Changes in estimated overall activity $\widehat{\kappa}_t$ in face-to-face networks. The following days are shown for each data set: (a) Hospital on December 8, 2010 (b) Workplace on June 28, 2015 (c) IC2S2-17 on July 12, 2017 and (d) WS-16 on November 30, 2016. Timelines below conference data (c) IC2S2-17 and (d) WS-16 identify time windows for scheduled events. Gray shading highlights unrestricted sessions i.e., registration, break, lunch, and poster session. Estimates of $\widehat{\kappa}_t$ are based on the model with probability $p_{ij,t} = \kappa a_i a_j$ from Eq. (4.2).

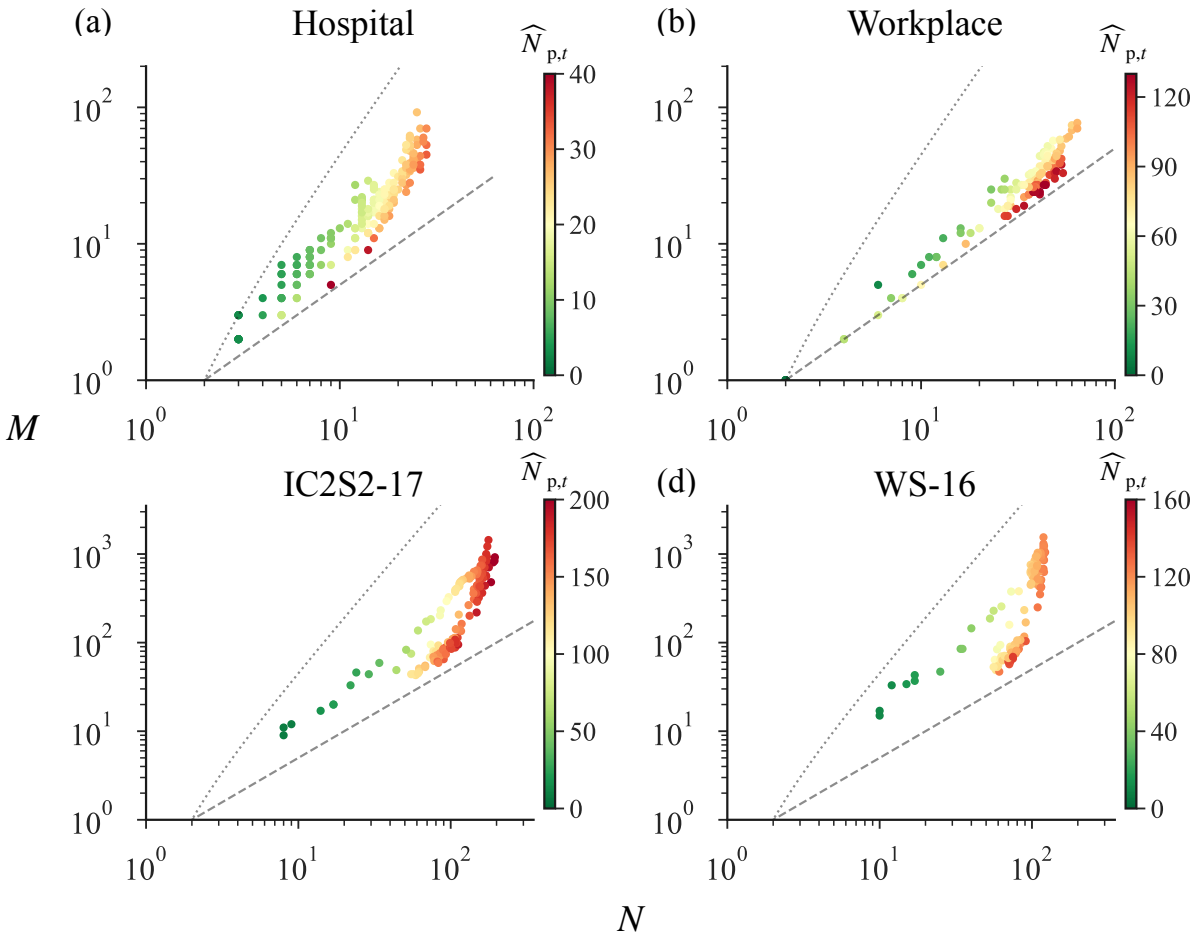

Figure 4.I.1: Densification scaling and changes in estimated population size in face-to-face networks. N-M scaling plots are shown for: (a) Hospital on December 8, 2010 (b) Workplace on June 28, 2015 (c) IC2S2-17 on July 12, 2017 and (d) WS-16 on November 30, 2016. Each marker represents a snapshot of the network and colors denote estimated population size $\widehat{N}_{p,t}$ based on the respective color bar. Gray dashed and dotted lines show theoretical lower ($M = N/2$) and upper ($M = N(N-1)/2$) bounds. Estimates of $N_{p,t}$ based on the model with probability $p_{ij,t} = 1 - e^{-\kappa a_i a_j}$ from Eq. (4.1).

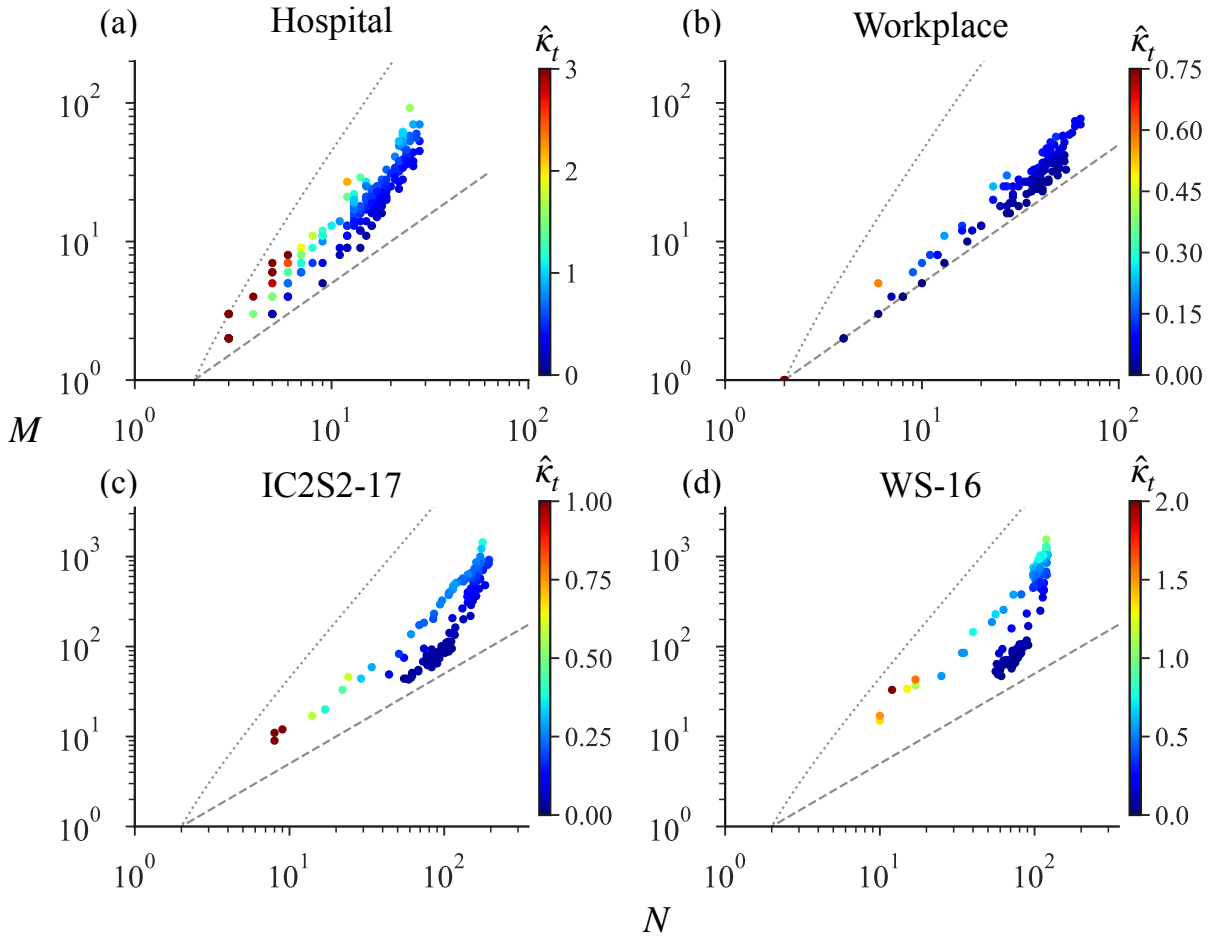

Figure 4.J.1: Densification scaling and changes in estimated overall activity in face-to-face networks. N-M scaling plots are shown for: (a) Hospital on December 8, 2010 (b) Workplace on June 28, 2015 (c) IC2S2-17 on July 12, 2017 and (d) WS-16 on November 30, 2016. Each marker represents a snapshot of the network and colors denote estimated activity level $\widehat{\kappa}_t$ based on the respective color bar. Gray dashed and dotted lines show theoretical lower ($M = N/2$) and upper ($M = N(N-1)/2$) bounds. Estimates of $\widehat{\kappa}_t$ based on the model with probability $p_{ij,t} = 1 - e^{-\kappa a_i a_j}$ from Eq. (4.1).

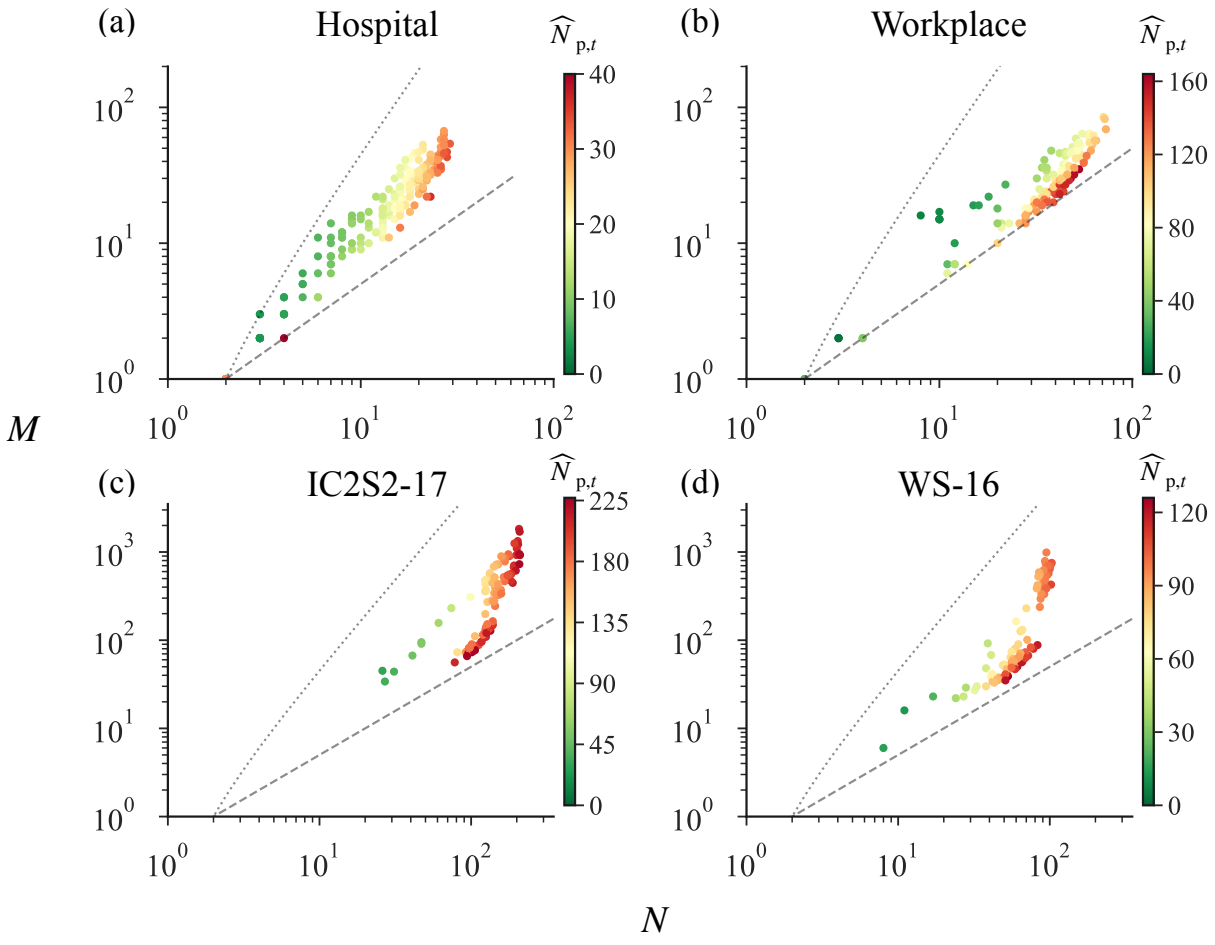

Figure 4.K.1: Densification scaling and changes in estimated population size in face-to-face networks. N-M scaling plots are shown for: a) Hospital on December 7, 2010 (b) Workplace on June 27, 2015 (c) IC2S2-17 on July 11, 2017 and (d) WS-16 on December 1, 2016. Each marker represents a snapshot of the network and colors denote estimated population size $\widehat{N}_{\mathrm{p},t}$ based on the respective color bar. Gray dashed and dotted lines show theoretical lower ($M = N/2$) and upper ($M = N(N-1)/2$) bounds. Estimates of $N_{\mathrm{p},t}$ based on the model with probability $p_{ij,t} = \kappa a_i a_j$ from Eq. (4.2).

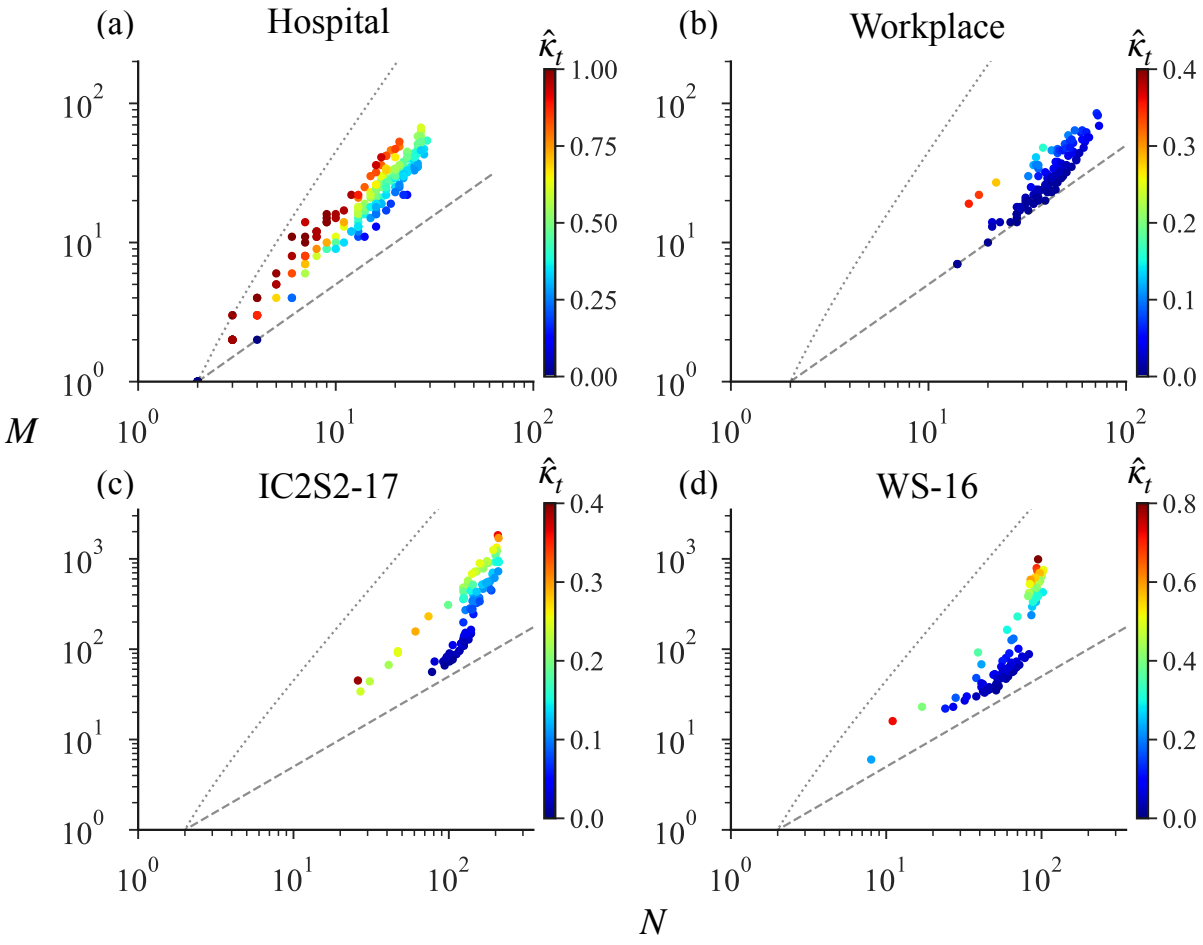

Figure 4.L.1: Densification scaling and changes in estimated overall activity in face-to-face networks. N-M scaling plots for: a) Hospital on December 7, 2010 (b) Workplace on June 27, 2015 (c) IC2S2-17 on July 11, 2017 and (d) WS-16 on December 1, 2016. Each marker represents a snapshot of the network and colors denote estimated activity level $\widehat{\kappa}_t$ based on the respective color bar. Gray dashed and dotted lines show theoretical lower ($M = N/2$) and upper ($M = N(N-1)/2$) bounds. Estimates of $\widehat{\kappa}_t$ based on the model with probability $p_{ij,t} = \kappa a_i a_j$ from Eq. (4.2).

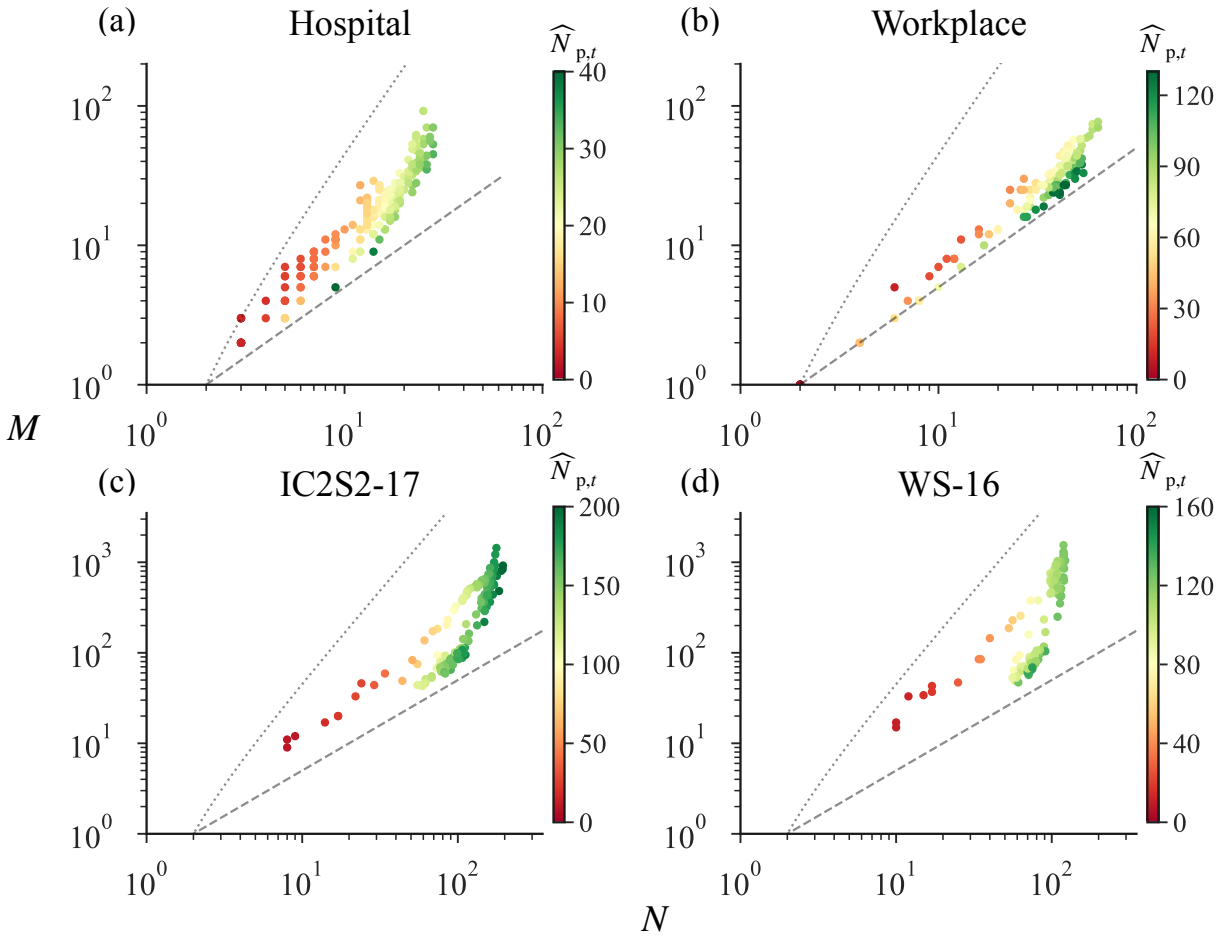

Figure 4.M.1: Densification and changes in estimated population size in face-to-face networks. N-M scaling plots are shown for: (a) Hospital on December 8, 2010 (b) Workplace on June 28, 2015 (c) IC2S2-17 on July 12, 2017 and (d) WS-16 on November 30, 2016. Each marker represents a snapshot of the network and colors denote estimated population size $\widehat{N}_{\mathrm{p},t}$ based on the respective color bar. Gray dashed and dotted lines show theoretical lower ($M = N/2$) and upper ($M = N(N-1)/2$) bounds. Estimates of $N_{\mathrm{p},t}$ based on the model with probability $p_{ij,t} = \kappa a_i a_j$ from Eq. (4.2).

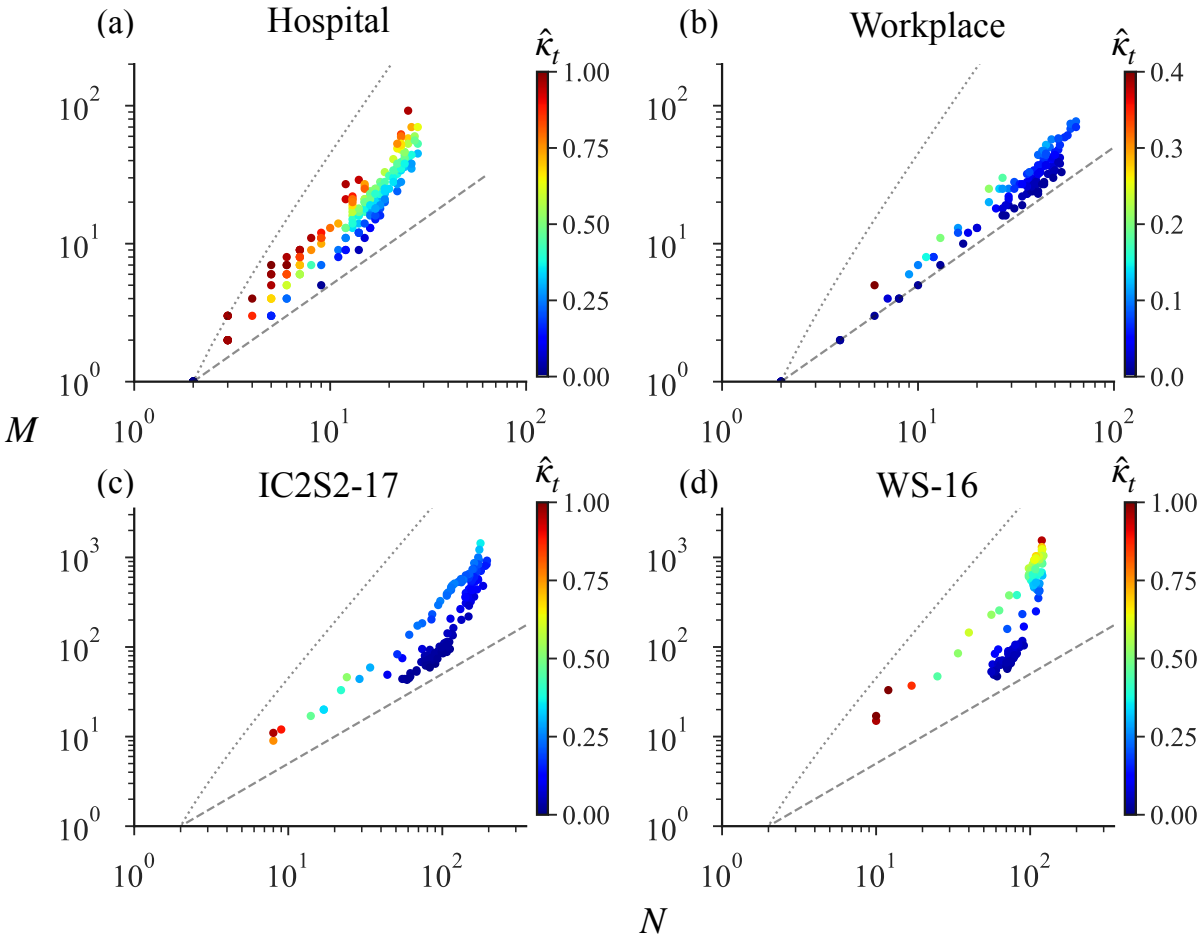

Figure 4.N.1: Densification and changes in the estimated overall activity in face-to-face networks. N-M scaling plots are shown for: (a) Hospital on December 8, 2010 (b) Workplace on June 28, 2015 (c) IC2S2-17 on July 12, 2017 and (d) WS-16 on November 30, 2016. Each marker represents a snapshot of the network and colors denote estimated activity level $\widehat{\kappa}_t$ based on the respective color bar. Gray dashed and dotted lines show theoretical lower ($M = N/2$) and upper ($M = N(N-1)/2$) bounds. Estimates of $\widehat{\kappa}_t$ based on the model with probability $p_{ij,t} = \kappa a_i a_j$ from Eq. (4.2).

CHAPTER 5

Concluding Remarks

In this work, we examined social and financial networks using data on: i) face-to-face contact between humans, and ii) bilateral transactions between banks in an interbank market. We showed that not only do they share the commonality of being vital to life in the modern world, but also that much more can be gained from taking a cross-disciplinary approach to studying them. Employing tools and methods from the more advanced area of social network analysis has seen a rapid advancement in our understanding of financial networks over the last two decades. At the same time, the occasional outbreak of infections, most recently the 2019 outbreak of coronavirus, indicates a consistent need to identify ways to maintain global health. We addressed in this dissertation, points that may be considered to be central to these objectives of maintaining the health of the global financial system and the well-being of humans worldwide.

We first addressed one of the gaps in financial systemic risk analysis, where time-varying properties are not reflective of the true timescale over which relationships are established and disbanded. This approach is an adaptation of time-varying analysis often employed in studies of how epidemics and social phenomena propagate given local activity in social networks. We find that the interbank system displays different degrees of fragility that is dependent on the time of day. In many ways, current policies aimed at maintaining stability in financial systems rely on information, almost entirely, about the architecture of the network. However, by incorporating temporal characteristics we showed that while market size affects risk at different times — when markets are the same size — high interconnectedness of risk between banks drives the system's fragility. The dimension of time in systemic risk analysis reflects more realistically, the setup of the interbank system and it can provide useful insights into how regulators may monitor and, to some extent, anticipate growing risk to guide the most appropriate responses that ensure stability.

Our investigation into the source of dynamical changes in the global network property of size was based on human contact networks. As mentioned earlier, the result of our study of systemic risk in

an interbank network highlighted that market size can in fact impact the magnitude of systemic risk; therefore, the source of changes in network size can be seen as a crucial factor with implications for the stability of systems. We developed a method that allows us identify the interplay between the driving mechanisms, namely overall activity and size of population. Given the fundamental nature of the metrics that our method relies on, we believe that its application is relevant to understand the dynamics of growth and shrinkage of any network in the real world.

Technology has certainly influenced how interaction occurs in social and financial systems which implies that advancements in technology may signal new areas of research. Here we highlight possibilities for future investigations. For social networks, more research is still needed on the multiple layers of interactions among individuals beyond the common assumption that individuals' dynamics are identical. In other words, individuals do not respond in the same way to influences emanating from different segments and at different times, and based on the literature, interactions between multiple network layers can materially affect the dynamics of systems and how they function.[324,426–432] Another aspect of the temporal network research in need of attention relates to how the results from empirical studies on spreading behavior can be extrapolated to large-scale networks.[122] Essentially, the objective is to use smaller more manageable empirical networks as the foundation for much larger data sets while avoiding the considerable biases that are expected to emerge due to the finite-size of the original data.

For financial networks, there is an urgent need for reliable early-warning signals of distress to enable appropriate responses that mitigate or prevent system-wide failures. Moreover, greater focus should also be aimed at extending the idea of network and/or structural controllability[433,434] to identify financial institutions most crucial to ensuring that the system is functioning well. Ideally, these considerations should incorporate the realistic structure of financial systems and the dynamical changes in structure over time. Advancements in these areas may require a whole new theoretical framework specific to financial networks; or as seen in the study by Delpini et al.[435] an application from existing controllability theory[433,434] on complex systems. Either way, such developments may be able to supplement quantitative indicators that can support the development of proactive and

effective policies of intervention. In other words, by taking on the aspect of the research on financial network analysis we would be progressing into the phase of predicting the future state of the system in order to preempt pernicious outcomes.

BIBLIOGRAPHY

[1] Holme, P. & Saramäki, J. Temporal networks. *Phys. Rep.* **519**, 97–125 (2012).

[2] Holme, P. & Saramäki, J. *Temporal Networks* (Springer-Verlag, Berlin, 2013).

[3] Masuda, N. & Lambiotte, R. *A Guide to Temporal Networks* (World Scientific Publishing, 2016).

[4] Holme, P. & Saramäki, J. *Temporal network theory*, vol. 2 (Springer, 2019).

[5] Newman, M. Network structure from rich but noisy data. *Nature Physics* 1 (2018).

[6] Valencia, M., Martinerie, J., Dupont, S. & Chavez, M. Dynamic small-world behavior in functional brain networks unveiled by an event-related networks approach. *Physical Review E* **77**, 050905 (2008).

[7] Tang, J., Scellato, S., Musolesi, M., Mascolo, C. & Latora, V. Small-world behavior in time-varying graphs. *Physical Review E* **81**, 055101 (2010).

[8] Starnini, M., Baronchelli, A. & Pastor-Satorras, R. Modeling human dynamics of face-to-face interaction networks. *Phys. Rev. Lett.* **110**, 168701 (2013).

[9] Szell, M., Sinatra, R., Petri, G., Thurner, S. & Latora, V. Understanding mobility in a social petri dish. *Scientific reports* **2**, 1–6 (2012).

[10] Yoneki, E., Greenfield, D. & Crowcroft, J. Dynamics of inter-meeting time in human contact networks. In *2009 International Conference on Advances in Social Network Analysis and Mining*, 356–361 (IEEE, 2009).

[11] Corsi, F., Lillo, F., Pirino, D. & Trapin, L. Measuring the propagation of financial distress with granger-causality tail risk networks. *Journal of Financial Stability* **38**, 18–36 (2018).

[12] Millán, A. P., Torres, J., Johnson, S. & Marro, J. Concurrence of form and function in developing networks and its role in synaptic pruning. *Nature communications* **9**, 1–10 (2018).

[13] Lambiotte, R., Rosvall, M. & Scholtes, I. From networks to optimal higher-order models of complex systems. *Nature physics* **15**, 313–320 (2019).

[14] Mazzarisi, P., Barucca, P., Lillo, F. & Tantari, D. A dynamic network model with persistent links and node-specific latent variables, with an application to the interbank market. *European Journal of Operational Research* **281**, 50–65 (2020).

[15] Williams, O. E., Lacasa, L., Millán, A. P. & Latora, V. The shape of memory in temporal networks. *Nature Communications* **13**, 1–8 (2022).

[16] Holme, P. & Saramäki, J. Temporal networks. *Physics reports* **519**, 97–125 (2012).

[17] Seabrook, I. E., Barucca, P. & Caccioli, F. Evaluating structural edge importance in temporal networks. *EPJ Data Science* **10**, 23 (2021).

[18] Elsinger, E. & Arnt, H. Contagion risk in the danish interbank market. *Danmarks Nationalbank Working Papers* **29** (2005).

[19] Lubloy, A. Domino effect in the Hungarian interbank market. *Hungarian Economic Review* **52**, 377–401 (2005).

[20] Karimi, F. & Raddant, M. Cascades in real interbank markets. *Computational Economics* **47**, 49–66 (2016).

[21] Sheldon, G. & Maurer, M. Interbank lending and systemic risk: an empirical analysis for switzerland. *Swiss Journal of Economics and Statistics* **134**, 685–704 (1998).

[22] Wells, S. Financial interlinkages in the United Kingdom's interbank market and the risk of contagion. *Bank of England Working Paper* **230** (2004).

[23] van Lelyveld, I. & Liedorp, F. Interbank contagion in the dutch banking sector: a sensitivity analysis. *International Journal of Central Banking* **2**, 99–133 (2006).

[24] Imakubo, K. & Soejima, Y. The transaction network in Japan's interbank money markets. *Monetary and Economic Studies* **28**, 107–150 (2010).

[25] Chan-Lau, J. A., Espinosa, M., Giesecke, K. & Solé, J. A. Assessing the systemic implications of financial linkages. *IMF global financial stability report* **2** (2009).

[26] Brunnermeier, M. K. Deciphering the liquidity and credit crunch 2007–2008. *The Journal of Economic Perspectives* **23**, 77–100 (2009).

[27] Gai, P. & Kapadia, S. Contagion in financial networks. *Proceedings of the Royal Society A* **466**, 2401–2423 (2010).

[28] Staum, J. Counterparty contagion in context: Contributions to systemic risk. In *Handbook on Systemic Risk*, 512–544 (Cambridge University Press, 2013).

[29] Acemoglu, D., Ozdaglar, A. & Tahbaz-Salehi, A. Systemic risk and stability in financial networks. *American Economic Review* **105**, 564–608 (2015).

[30] Battiston, S., Caldarelli, G., May, R. M., Roukny, T. & Stiglitz, J. E. The price of complexity in financial networks. *Proceedings of the National Academy of Sciences* **113**, 10031–10036 (2016).

[31] De Bandt, O. & Hartmann, P. Systemic risk: a survey. *Available at SSRN 258430* (2000).

[32] De Bandt, O., Hartmann, P. & Peydro, J.-L. Systemic risk in banking: An update. *Berger, A., MP, Wilson, J.(Eds.), Oxfoord Handbook of Banking. Oxford University Press, Oxford* (2009).

[33] Hüser, A.-C., Hałaj, G., Kok, C., Perales, C. & van der Kraaij, A. The systemic implications of bail-in: a multi-layered network approach. *Journal of Financial Stability* **38**, 81–97 (2018).

[34] Eisenberg, L. & Noe, T. Systemic risk in financial systems. *Management Science* **47**, 236–249 (2001).

[35] Nier, E., Yang, J., Yorulmazer, T. & Alentorn, A. Network models and financial stability. *Journal of Economic Dynamics and Control* **31**, 2033–2060 (2007).

[36] Gai, P., Haldane, A. & Kapadia, S. Complexity, concentration and contagion. *Journal of Monetary Economics* **58**, 453–470 (2011).

[37] Furfine, C. Interbank exposures: quantifying the risk of contagion. *Journal of Money, Credit and Banking* **35**, 111–128 (2003).

[38] Mistrulli, P. Assessing financial contagion in the interbank market: a comparison between estimated and observed bilateral exposures. *Banca d'Italia Temi di Discussione (Working Papers)* **641** (2007).

[39] Elsinger, H., Lehar, A. & Summer, M. Risk assessment for banking systems. *Management Science* **52**, 1301–1314 (2006).

[40] Elsinger, H., Lehar, A. & Summer, M. Using market information for banking system risk assessement. *International Journal of Central Banking* **2**, 137–165 (2006).

[41] Mistrulli, P. E. Assessing financial contagion in the interbank market: Maximum entropy versus observed interbank lending patterns. *Journal of Banking & Finance* **35**, 1114–1127 (2011).

[42] Takaguchi, T., Masuda, N. & Holme, P. Bursty communication patterns facilitate spreading in a threshold-based epidemic dynamics. *PLOS ONE* **8**, e68629 (2013).

[43] Karimi, F. & Holme, P. Threshold model of cascades in empirical temporal networks. *Physica A* **392**, 3476–3483 (2013).

[44] Barabási, A. L. The origin of bursts and heavy tails in human dynamics. *Nature* **435**, 207–211 (2005).

[45] Vázquez, A. *et al.* Modeling bursts and heavy tails in human dynamics. *Phys. Rev. E* **73**, 036127 (2006).

[46] Karsai, M. *et al.* Small but slow world: How network topology and burstiness slow down spreading. *Phys. Rev. E* **83**, 025102(R) (2011).

[47] Miritello, G., Moro, E. & Lara, R. Dynamical strength of social ties in information spreading. *Phys. Rev. E* **83**, 045102(R) (2011).

[48] Stehlé, J. *et al.* Simulation of an SEIR infectious disease model on the dynamic contact network of conference attendees. *BMC Medicine* **9**, 87 (2011).

[49] Rocha, L. E. C., Liljeros, F. & Holme, P. Simulated epidemics in an empirical spatiotemporal network of 50,185 sexual contacts. *PLOS Comput. Biol.* **7**, e1001109 (2011).

[50] Holme, P. Epidemiologically optimal static networks from temporal network data. *PLOS Comput. Biol.* **9**, e1003142 (2013).

[51] Saramäki, J. & Moro, E. From seconds to months: an overview of multi-scale dynamics of mobile telephone calls. *The European Physical Journal B* **88**, 1–10 (2015).

[52] Darst, R. K. *et al.* Detection of timescales in evolving complex systems. *Scientific reports* **6**, 1–8 (2016).

[53] Masuda, N. & Holme, P. Detecting sequences of system states in temporal networks. *Sci. Rep.* **9** (2019).

[54] Gelardi, V., Le Bail, D., Barrat, A. & Claidiere, N. From temporal network data to the dynamics of social relationships. *Proceedings of the Royal Society B* **288**, 20211164 (2021).

[55] Kobayashi, T. & Takaguchi, T. Social dynamics of financial networks. *EPJ Data Science* **7**, 15 (2018).

[56] Cattuto, C. *et al.* Dynamics of person-to-person interactions from distributed rfid sensor networks. *PLOS ONE* **5**, 1–9 (2010).

[57] Kobayashi, T. & Génois, M. Two types of densification scaling in the evolution of temporal networks. *Phys. Rev. E* **102**, 052302 (2020).

[58] Kobayashi, T. & Génois, M. The switching mechanisms of social network densification. *Scientific Reports* **11** (2021).

[59] Leskovec, J., Kleinberg, J. & Faloutsos, C. Graph evolution: Densification and shrinking diameters. *ACM Transactions on Knowledge Discovery from Data (TKDD)* **1**, 2 (2007).

[60] Leskovec, J., Kleinberg, J. & Faloutsos, C. Graph evolution: Densification and shrinking diameters. *ACM Trans. Knowl. Discov. Data* **1**, 2 (2007).

[61] Soramäki, K. & Cook, S. *Network theory and financial risk* (Risk Books, 2016).

[62] Caldarelli, G. *Scale-free networks: complex webs in nature and technology* (Oxford University Press, 2007).

[63] Newman, M. *Networks* (Oxford university press, 2018).

[64] Barabási, A.-l. *Network Science* (Cambridge: Cambridge University Press, Cambridge, 2016).

[65] Latora, V., Nicosia, V. & Russo, G. *Complex Networks — Principles, Methods and Applications* (Cambridge University Press, Cambridge, 2017).

[66] Albert, R., Jeong, H. & Barabási, A.-L. Internet: Diameter of the world-wide web. *Nature* **401**, 130–131 (1999).

[67] Barabási, A.-L. & Albert, R. Emergence of scaling in random networks. *Science* **286**, 509–512 (1999).

[68] Faloutsos, M., Faloutsos, P. & Faloutsos, C. On power-law relationships of the internet topology. *ACM SIGCOMM Computer Communication Review* **29**, 251–262 (1999).

[69] Li, W. & Cai, X. Statistical analysis of airport network of china. *Physical Review E* **69** (2004).

[70] Newman, M. E. J. *Networks — An Introduction* (Oxford University Press, Oxford, 2010).

[71] Motter, A. E. & Lai, Y. C. Cascade-based attacks on complex networks. *Phys. Rev. E* **66**, 065102(R) (2002).

[72] Huang, X., Vodenska, I., Havlin, S. & Stanley, H. E. Cascading failures in bi-partite graphs: model for systemic risk propagation. *Scientific Reports* **3** (2013).

[73] Helbing, D. Globally networked risks and how to respond. *Nature* **497**, 51–59 (2013).

[74] Sakamoto, Y. & Vodenska, I. Impact of bankruptcy through asset portfolios. *The European Physical Journal Special Topics* **225**, 1311–1316 (2016).

[75] Sakamoto, Y. & Vodenska, I. Systemic risk propagation in bank-asset network: New perspective on japanese banking crisis in the 1990s. *IMA Journal of Complex Networks (2015)* (2015).

[76] Duan, D. *et al.* Universal behavior of cascading failures in interdependent networks. *Proceedings of the National Academy of Sciences* **116**, 22452–22457 (2019).

[77] Smolyak, A., Levy, O., Vodenska, I., Buldyrev, S. & Havlin, S. Mitigation of cascading failures in complex networks. *Scientific reports* **10**, 1–12 (2020).

[78] Domingos, P. & Richardson, M. Mining the network value of customers. In *Proceedings of the seventh ACM SIGKDD international conference on Knowledge discovery and data mining*, 57–66 (2001).

[79] Kempe, D., Kleinberg, J. & Tardos, É. Maximizing the spread of influence through a social network. In *Proceedings of the Ninth ACM SIGKDD International Conference on Knowledge Discovery and Data Mining*, 137–146 (ACM, 2003).

[80] Radicchi, F. & Castellano, C. Fundamental difference between superblockers and superspreaders in networks. *Physical Review E* **95**, 012318 (2017).

[81] Scott, J. Social network analysis. *Sociology* **22**, 109–127 (1988).

[82] Wasserman, S., Faust, K. *et al. Social network analysis: Methods and applications* (Cambridge university press, 1994).

[83] Costa, L. d. F., Rodrigues, F. A., Travieso, G. & Villas Boas, P. R. Characterization of complex networks: A survey of measurements. *Advances in physics* **56**, 167–242 (2007).

[84] White, H. C. *Chains of opportunity* (Harvard University Press, 2013).

[85] Barbosa, H. *et al.* Human mobility: Models and applications. *Physics Reports* **734**, 1–74 (2018).

[86] Alessandretti, L., Aslak, U. & Lehmann, S. The scales of human mobility. *Nature* **587**, 402–407 (2020).

[87] Kraemer, M. U. *et al.* The effect of human mobility and control measures on the covid-19 epidemic in china. *Science* **368**, 493–497 (2020).

[88] Song, X., Zhang, Q., Sekimoto, Y. & Shibasaki, R. Prediction of human emergency behavior and their mobility following large-scale disaster. In *Proceedings of the 20th ACM SIGKDD international conference on Knowledge discovery and data mining*, 5–14 (2014).

[89] Becker, F. & Axhausen, K. W. Literature review on surveys investigating the acceptance of automated vehicles. *Transportation* **44**, 1293–1306 (2017).

[90] Eboli, M. Systemic risk in financial networks: a graph theoretic approach. *Universita di Chieti Pescara* (2004).

[91] Haldane, A. Rethinking the financial network. speech at the financial student association, amsterdam, 28 april. *Systemic Risk and Contingent Claim Analysis* **285** (2009).

[92] Albert, R. & Barabási, A. L. Statistical mechanics of complex networks. *Rev. Mod. Phys.* **74**, 47–97 (2002).

[93] Bardoscia, M. *et al.* The physics of financial networks. *Nature Reviews Physics* 1–18 (2021).

[94] Erdős, P. & Rényi, A. On random graphs i. *Publ. Math.* **6**, 290–297 (1959).

[95] Milgram, S. The small world problem. *Psychology today* **2**, 60–67 (1967).

[96] Watts, D. J. & Strogatz, S. H. Collective dynamics of 'small-world' networks. *Nature* **393**, 440–442 (1998).

[97] Jeong, H., Tombor, B., Albert, R., Oltvai, Z. N. & Barabási, A.-L. The large-scale organization of metabolic networks. *Nature* **407**, 651–654 (2000).

[98] Redner, S. How popular is your paper? an empirical study of the citation distribution. *The European Physical Journal B-Condensed Matter and Complex Systems* **4**, 131–134 (1998).

[99] Liljeros, F., Edling, C., Amaral, L. & Åberg, H. E. S. . Y. The web of human sexual contacts. *Nature* **411**, 907–908 (2001).

[100] Barabási, A. L., Albert, R. & Jeong, H. Mean-field theory for scale-free random networks. *Physica A* **272**, 173–187 (1999).

[101] Jeong, H., Mason, S. P., Barabási, A.-L. & Oltvai, Z. N. Lethality and centrality in protein networks. *Nature* **411**, 41–42 (2001).

[102] Navlakha, S., He, X., Faloutsos, C. & Bar-Joseph, Z. Topological properties of robust biological and computational networks. *Journal of the Royal Society Interface* **11**, 20140283 (2014).

[103] May, R. M., Levin, S. A. & Sugihara, G. Complex systems: Ecology for bankers. *Nature* **451**, 893–895 (2008).

[104] Haldane, A. G. & May, R. M. Systemic risk in banking ecosystems. *Nature* **469**, 351–355 (2011).

[105] Allen, F. & Gale, D. Financial contagion. *Journal of political economy* **108**, 1–33 (2000).

[106] Macchiati, V. *et al.* Systemic liquidity contagion in the european interbank market. *Journal of Economic Interaction and Coordination* **17**, 443–474 (2022).

[107] Boss, M., Elsinger, H., Summer, M. & Thurner, S. Network topology of the interbank market. *Quantitative Finance* **4**, 677–684 (2004).

[108] De Masi, G., Iori, G. & Caldarelli, G. Fitness model for the Italian interbank money market. *Phys. Rev. E* **74**, 066112 (2006).

[109] León, C. & Berndsen, R. J. Rethinking financial stability: challenges arising from financial networks' modular scale-free architecture. *Journal of Financial Stability* **15**, 241–256 (2014).

[110] Soramäki, K., Bech, M. L., Arnold, J., Glass, R. J. & Beyeler, W. E. The topology of interbank payment flows. *Physica A: Statistical Mechanics and its Applications* **379**, 317 – 333 (2007).

[111] Iori, G., De Masi, G., Precup, O. V., Gabbi, G. & Caldarelli, G. A network analysis of the Italian overnight money market. *Journal of Economic Dynamics and Control* **32**, 259–278 (2008).

[112] Bech, M. L. & Atalay, E. The topology of the federal funds market. *Physica A: Statistical Mechanics and its Applications* **389**, 5223–5246 (2010).

[113] Fricke, D. & Lux, T. Core–periphery structure in the overnight money market: evidence from the e-MID trading platform. *Computational Economics* **45**, 359–395 (2015).

[114] Albert, R., Jeong, H. & Barabási, A.-L. Error and attack tolerance of complex networks. *Nature* **406**, 378–382 (2000).

[115] Langfield, S. & Soramäki, K. Interbank exposure networks. *Computational Economics* **47**, 3–17 (2016).

[116] Bargigli, L., Di Iasio, G., Infante, L., Lillo, F. & Pierobon, F. The multiplex structure of interbank networks. *Quantitative Finance* **15**, 673–691 (2015).

[117] Langfield, S., Liu, Z. & Ota, T. Mapping the uk interbank system. *Journal of Banking & Finance* **45**, 288–303 (2014).

[118] Montagna, M. & Kok, C. Multi-layered Interbank Model for Assessing Systemic Risk. *Kiel Working Papers no.1873* (2013).

[119] Tu, Y. How robust is the internet. *Nature Communications* **406** (2000).

[120] Callaway, D. S., Newman, M. E. J., Strogatz, S. H. & Watts, D. J. Network robustness and fragility: Percolation on random graphs. *Phys. Rev. Lett.* **85**, 5468–5471 (2000).

[121] Squartini, T., van Lelyveld, I. & Garlaschelli, D. Early-warning signals of topological collapse in interbank networks. *Scientific Reports* **3**, 3357 (2013).

[122] Holme, P. Modern temporal network theory: A colloquium. *Eur. Phys. J. B* **88**, 234 (2015).

[123] Latapy, M., Viard, T. & Magnien, C. Stream graphs and link streams for the modeling of interactions over time. *Social Network Analysis and Mining* **8**, 1–29 (2018).

[124] Zhao, K., Stehlé, J., Bianconi, G. & Barrat, A. Social network dynamics of face-to-face interactions. *Physical Review E* **83**, 056109 (2011).

[125] Karsai, M., Perra, N. & Vespignani, A. Time varying networks and the weakness of strong ties. *Sci. Rep.* 4001 (2014).

[126] Battiston, S. *et al.* Complexity theory and financial regulation. *Science* **351**, 818–819 (2016).

[127] Isella, L. *et al.* Close encounters in a pediatric ward: measuring face-to-face proximity and mixing patterns with wearable sensors. *PLOS ONE* **6**, e17144 (2011).

[128] Karimi, F. & Holme, P. A temporal network version of watts's cascade model. In *Temporal Networks*, 315–329 (Springer, 2013).

[129] Allen, F. & Babus, A. Networks in finance. *The network challenge: strategy, profit, and risk in an interlinked world* **367** (2009).

[130] Chinazzi, M. & Fagiolo, G. Systemic risk, contagion, and financial networks: A survey. *Institute of Economics, Scuola Superiore Sant*

Anna, Laboratory of Economics and Management (LEM) Working Paper Series (2015).

[131] Benoit, S., Colliard, J.-E., Hurlin, C. & Pérignon, C. Where the risks lie: A survey on systemic risk. *Review of Finance* **21**, 109–152 (2017).

[132] Upper, C. Simulation methods to assess the danger of contagion in interbank markets. *Journal of Financial Stability* **7**, 111–125 (2011).

[133] Elsinger, H., Lehar, A. & Summer, M. Network models and systemic risk assessment. *Handbook on Systemic Risk* **1**, 287–305 (2013).

[134] Summer, M. Financial contagion and network analysis. *Annu. Rev. Financ. Econ.* **5**, 277–297 (2013).

[135] Caccioli, F., Barucca, P. & Kobayashi, T. Network models of financial systemic risk: a review. *Journal of Computational Social Science* **1**, 81–114 (2018).

[136] Jackson, M. O. & Pernoud, A. Systemic risk in financial networks: A survey. *Annual Review of Economics* **13**, 171–202 (2021).

[137] http://www.sociopatterns.org/ Accessed on January 8, 2022.

[138] Cattuto, C. *et al.* Dynamics of person-to-person interactions from distributed RFID sensor networks. *PLOS ONE* **5**, e11596 (2010).

[139] Onnela, J.-P. *et al.* Structure and tie strengths in mobile communication networks. *Proc. Natl. Acad. Sci. USA* **104**, 7332–7336 (2007).

[140] Kobayashi, T., Takaguchi, T. & Barrat, A. The structured backbone of temporal social ties. *Nature communications* **10** (2019).

[141] Holme, P. & Saramäki, J. Temporal networks. *Physics reports* **519**, 97–125 (2012).

[142] Cohen, R., Erez, K., Ben-Avraham, D. & Havlin, S. Resilience of the Internet to random breakdowns. *Phys. Rev. Lett.* **85**, 4626–4628 (2000).

[143] Pastor-Satorras, R. & Vespignani, A. Epidemic spreading in scale-free networks. *Phys. Rev. Lett.* **86**, 3200–3203 (2001).

[144] Liljeros, F., Giesecke, J. & Holme, P. The contact network of inpatients in a regional healthcare system. a longitudinal case study, mathematical population studies. *Math. Popul. Stud.* **14**, 269–284 (2012).

[145] Walker, A. *et al.* Characterisation of clostridium difficile hospital ward–based transmission using extensive epidemiological data and molecular typing. *PLoS Med* **9**, e1001172 (2012).

[146] Génois, M., Vestergaard, C. L., Cattuto, C. & Barrat, A. Compensating for population sampling in simulations of epidemic spread on temporal contact networks. *Nature Communications* **6** (2015).

[147] Gehrke, J., Ginsparg, P. & Kleinberg, J. Overview of the 2003 kdd cup. *ACM SIGKDD Explorations Newsletter* **5**, 149–151 (2003).

[148] Barrat, A., Barthélemy, M., Pastor-Satorras, R. & Vespignani, A. The architecture of complex weighted networks. *Proc. Natl. Acad. Sci. USA* **101**, 3747–3752 (2004).

[149] Newman, M. E. J. The structure of scientific collaboration networks. *Proc. Natl. Acad. Sci. USA* **98**, 404–409 (2001).

[150] Zhan, X., Hanjalic, A. & Wang, H. Information diffusion backbones in temporal networks. *Sci. Rep.* **9** (2019).

[151] Hulovatyy, Y., Chen, H. & Milenković. Exploring the structure and function of temporal networks with dynamic graphlets. *Bioinformatics* **31** (2015).

[152] Goh, K.-I. & Barabási, A.-L. Burstiness and memory in complex systems. *EPL (Europhysics Letters)* **81**, 48002 (2008).

[153] Jo, H. H. Modeling correlated bursts by the bursty-get-burstier mechanism. *Phys. Rev. E* **96**, 062131 (2017).

[154] Karsai, M., Jo, H. H. & Kaski, K. *Bursty human dynamics* (Springer Berlin, 2018).

[155] Karsai, M., Kaski, K., Barabási, A. L. & Kertész, J. Universal features of correlated bursty behaviour. *Sci. Rep.* **2**, 397 (2012).

[156] Holme, P. Efficient local strategies for vaccination and network attack. *Europhys. Lett.* **68**, 908–914 (2004).

[157] Johansen, A. Probing human response times. *Phys. A* **330**, 286–291 (2004).

[158] Vázquez, A., Pastor-Satorras, R. & Vespignani, A. Large-scale topological and dynamical properties of the internet. *Physical review. E, Statistical, nonlinear, and soft matter physics* **65 6 Pt 2**, 066130 (2002).

[159] Newman, M. E. J. Power laws, Pareto distributions and Zipf's law. *Contem. Phys.* **46**, 323–351 (2005).

[160] Rocha, L. E. C., Liljeros, F. & Holme, P. Information dynamics shape the sexual networks of Internet-mediated prostitution. *Proc. Natl. Acad. Sci. USA* **107**, 5706–5711 (2010).

[161] Jo, H.-H. & Hiraoka, T. Bursty time series analysis for temporal networks. In Holme, P. & Saramäki, J. (eds.) *Temporal Network Theory* (Springer-Nature, New York, 2019).

[162] Goh, K. I. & Barabási, A. L. Burstiness and memory in complex systems. *Europhys. Lett.* **81**, 48002 (2008).

[163] Min, B., Goh, K. I. & Vazquez, A. Spreading dynamics following bursty human activity patterns. *Phys. Rev. E* **83**, 036102 (2011).

[164] Horváth, D. X. & Kertész, J. Spreading dynamics on networks: The role of burstiness, topology and non-stationarity. *New J. Phys.* **16**, 073037 (2014).

[165] Iribarren, J. L. & Moro, E. Branching dynamics of viral information spreading. *Phys. Rev E* **84**, 046116 (2011).

[166] Unicomb, S., Iñiguez, G., Gleeson, J. & Karsai, M. Dynamics of cascades on burstiness-controlled temporal networks. *Nature Communications* **12** (2021).

[167] Schweitzer, F. *et al.* Economic networks: The new challenges. *science* **325**, 422–425 (2009).

[168] Mishkin, F. S. Monetary policy strategy: lessons from the crisis. *NBER Working Paper* **16755** (2011).

[169] Atkinson, T., Luttrell, D. & Rosenblum, H. How bad is it? the costs and consequences of the 2007–09 financial crisis. *Dallas Fed Staff Papers* **20** (2013).

[170] Castellano, C., Fortunato, S. & Loreto, V. Statistical physics of social dynamics. *Rev. Mod. Phys.* **81**, 591–646 (2009).

[171] Lloyd, A. L. & May, R. M. How viruses spread among computers and people. *Science* **292**, 1316–1317 (2001).

[172] Newman, M. E. Spread of epidemic disease on networks. *Physical Review E* **66**, 016128 (2002).

[173] Hsu, W. H., King, A. L., Paradesi, M. S., Pydimarri, T. & Weninger, T. Collaborative and structural recommendation of friends using weblog-based social network analysis. In *AAAI Spring Symposium: Computational Approaches to Analyzing Weblogs*, vol. 6, 55–60 (2006).

[174] Liben-Nowell, D. & Kleinberg, J. The link-prediction problem for social networks. *J. Am. Soc. Inf. Sci. Tech.* **58**, 1019–1031 (2007).

[175] Leskovec, J., Adamic, L. A. & Huberman, B. A. The dynamics of viral marketing. *ACM Transactions on the Web (TWEB)* **1**, 5–es (2007).

[176] Zeng, D., Chen, H., Lusch, R. & Li, S.-H. Social media analytics and intelligence. *IEEE Intelligent Systems* **25**, 13–16 (2010).

[177] Moreno, Y., Nekovee, M. & Pacheco, A. F. Dynamics of rumor spreading in complex networks. *Physical review E* **69**, 066130 (2004).

[178] Ricardo, D. *On the principles of political economy* (J. Murray London, 1821).

[179] Stäheli, U. Seducing the crowd: The leader in crowd psychology. *New German Critique* **38**, 63–77 (2011).

[180] Hansen, K. B. Financial contagion: problems of proximity and connectivity in financial markets. *Journal of Cultural Economy* **14**, 388–402 (2021).

[181] Jones, E. D. *Economic crises* (New York: The Macmillan Company; London: Macmillan and Company, Limited, 1900).

[182] Sidis, B. *The psychology of suggestion: A research into the subconscious nature of man and society* (D. Appleton, 1898).

[183] Rafter, N. H. Gabriel tarde: Imitation and crime, 1890. In *The Origins of Criminology*, 341–345 (Routledge-Cavendish, 2009).

[184] Mitchell, W. C. *Business cycles*, vol. 3 (University of California Press, 1913).

[185] Bikhchandani, S., Hirshleifer, D. & Welch, I. A theory of fads, fashion, custom, and cultural change as informational cascades. *J. Polit. Econ.* 992–1026 (1992).

[186] Kindleberger, C. P., Manias, P. & Crashes, A. History of financial crises (1996).

[187] Aliber, R. Z. & Kindleberger, C. P. *Manias, panics, and crashes: A history of financial crises* (Springer, 2015).

[188] Stiglitz, J. E. Contagion, liberalization, and the optimal structure of globalization. *Journal of Globalization and Development* **1** (2010).

[189] Minoiu, C. & Reyes, J. A. A network analysis of global banking: 1978–2010. *Journal of Financial Stability* **9**, 168–184 (2013).

[190] Perera, S., Bell, M. G. & Bliemer, M. C. Network science approach to modelling the topology and robustness of supply chain networks: a review and perspective. *Applied network science* **2**, 1–25 (2017).

[191] Brankston, G., Gitterman, L., Hirji, Z., Lemieux, C. & Gardam, M. Transmission of influenza a in human beings. *The Lancet infectious diseases* **7**, 257–265 (2007).

[192] Read, J. M., Eames, K. T. & Edmunds, W. J. Dynamic social networks and the implications for the spread of infectious disease. *Journal of The Royal Society Interface* **5**, 1001–1007 (2008).

[193] Funk, S., Salathé, M. & Jansen, V. A. Modelling the influence of human behaviour on the spread of infectious diseases: a review. *Journal of the Royal Society Interface* **7**, 1247–1256 (2010).

[194] Salathé, M. *et al.* A high-resolution human contact network for infectious disease transmission. *Proceedings of the National Academy of Sciences* **107**, 22020–22025 (2010).

[195] Leung, N. H. Transmissibility and transmission of respiratory viruses. *Nature Reviews Microbiology* **19**, 528–545 (2021).

[196] Mossong, J. *et al.* Social contacts and mixing patterns relevant to the spread of infectious diseases. *PLoS medicine* **5**, e74 (2008).

[197] Sommer, R. Studies in personal space. *Sociometry* **22**, 247–260 (1959).

[198] Hui, P. *et al.* Pocket switched networks and human mobility in conference environments. In *Proceedings of the 2005 ACM SIGCOMM workshop on Delay-tolerant networking*, 244–251 (2005).

[199] Eagle, N. & Pentland, A. Reality mining: sensing complex social systems. *Pers. Ubiquit. Comput.* **10**, 255–268 (2006).

[200] O'Neill, E. *et al.* Instrumenting the city: Developing methods for observing and understanding the digital cityscape. In *International Conference on Ubiquitous Computing*, 315–332 (Springer, 2006).

[201] Scherrer, A., Borgnat, P., Fleury, E., Guillaume, J.-L. & Robardet, C. Description and simulation of dynamic mobility networks. *Computer Networks* **52**, 2842–2858 (2008).

[202] Liu, T., Yang, L., Liu, S. & Ge, S. Inferring and analysis of social networks using rfid check-in data in china. *PloS one* **12**, e0178492 (2017).

[203] Stopczynski, A., Pentland, A. & Lehmann, S. How physical proximity shapes complex social networks. *Scientific reports* **8**, 1–10 (2018).

[204] Dunbar, R., Arnaboldi, V., Conti, M. & Passarella, A. The structure of online social networks mirrors those in the offline world. *Social Networks* **43**, 39–47 (2015).

[205] Jo, H. H., Karsai, M., Kertesz, J. & Kaski, K. Circadian pattern and burstiness in mobile phone communication. *New J. Phys.* **14**, 013055 (2012).

[206] Kovanen, L., Saramaki, J. & Kaski, K. Reciprocity of mobile phone calls (2010). 1002.0763.

[207] Schläpfer, M. *et al.* The scaling of human interactions with city size. *J. R. Soc.* **11** (2014).

[208] Ghosh, A., Monsivais, D., Bhattacharya, K., Dunbar, R. I. & Kaski, K. Quantifying gender preferences in human social interactions using a large cellphone dataset. *EPJ Data Sci.* **8** (2019).

[209] Klimt, B. & Yang, Y. The enron corpus: A new dataset for email classification research. In *Machine Learning: ECML 2004*, 217–226 (Springer, 2004).

[210] Wilson, J. Q. & Kelling, G. L. Broken windows. *Atlantic monthly* **249**, 29–38 (1982).

[211] Bullmore, E. & Sporns, O. Complex brain networks: graph theoretical analysis of structural and functional systems. *Nature reviews neuroscience* **10**, 186–198 (2009).

[212] Szell, M., Lambiotte, R. & Thurner, S. Multirelational organization of large-scale social networks in an online world. *Proceedings of the National Academy of Sciences* **107**, 13636–13641 (2010).

[213] Consortium, A. I. M. *et al.* Evidence for network evolution in an arabidopsis interactome map. *Science* **333**, 601–607 (2011).

[214] Vespignani, A. Modelling dynamical processes in complex socio-technical systems. *Nature physics* **8**, 32–39 (2012).

[215] Dorogovtsev, S. N. & Mendes, J. F. F. *Evolution of Networks: From Biological Nets to the Internet and WWW* (Oxford University Press, Oxford, 2003).

[216] Krause, J., Ruxton, G. D. & Krause, S. Swarm intelligence in animals and humans. *Trends Ecol. Evol.* **25**, 28–34 (2010).

[217] Brent, L. J. Friends of friends: are indirect connections in social networks important to animal behaviour? *Animal behaviour* **103**, 211–222 (2015).

[218] Croft, D. P., James, R. & Krause, J. *Exploring animal social networks* (Princeton University Press, 2008).

[219] Wey, T., Blumstein, D. T., Shen, W. & Jordán, F. Social network analysis of animal behaviour: a promising tool for the study of sociality. *Animal behaviour* **75**, 333–344 (2008).

[220] Falkenberg, M. *et al.* Identifying time dependence in network growth. *Physical Review Research* **2**, 023352 (2020).

[221] Eisenberg, E. & Levanon, E. Y. Preferential attachment in the protein network evolution. *Physical review letters* **91**, 138701 (2003).

[222] Szell, M. & Thurner, S. Measuring social dynamics in a massive multiplayer online game. *Social networks* **32**, 313–329 (2010).

[223] Perc, M. Evolution of the most common english words and phrases over the centuries. *Journal of The Royal Society Interface* **9**, 3323–3328 (2012).

[224] Kondor, D., Pósfai, M., Csabai, I. & Vattay, G. Do the rich get richer? an empirical analysis of the bitcoin transaction network. *PloS one* **9**, e86197 (2014).

[225] Ronda-Pupo, G. A. & Pham, T. The evolutions of the rich get richer and the fit get richer phenomena in scholarly networks: the case of the strategic management journal. *Scientometrics* **116**, 363–383 (2018).

[226] Sheridan, P. & Onodera, T. A preferential attachment paradox: How preferential attachment combines with growth to produce networks with log-normal in-degree distributions. *Scientific reports* **8**, 1–11 (2018).

[227] Bazzi, M., Jeub, L. G., Arenas, A., Howison, S. D. & Porter, M. A. A framework for the construction of generative models for mesoscale structure in multilayer networks. *Physical Review Research* **2**, 023100 (2020).

[228] Bianconi, G. & Barabási, A.-L. Competition and multiscaling in evolving networks. *EPL (Europhysics Letters)* **54**, 436 (2001).

[229] Caldarelli, G., Capocci, A., De Los Rios, P. & Muñoz, M. A. Scale-free networks from varying vertex intrinsic fitness. *Phys. Rev. Lett.* **89**, 258702 (2002).

[230] Boguñá, M. & Pastor-Satorras, R. Class of correlated random networks with hidden variables. *Phys. Rev. E* **68**, 036112 (2003).

[231] Starnini, M. & Pastor-Satorras, R. Topological properties of a time-integrated activity-driven network. *Phys. Rev. E* **87**, 062807 (2013).

[232] Leskovec, J., Kleinberg, J. & Faloutsos, C. Graphs over time: densification laws, shrinking diameters and possible explanations. In *Proceedings of the Eleventh ACM SIGKDD International Conference on Knowledge Discovery in Data Mining*, 177–187 (ACM, 2005).

[233] Bettencourt, L. M., Kaiser, D. I. & Kaur, J. Scientific discovery and topological transitions in collaboration networks. *Journal of Informetrics* **3**, 210–221 (2009).

[234] Pastor-Satorras, R., Castellano, C., Van Mieghem, P. & Vespignani, A. Epidemic processes in complex networks. *Rev. Mod. Phys.* **87**, 925–979 (2015).

[235] Min, B., Gwak, S.-H., Lee, N. & Goh, K.-I. Layer-switching cost and optimality in information spreading on multiplex networks. *Scientific reports* **6**, 1–12 (2016).

[236] Zheng, M., Zhao, M., Min, B. & Liu, Z. Synchronized and mixed outbreaks of coupled recurrent epidemics. *Scientific reports* **7**, 1–11 (2017).

[237] Centola, D. & Macy, M. W. Complex contagion and the weakness of long ties. *American Journal of Sociology* **113**, 702–734 (2007).

[238] Centola, D., Eguíluz, V. & Macy, M. W. Cascade dynamics of complex propagation. *Physica A* **374**, 449–456 (2007).

[239] Borge-Holthoefer, J., Banos, R. A., González-Bailón, S. & Moreno, Y. Cascading behaviour in complex socio-technical networks. *Journal of Complex Networks* **1**, 3–24 (2013).

[240] Min, B. & San Miguel, M. Competing contagion processes: Complex contagion triggered by simple contagion. *Sci. Rep.* (2018).

[241] Guille, A., Hacid, H., Favre, C. & Zighed, D. A. Information diffusion in online social networks: A survey. *ACM Sigmod Record* **42**, 17–28 (2013).

[242] Newman, M. E. J. Assortative mixing in networks. *Phys. Rev. Lett.* **89**, 208701 (2002).

[243] Granovetter, M. Threshold models of collective behavior. *American Journal of Sociology* **83**, 1420–1443 (1978).

[244] Watts, D. J. A simple model of global cascades on random networks. *PNAS* **99**, 5766–5771 (2002).

[245] Dodds, P. S. & Watts, D. J. Universal behavior in a generalized model of contagion. *Physical review letters* **92**, 218701 (2004).

[246] Hoppe, K. & Rodgers, G. Mutual selection in time-varying networks. *Physical Review E* **88**, 042804 (2013).

[247] Fernández-Gracia, J., Eguíluz, V. M. & Miguel, M. S. Timing interactions in social simulations: The voter model. *arXiv preprint arXiv:1306.4735* (2013).

[248] Chung, K., Baek, Y., Kim, D., Ha, M. & Jeong, H. Generalized epidemic process on modular networks. *Physical Review E* **89**, 052811 (2014).

[249] Gómez-Gardeñes, J., de Barros, A. S., Pinho, S. T. & Andrade, R. F. Abrupt transitions from reinfections in social contagions. *EPL (Europhysics Letters)* **110**, 58006 (2015).

[250] Choi, W., Lee, D. & Kahng, B. Mixed-order phase transition in a two-step contagion model with a single infectious seed. *Physical Review E* **95**, 022304 (2017).

[251] Ugander, J., Backstrom, L., Marlow, C. & Kleinberg, J. Structural diversity in social contagion. *Proceedings of the national academy of sciences* **109**, 5962–5966 (2012).

[252] Anderson, R. M. & May, R. M. *Infectious diseases of humans* (Oxford University Press, Oxford, 1991).

[253] Watts, D. J. Networks, dynamics, and the small-world phenomenon. *American Journal of sociology* **105**, 493–527 (1999).

[254] Barthélemy, M., Barrat, A., Pastor-Satorras, R. & Vespignani, A. Velocity and hierarchical spread of epidemic outbreaks in scale-free networks. *Phys. Rev. Lett.* **92**, 178701 (2004).

[255] Isella, L. *et al.* What's in a crowd? analysis of face-to-face behavioral networks. *J. Theor. Biol.* **271**, 166–180 (2011).

[256] Dodds, P. S. & Watts, D. J. A generalized model of social and biological contagion. *Journal of theoretical biology* **232**, 587–604 (2005).

[257] Granovetter, M. Threshold models of collective behavior. *Am. J. Sociol.* **83**, 1420–1443 (1978).

[258] Watts, D. J. & Dodds, P. S. Influentials, networks, and public opinion formation. *Journal of Consumer Research* **34**, 441–458 (2007).

[259] Centola, D. The spread of behavior in an online social network experiment. *Science* **329**, 1194–1197 (2010).

[260] Backlund, V.-P., Saramäki, J. & Pan, R. K. Effects of temporal correlations on cascades: Threshold models on temporal networks. *Physical Review E* **89**, 062815 (2014).

[261] Kobayashi, T. Trend-driven information cascades on random networks. *Physical Review E* **92**, 062823 (2015).

[262] Schelling, T. C. Dynamic models of segregation. *J. Math. Sociol.* **1**, 143–186 (1971).

[263] Valente, T. W. Social network thresholds in the diffusion of innovations. *Soc. Netw.* **18**, 69–89 (1996).

[264] Brockmann, D., Hufnagel, L. & Geisel, T. The scaling laws of human travel. *Nature* **439**, 462–465 (2006).

[265] Gonzalez, M. C., Hidalgo, C. A. & Barabasi, A.-L. Understanding individual human mobility patterns. *Nature* **453**, 779–782 (2008).

[266] Lazer, D. *et al.* Computational Social Science. *Science* **323**, 721–723 (2009).

[267] Vespignani, A. Predicting the behavior of techno-social systems. *Science* **325**, 425–428 (2009).

[268] Eckmann, J. P., Moses, E. & Sergi, D. Entropy of dialogues creates coherent structures in e-mail traffic. *Proc. Natl. Acad. Sci. USA* **101**, 14333–14337 (2004).

[269] Said, A. Identifying and utilizing contextual data in hybrid recommender systems. In *Proceedings of the fourth ACM conference on Recommender systems*, 365–368 (2010).

[270] Wang, Z., Du, C., Fan, J. & Xing, Y. Ranking influential nodes in social networks based on node position and neighborhood. *Neurocomputing* **260**, 466–477 (2017).

[271] Xu, Z., Rui, X., He, J., Wang, Z. & Hadzibeganovic, T. Superspreaders and superblockers based community evolution tracking in dynamic social networks. *Knowledge-Based Systems* **192**, 105377 (2020).

[272] May, R. M. & Anderson, R. M. The transmission dynamics of human immunodeficiency virus (HIV). *Phil. Trans. R. Soc. Lond. Ser. B* **321**, 565–607 (1988).

[273] Woolhouse, M. E. *et al.* Heterogeneities in the transmission of infectious agents: implications for the design of control programs. *Proceedings of the National Academy of Sciences* **94**, 338–342 (1997).

[274] Lloyd-Smith, J. O., Getz, W. M. & Westerhoff, H. V. Frequency–dependent incidence in models of sexually transmitted diseases: portrayal of pair–based transmission and effects of illness on contact behaviour. *Proceedings of the Royal Society of London. Series B: Biological Sciences* **271**, 625–634 (2004).

[275] Lloyd-Smith, J. O., Schreiber, S. J., Kopp, P. E. & Getz, W. M. Superspreading and the effect of individual variation on disease emergence. *Nature* **438**, 355–359 (2005).

[276] Altarelli, F., Braunstein, A., Dall'Asta, L., Wakeling, J. R. & Zecchina, R. Containing epidemic outbreaks by message-passing techniques. *Phys. Rev. X* **4**, 021024 (2014).

[277] Zhang, J.-X., Chen, D.-B., Dong, Q. & Zhao, Z.-D. Identifying a set of influential spreaders in complex networks. *Scientific reports* **6**, 1–10 (2016).

[278] Kitsak, M. *et al.* Identifying influential spreaders in complex networks. *Nature Physics 6, 888* (2010).

[279] Radicchi, F. & Castellano, C. Beyond the locally treelike approximation for percolation on real networks. *Phys. Rev. E* **93**, 030302(R) (2016).

[280] Cont, R., Moussa, A. & Santos, E. B. Network structure and systemic risk in banking systems. In Fouque, J.-P. & Langsam, J. A. (eds.) *Handbook on Systemic Risk* (Cambridge University Press, New York, 2013).

[281] Bricco, M. J. & Xu, M. T. *Interconnectedness and contagion analysis: a practical framework* (International Monetary Fund, 2019).

[282] ANDERSON, R. *et al.* Macroprudential stress tests and policies: Searching for robust and implementable frameworks, washington dc. *International Monetary Fund, Working Paper WP/18/197* (2018).

[283] Anderson, R. *et al. Macroprudential stress tests and policies: Searching for robust and implementable frameworks* (International Monetary Fund, 2018).

[284] Hurd, T. R. Bank panics and fire sales, insolvency and illiquidity. *International Journal of Theoretical and Applied Finance* **21**, 1850040 (2018).

[285] Roukny, T., Battiston, S. & Stiglitz, J. E. Interconnectedness as a source of uncertainty in systemic risk. *Journal of Financial Stability* **35**, 93–106 (2018).

[286] Yang, J. & Leskovec, J. Defining and evaluating network communities based on ground-truth. *Knowledge and Information Systems* **42**, 181–213 (2015).

[287] Eagle, N., Pentland, A. S. & Lazer, D. Inferring friendship network structure by using mobile phone data. *Proceedings of the national academy of sciences* **106**, 15274–15278 (2009).

[288] Fudolig, M. I. D., Monsivais, D., Bhattacharya, K., Jo, H.-H. & Kaski, K. Different patterns of social closeness observed in mobile phone communication. *Journal of Computational Social Science* **3**, 1–17 (2020).

[289] Enron Email Dataset (May 7, 2015 version). http://www.cs.cmu.edu/~enron/. Accessed July 20, 2021.

[290] Opsahl, T. & Panzarasa, P. Clustering in weighted networks. *Social networks* **31**, 155–163 (2009).

[291] Yin, H., Benson, A. R., Leskovec, J. & Gleich, D. F. Local higher-order graph clustering. In *Proceedings of the 23rd ACM SIGKDD international conference on knowledge discovery and data mining*, 555–564 (2017).

[292] Cajueiro, D. O. & Tabak, B. M. The role of banks in the Brazilian Interbank Market: Does bank type matter? Working Papers Series 130, Central Bank of Brazil, Research Department (2007).

[293] e Santos, E. B. & Cont, R. The Brazilian Interbank Network Structure and Systemic Risk. Working Papers Series 219, Central Bank of Brazil, Research Department (2010).

[294] Degryse, H., Nguyen, G. *et al.* Interbank exposures: An empirical examination of contagion risk in the belgian banking system. *International Journal of Central Banking* **3**, 123–171 (2007).

[295] Craig, B. & Von Peter, G. Interbank tiering and money center banks. *Journal of Financial Intermediation* **23**, 322–347 (2014).

[296] Finger, K., Fricke, D. & Lux, T. Network analysis of the e-mid overnight money market: the informational value of different aggregation levels for intrinsic dynamic processes. *Computational Management Science* **10**, 187–211 (2013).

[297] Martinez-Jaramillo, S., Alexandrova-Kabadjova, B., Bravo-Benitez, B. & Solórzano-Margain, J. P. An empirical study of the mexican banking system's network and its implications for systemic risk. *Journal of Economic Dynamics and Control* **40**, 242–265 (2014).

[298] Müller, J. Interbank credit lines as a channel of contagion. *Journal of Financial Services Research* **29**, 37–60 (2006).

[299] Demiralp, S., Preslopsky, B. & Whitesell, W. Overnight interbank loan markets. *Journal of Economics and Business* **58**, 67–83 (2006).

[300] Upper, C. & Worms, A. Estimating bilateral exposures in the german interbank market: Is there a danger of contagion? *European Economic Review* **48**, 827 – 849 (2004).

[301] Kiff, J. *et al.* Making over-the-counter derivatives safer: The role of central counterparties. *Global Financial Stability Report* (2010).

[302] Faruqui, U., Huang, W. & Takáts, E. Clearing risks in OTC derivatives markets: the CCP-bank nexus. *BIS Quarterly Review* 73–90 (2018).

[303] Domanski, D., Gambacorta, L. & Picillo, C. Central clearing: trends and current issues. *BIS Quarterly Review* 59–76 (2015).

[304] Duffie, D. & Zhu, H. Does a central clearing counterparty reduce counterparty risk? *The Review of Asset Pricing Studies* **1**, 74–95 (2011).

[305] Garratt, R. & Zimmerman, P. Does central clearing reduce counterparty risk in realistic financial networks? *FRB of New York Staff Report* (2015).

[306] Hirata, W. & Ojima, M. Competition and bank systemic risk: New evidence from japan's regional banking. *Pacific-Basin Finance Journal* **60**, 101283 (2020).

[307] Greenwood, R. & Thesmar, D. Stock price fragility. *Journal of Financial Economics* **102**, 471–490 (2011).

[308] Anton, M. & Polk, C. Connected stocks. *The Journal of Finance* **69**, 1099–1127 (2014).

[309] Vodenska, I. *et al.* From stress testing to systemic stress testing: the importance of macroprudential regulation. *Journal of Financial Stability* **52**, 100803 (2021).

[310] Caccioli, F., Shrestha, M., Moore, C. & Farmer, J. D. Stability analysis of financial contagion due to overlapping portfolios. *Journal of Banking & Finance* **46**, 233–245 (2014).

[311] Gualdi, S., Cimini, G., Primicerio, K., Di Clemente, R. & Challet, D. Statistically validated network of portfolio overlaps and systemic risk. *Scientific Reports* **6** (2016).

[312] Greenwood, R., Landier, A. F. & Thesmar, D. Vulnerable Banks. *Journal of Financial Economics* **115**, 471–485 (2015).

[313] Cont, R. & Wagalath, L. Fire sales forensics: measuring endogenous risk. *Mathematical finance* **26**, 835–866 (2016).

[314] Cifuentes, R., Ferrucci, G. & Shin, H. S. Liquidity risk and contagion. *Journal of the European Economic Association* **3**, 556–566 (2005).

[315] Caccioli, F., Farmer, J. D., Foti, N. & Rockmore, D. Overlapping portfolios, contagion, and financial stability. *Journal of Economic Dynamics and Control* **51**, 50–63 (2015).

[316] Caccioli, F., Ferrara, G. & Ramadiah, A. Modelling fire sale contagion across banks and non-banks. *Bank of England Working Paper* (2020).

[317] Boccaletti, S. *et al.* The structure and dynamics of multilayer networks. *Physics Reports* **544**, 1–122 (2014).

[318] Bianconi, G. *Multilayer networks: structure and function* (Oxford university press, 2018).

[319] Battiston, S., Caldarelli, G. & Garas, A. *Multiplex and multilevel networks* (Oxford University Press, 2018).

[320] Fischer, T. No-arbitrage pricing under systemic risk: Accounting for cross-ownership. *Mathematical Finance: An International Journal of Mathematics, Statistics and Financial Economics* **24**, 97–124 (2014).

[321] Brummitt, C. D. & Kobayashi, T. Cascades in multiplex financial networks with debts of different seniority. *PRE* **91**, 062813 (2015).

[322] Kusnetsov, M. & Maria Veraart, L. A. Interbank clearing in financial networks with multiple maturities. *SIAM Journal on Financial Mathematics* **10**, 37–67 (2019).

[323] Feinstein, Z. Obligations with physical delivery in a multilayered financial network. *SIAM Journal on Financial Mathematics* **10**, 877–906 (2019).

[324] Brummitt, C. D., Lee, K.-M. & Goh, K.-I. Multiplexity-facilitated cascades in networks. *PRE* **85**, 045102(R) (2012).

[325] Poledna, S., Molina-Borboa, J. L., Martnez-Jaramillo, S., van der Leij, M. & Thurner, S. The multilayer network nature of systemic risk and its implications for the costs of financial crises. *Journal of Financial Stability* **20**, 70–81 (2015).

[326] Montagna, M. & Kok, C. Multi-layered interbank model for assessing systemic risk. *ECB Working Paper* (2016).

[327] Barucca, P. & Lillo, F. Disentangling bipartite and core-periphery structure in financial networks. *Chaos, Solitons & Fractals* **88**, 244–253 (2016).

[328] Barucca, P. & Lillo, F. The organization of the interbank network and how ecb unconventional measures affected the e-mid overnight market. *Computational Management Science* **15**, 33–53 (2018).

[329] Kobayashi, T., Sapienza, A. & Ferrara, E. Extracting the multi-timescale activity patterns of online financial markets. *Scientific Reports* **8**, 11184 (2018).

[330] Caccioli, F., Barucca, P. & Kobayashi, T. Network models of financial systemic risk: A review. *arXiv:1710.11512v1* (2017).

[331] Raddant, M. Structure in the Italian overnight loan market. *Journal of International Money and Finance* **41**, 197–213 (2014).

[332] Elliott, M., Golub, B. & Jackson, M. O. Financial networks and contagion. *American Economic Review* **104**, 3115–53 (2014).

[333] Freixas, X., Parigi, B. M. & Rochet, J.-C. Systemic risk, interbank relations, and liquidity provision by the central bank. *Journal of Money, Credit and Banking* **32**, 611–638 (2000).

[334] Boss, M., Krenn, G., Puhr, C. & Summer, M. Systemic Risk Monitor: A Model for Systemic Risk Analysis and Stress Testing of Banking Systems. *Financial Stability Report* 83–95 (2006).

[335] Iori, G., Jafarey, S. & Padilla, F. G. Systemic risk on the interbank market. *Journal of Economic Behavior & Organization* **61**, 525–542 (2006).

[336] Glasserman, P. & Young, H. P. Contagion in financial networks. *Journal of Economic Literature* **54**, 779–831 (2016).

[337] Nier, E., Yang, J., Yorulmazer, T. & Alentorn, A. Network models and financial stability. *Bank of England Working Paper* **No. 346** (2008).

[338] Gallegati, M., Greenwald, B., Richiardi, M. G. & Stiglitz, J. E. The asymmetric effect of diffusion processes: Risk sharing and contagion. *Global Economy Journal* **8**, 1850141 (2008).

[339] Battiston, S., Gatti, D. D., Gallegati, M., Greenwald, B. & Stiglitz, J. E. Liaisons dangereuses: Increasing connectivity, risk sharing, and systemic risk. *Journal of economic dynamics and control* **36**, 1121–1141 (2012).

[340] Anand, K., Gai, P. & Marsili, M. Rollover risk, network structure and systemic financial crises. *Journal of Economic Dynamics and Control* **36**, 1088–1100 (2012).

[341] Arinaminpathy, N., Kapadia, S. & May, R. M. Size and complexity in model financial systems. *Proceedings of the National Academy of Sciences* **109**, 18338–18343 (2012).

[342] Shirado, H., Crawford, F. W. & Christakis, N. A. Collective communication and behaviour in response to uncertain 'danger'in network experiments. *Proceedings of the Royal Society A* **476**, 20190685 (2020).

[343] Abbe, E. A., Khandani, A. E. & Lo, A. W. Privacy-preserving methods for sharing financial risk exposures. *American Economic Review* **102**, 65–70 (2012).

[344] D'Errico, M. & Roukny, T. Compressing over-the-counter markets. *ESRB: Working Paper Series* (2017).

[345] Roukny, T., Bersini, H., Pirotte, H., Caldarelli, G. & Battiston, S. Default cascades in complex networks: Topology and systemic risk. *Scientific reports* **3**, 1–8 (2013).

[346] Leitner, Y. Financial networks: contagion, committment and private sector bailouts. *Journal of Finance* (2005).

[347] Lee, S. Measuring systemic funding liquidity risk in the interbank foreign currency ending market. *Bank of Korea Institute for Monetary and Economic Research Working Paper* **418** (2010).

[348] Lenzu, S. & Tedeschi, G. Systemic risk on different interbank network topologies. *Physica A: Statistical Mechanics and its Applications* **391**, 4331–4341 (2012).

[349] Shleifer, A. & Vishny, R. W. Liquidation values and debt capacity: A market equilibrium approach. *The journal of finance* **47**, 1343–1366 (1992).

[350] Shleifer, A. & Vishny, R. Fire sales in finance and macroeconomics. *Journal of economic perspectives* **25**, 29–48 (2011).

[351] Levy-Carciente, S., Kenett, D. Y., Avakian, A., Stanley, H. E. & Havlin, S. Dynamical macroprudential stress testing using network theory. *Journal of Banking & Finance* **59**, 164–181 (2015).

[352] Tasca, P., Battiston, S. & Deghi, A. Portfolio diversification and systemic risk in interbank networks. *Journal of Economic dynamics and control* **82**, 96–124 (2017).

[353] Squartini, T. *et al.* Enhanced capital-asset pricing model for the reconstruction of bipartite financial networks. *Physical Review E* **96**, 032315 (2017).

[354] Braouezec, Y. & Wagalath, L. Strategic fire-sales and price-mediated contagion in the banking system. *European Journal of Operational Research* **274**, 1180–1197 (2019).

[355] Sasidevan, V. & Bertschinger, N. Systemic risk: Fire-walling financial systems using network-based approaches. In *Network Theory and Agent-Based Modeling in Economics and Finance*, 313–330 (Springer, 2019).

[356] Kossinets, G. & Watts, D. J. Empirical analysis of an evolving social network. *Science* **311**, 88–90 (2006).

[357] Palla, G., Barabási, A. L. & Vicsek, T. Quantifying social group evolution. *Nature* **446**, 664–667 (2007).

[358] Cabrales, A., Gottardi, P. & Vega-Redondo, F. Risk sharing and contagion in networks. *The Review of Financial Studies* **30**, 3086–3127 (2017).

[359] Rogers, L. C. G. & Veraart, L. A. M. Failure and Rescue in an Interbank Network. *Management Science* **59**, 882–898 (2013).

[360] Ferrara, G., Langfield, S., Liu, Z. & Ota, T. Systemic illiquidity in the interbank network. *Working paper series* (2018).

[361] May, R. M., Levin, S. A. & Sugihara, G. Ecology for bankers. *Nature* **451**, 893–894 (2008).

[362] May, R. M. & Arinaminpathy, N. Systemic risk: the dynamics of model banking systems. *Journal of the Royal Society Interface* **7**, 823–838 (2010).

[363] Moreno, Y., Pastor-Satorras, R. & Vespignani, A. Epidemic outbreaks in complex heterogeneous networks. *Eur. Phys. J. B* **26**, 521–529 (2002).

[364] Yağan, O. & Gligor, V. Analysis of complex contagions in random multiplex networks. *PRE* **86**, 036103 (2012).

[365] Lee, K.-M., Brummitt, C. D. & Goh, K.-I. Threshold cascades with response heterogeneity in multiplex networks. *PRE* **90** (2014).

[366] Gleeson, J. & Cahalane, D. Seed size strongly affects cascades on random networks. *PRE* **75**, 56103 (2007).

[367] Gabbi, G., Iori, G., Jafarey, S. & Porter, J. Financial regulations and bank credit to the real economy. *Journal of Economic Dynamics and Control* **50**, 117–143 (2015).

[368] Borio, C. Iii. special feature: Market liquidity and stress: selected issues and policy implications. *BIS Quarterly Review* (2000).

[369] Fourel, V., Heam, J.-C., Salakhova, D. & Tavolaro, S. Domino effects when banks hoard liquidity: The french network. *Banque de France Working Paper* (2013).

[370] Diamond, D. W. & Rajan, R. G. Fear of fire sales, illiquidity seeking, and credit freezes. *The Quarterly Journal of Economics* **126**, 557–591 (2011).

[371] Lee, S. H. Systemic liquidity shortages and interbank network structures. *Journal of Financial Stability* **9**, 1–12 (2013).

[372] Lux, T. Emergence of a core-periphery structure in a simple dynamic model of the interbank market. *Journal of Economic Dynamics and Control* **52**, A11–A23 (2015).

[373] Lagunoff, R. & Schreft, S. L. A model of financial fragility. *Journal of Economic Theory* **99**, 220–264 (2001).

[374] Khandani, A. E. & Lo, A. W. What happened to the quants in august 2007? evidence from factors and transactions data. *Journal of Financial Markets* **14**, 1–46 (2011).

[375] Cont, R. & Schaanning, E. Fire sales, indirect contagion and systemic stress testing. *Available at SSRN* (2017).

[376] Watson, H. W. & Galton, F. On the probability of the extinction of families. *The Journal of the Anthropological Institute of Great Britain and Ireland* **4**, 138–144 (1875).

[377] Borgatti, S. P. Centrality and network flow. *Social networks* **27**, 55–71 (2005).

[378] Duarte, F. & Jones, C. *Empirical network contagion for US financial institutions* (FRB of NY Staff Report, 2017).

[379] Engle, R. F. & Ruan, T. Measuring the probability of a financial crisis. *Proceedings of the National Academy of Sciences* **116**, 18341–18346 (2019).

[380] Billio, M., Getmansky, M., Lo, A. W. & Pelizzon, L. Econometric measures of connectedness and systemic risk in the finance and insurance sectors. *Journal of financial economics* **104**, 535–559 (2012).

[381] Battiston, S., Puliga, M., Kaushik, M., Tasca, P. & Calderelli, G. DebtRank: Too Central to Fail? Financial Networks, the FED and Systemic Risk. *Sci. Rep.* **2**, 541 (2012).

[382] Nicosia, V., Criado, R., Romance, M., Russo, G. & Latora, V. Controlling centrality in complex networks. *Scientific reports* **2**, 1–7 (2012).

[383] Brin, S. & Page, L. Anatomy of a large-scale hypertextual web search engine. *Proceedings of the Seventh International World Wide Web Conference* 107–117 (1998).

[384] Page, L., Brin, S., Motwani, R. & Winograd, T. The pagerank citation ranking: Bringing order to the web. Tech. Rep., Stanford InfoLab (1999).

[385] Soramäki, K. & Cook, S. Sinkrank: An algorithm for identifying systemically important banks in payment systems. *Economics* **7** (2013).

[386] Arregui, M. N. *et al.* Addressing interconnectedness: Concepts and prudential tools. *International Monetary Fund* (2013).

[387] Banks, G. S. I. Updated assessment methodology and the higher loss absorbency requirement. *Basel Committee on Banking Supervision: Basel, Switzerland* (2013).

[388] Bluhm, M., Faia, E. & Krahnen, J. P. Monetary policy implementation in an interbank network: Effects on systemic risk. *SAFE Working Paper* (2014).

[389] Aldasoro, I., Gatti, D. D. & Faia, E. Bank networks: Contagion, systemic risk and prudential policy. *Journal of Economic Behavior & Organization* **142**, 164–188 (2017).

[390] Aldasoro, I. & Faia, E. Systemic loops and liquidity regulation. *Journal of Financial Stability* **27**, 1–16 (2016).

[391] Battiston, S. & Martinez-Jaramillo, S. Financial networks and stress testing: Challenges and new research avenues for systemic risk analysis and financial stability implications (2018).

[392] Beale, N. *et al.* Individual versus systemic risk and the regulator's dilemma. *PNAS* **108**, 12647–12652 (2011).

[393] Fouque, J.-P. & Langsam, J. A. *Handbook on Systemic Risk* (Cambridge University Press, 2013).

[394] Cimini, G., Squartini, T., Garlaschelli, D. & Gabrielli, A. Systemic risk analysis on reconstructed economic and financial networks. *Scientific reports* **5**, 1–12 (2015).

[395] Squartini, T., Caldarelli, G., Cimini, G., Gabrielli, A. & Garlaschelli, D. Reconstruction methods for networks: The case of economic and financial systems. *Physics reports* **757**, 1–47 (2018).

[396] Gleeson, J. P. Cascades on correlated and modular random networks. *Phys. Rev. E* **77**, 46117 (2008).

[397] Kobayashi, T. A model of financial contagion with variable asset returns may be replaced with a simple threshold model of cascades. *Economics Letters* **124**, 113–116 (2014).

[398] Kobayashi, T. & Takaguchi, T. Identifying relationship lending in the interbank market: A network approach. *Journal of Banking & Finance* **97**, 20–36 (2018).

[399] Gabbi, G., Germano, G., Hatzopoulos, V., Iori, G. & Politi, M. Market microstructure, banks' behaviour, and interbank spreads. *Banks' Behaviour, and Interbank Spreads (October 2, 2013)* (2013).

[400] Jo, H. H., Perotti, J. I., Kaski, K. & Kertész, J. Analytically solvable model of spreading dynamics with non-Poissonian processes. *Phys. Rev. X* **4**, 011041 (2014).

[401] Rocha, L. E. C. & Blondel, V. D. Bursts of vertex activation and epidemics in evolving networks. *PLOS Comput. Biol.* **9**, e1002974 (2013).

[402] Iribarren, J. L. & Moro, E. Impact of human activity patterns on the dynamics of information diffusion. *Phys. Rev. Lett.* **103**, 038702 (2009).

[403] Min, B., Goh, K. I. & Kim, I. M. Suppression of epidemic outbreaks with heavy-tailed contact dynamics. *EPL* **103**, 50002 (2013).

[404] Vazquez, A., Rácz, B., Lukács, A. & Barabási, A. L. Impact of non-Poissonian activity patterns on spreading processes. *Phys. Rev. Lett.* **98**, 158702 (2007).

[405] Garlaschelli, D. & Loffredo, M. I. Generalized bose-fermi statistics and structural correlations in weighted networks. *Physical review letters* **102**, 038701 (2009).

[406] Mastrandrea, R., Squartini, T., Fagiolo, G. & Garlaschelli, D. Enhanced reconstruction of weighted networks from strengths and degrees. *New Journal of Physics* **16**, 043022 (2014).

[407] Kingma, D. P. & Ba, J. Adam: A method for stochastic optimization. *arXiv preprint arXiv:1412.6980* (2014).

[408] Opsahl, T., Colizza, V., Panzarasa, P. & Ramasco, J. J. Prominence and control: the weighted rich-club effect. *Phys. Rev. Lett.* **101**, 168702 (2008).

[409] Panzarasa, P., Opsahl, T. & Carley, K. M. Patterns and dynamics of users' behavior and interaction: network analysis of an online community. *J. Am. Soc. Inf. Sci. Technol.* **60**, 911–932 (2009).

[410] Barrat, A. & Cattuto, C. Temporal networks of face-to-face human interactions. *Temporal Networks* 191–216 (2013).

[411] Génois, M. *et al.* Data on face-to-face contacts in an office building suggest a low-cost vaccination strategy based on community linkers. *Network Science* **3**, 326–347 (2015).

[412] Holme, P. Modern temporal network theory: a colloquium. *The European Physical Journal B* **88**, 234 (2015).

[413] Hamilton, J. D. *Time Series Analysis* (Princeton University Press, Princeton, NJ, 1995).

[414] Hamilton, J. D. Regime switching models. In *Macroeconometrics and time series analysis*, 202–209 (Springer, 2010).

[415] Vanhems, P. *et al.* Estimating potential infection transmission routes in hospital wards using wearable proximity sensors. *PLoS ONE* **8**, e73970 (2013).

[416] Génois, M. & Barrat, A. Can co-location be used as a proxy for face-to-face contacts? *arXiv:1712.06346* (2017).

[417] Génois, M., Zens, M., Lechner, C., Rannstedt, B. & Strohmaier, M. Building connections: How scientists meet each other during a conference. *arXiv preprint arXiv:1706.00230* (2019).

[418] Stehlé, J. *et al.* High-Resolution Measurements of Face-to-Face Contact Patterns in a Primary School. *PLoS ONE* **6**, e23176 (2011).

[419] Masuda, N. & Holme, P. *Temporal network epidemiology* (Springer, 2017).

[420] Cazabet, R. & Rosetti, G. Challenges in community discovery on temporal networks. In Holme, P. & Saramäki, J. (eds.) *Temporal Network Theory* (Springer-Nature, New York, 2019).

[421] Barrat, A., Cattuto, C., Szomszor, M., Broeck, W. V. d. & Alani, H. Social dynamics in conferences: analyses of data from the live social semantics application. In *International semantic web conference*, 17–33 (Springer, 2010).

[422] Barrat, A. *et al.* Empirical temporal networks of face-to-face human interactions. *The European Physical Journal Special Topics* **222**, 1295–1309 (2013).

[423] Kibanov, M. *et al.* Is web content a good proxy for real-life interaction? a case study considering online and offline interactions of computer scientists. In *Proceedings of the 2015 IEEE/ACM International Conference on Advances in Social Networks Analysis and Mining 2015*, 697–704 (2015).

[424] IC2S2 2017 program. https://quanttext.com/wp-content/uploads/2018/09/IC2S2-2017-program.pdf. Accessed May 29, 2022.

[425] Computational Social Science Winter Symposium 2016 program. https://www.gesis.org/en/css-wintersymposium/program/schedule. Accessed May 29, 2022.

[426] Kivelä, M. *et al.* Multilayer networks. *Journal of Complex Networks* **2**, 203–271 (2014).

[427] Min, B., Yi, S. D., Lee, K.-M. & Goh, K.-I. Network robustness of multiplex networks with interlayer degree correlations. *Phys. Rev. E* **89**, 042811 (2014). URL http://link.aps.org/doi/10.1103/PhysRevE.89.042811.

[428] Nicosia, V., Bianconi, G., Latora, V. & Barthelemy, M. Growing multiplex networks. *Physical review letters* **111**, 058701 (2013).

[429] Lee, K.-M., Goh, K.-I. & Kim, I.-M. Sandpiles on multiplex networks. *Journal of the Korean Physical Society* **60**, 641–647 (2012). URL http://dx.doi.org/10.3938/jkps.60.641.

[430] Gómez, S. *et al.* Diffusion dynamics on multiplex networks. *Phys. Rev. Lett.* **110**, 028701 (2013).

[431] Kim, J. Y. & Goh, K.-I. Coevolution and correlated multiplexity in multiplex networks. *Physical review letters* **111**, 058702 (2013).

[432] Gao, J., Buldyrev, S. V., Stanley, H. E. & Havlin, S. Networks formed from interdependent networks. *Nature physics* **8**, 40–48 (2012).

[433] Liu, Y.-Y., Slotine, J.-J. & Barabási, A.-L. Controllability of complex networks. *nature* **473**, 167–173 (2011).

[434] Lin, C.-T. Structural controllability. *IEEE Transactions on Automatic Control* **19**, 201–208 (1974).

[435] Delpini, D. *et al.* Evolution of controllability in interbank networks. *Scientific reports* **3**, 1–5 (2013).